Local Calibration of AASHTOWare® Using Ontario Pavement Management System Data PMS2

by

Amin Hamdi

A thesis
presented to the University of Waterloo
in fulfillment of the
thesis requirement for the degree of
Doctor of Philosophy
in
Civil Engineering

Waterloo, Ontario, Canada, 2015

AUTHOR'S DECLARATION

I hereby declare that I am the sole author of this thesis. This is a true copy of the thesis, including any required final revisions, as accepted by my examiners.

I understand that my thesis may be made electronically available to the public.

Abstract

Well designed built and maintained pavements will sustain the safe and comfortable transportation of people and goods. Effective monitoring requires information about evolving pavement condition, including details about factors such as pavement distresses, climate conditions and traffic pattern which are important factors impacting the pavement conditions. Keeping track of the degree of distress over time can help extending the pavement life by applying the suitable maintenance and rehabilitation at the right time. Pavement management systems (PMSs) were originally created to archive this kind of data so that decision makers could predict future pavement performance. The Ministry of Transportation of Ontario (MTO) employs an advanced PMS tool, entitled PMS2, to record, store, and analyze data about the current and past pavement performance conditions of its network of 16,500 centre-lane kilometers of freeways, collectors, arterials, and local roads.

The research presented in this thesis was focused on the use of PMS2 data for the calibration of flexible pavement performance models coefficients for Ontario as a case study Performance model coefficients were created for application with the *Mechanistic-Empirical Pavement Design Guide* (MEPDG), now known as AASHTOWare®, and were calibrated using statistical tools through a series of analyses of historical pavement condition data that were collected in the field. The data were classified according to pavement type and annual average daily traffic. For this study, three categories were examined and calibrated: low traffic volume (AADT < 10,000), high traffic volume (AADT > 10,000), and overall network. The spilt in data was Eighty-five percent to be used in calibration development of the performance model calibration coefficients and the remaining fifteen percent of the data were employed for validating the performance models using a variety of statistical tools. A comparison of the results with the field measurements revealed that rutting model coefficients should be locally calibrated for each category. For the low-volume, high-volume, and overall network categories, local calibration produced significant reductions in the rutting root-mean-square error (RMSE) of 30, 37, and 37 %, respectively, and in the IRI showed there was no significant correlation.

The procedure and analysis methodology used in the calibration of the performance model coefficients provide a framework for the local calibration of AASHTOWare® based on a comparison of the predicted pavement distress and that documented in the PMS. This work will have important benefits to the transportation agencies as it will enable them to evaluate the feasibility of using the ASHTOWare® Design system to improve pavement management and to enhance future design and construction strategies.

Acknowledgements

I wish to thank my supervisor, Professor Susan Tighe, of the Department of Civil and Environmental Engineering at the University of Waterloo. It was an honor to work under her supervision. Many thanks for Dr. Li Ningyuan from the MTO as well as Dr. Khaled Helali, Dr. Amir Abd El Halim, and Dr. Mohab El-Hakim of Stantec Ltd. for their guidance and encouragement in support of my research.

I would like to acknowledge the Ministry of Transportation of Ontario (MTO) for its technical help; the Centre for Pavement and Transportation Technology (CPATT); Stantec Ltd.; and King Abdul Aziz University (KAU), Jeddah, Saudi Arabia, for their scholarship and for sponsoring my studies.

For their countless hours of assistance, I extend profound gratitude to the professionals, colleagues and co-op students who assisted me with this research: Becca Lane from the MTO, Laura Bland, Andrew Northmore, Magdy Shaheen, Zaid Alyami, Marcelo Gonzales, Mohmmad Hegazi, Doubra Ambaiowei, Xiomara Sanchez, Cheng Zhang, Jodi Norris, Vimy Henderson, Rabiah Rizbi, Federico Irali, Gulfam Jannat, Aleks Kivi, Aleli Osorio, Daniel Pickel, Sonia Rahman, Janki Bhavsar, Sina Varamini, and Hanaa Al-Bayat. I would like to thank you all for your support, help, and research collaboration.

Dedication

I dedicate this thesis to my father, a medical doctor and member of the academic staff at King Abdulaziz University (KAU), Jeddah, Saudi Arabia, who passed away suddenly in 2009 at the age of 60, and to my mother and brother, with gratitude for supporting me throughout the years of my academic study and my professional career. I would like to thank my adorable wife, Duaa, and my dear children Hashim, Yousef, and Youmna for their constant encouragement and reinforcement throughout my graduate studies. I also extend this dedication to include my colleagues and friends at the University of Waterloo and in Saudi Arabia, with appreciation for their endless support.

Table of Contents

AUTHOR'S DECLARATION ii
Abstract iii
Acknowledgements iv
Dedication v
Table of Contents vi
Chapter 1 Introduction 1
1.1 Background 1
1.2 Problem Definition 2
1.3 Research Scope and Objectives 2
1.4 Local Calibration Methodology 3
1.4.1 Introduction 3
1.4.2 Research Plan 4
1.5 Organization of the Thesis 6
Chapter 2 Literature Review 8
2.1 Introduction 8
2.2 Pavement Management Systems 9
2.3 PMS Key Performance Indicators 12
2.3.1 International Roughness Index 12
2.3.2 Cracking 12
2.3.3 Rutting 13
2.3.4 Pavement Condition Index 14
2.4 Pavement Design Methods 15
2.4.1 Pavement Design Approaches 16
2.4.2 Mechanistic-Empirical Pavement Design Guide 16
2.5 Pertinent Studies of Local Calibration of the MEPDG 20
2.6 Summary of Findings 33
Chapter 3 Data Sources and AASHTOWare® Input 34
3.1 Introduction 34
3.2 Data Collection 35
3.3 Collection of Performance Data 36

3.3.1 IRI 36
3.3.2 Rutting 36
3.4 AASHTOWare® Input 37
3.4.1 General Site Information 38
3.4.2 Traffic Information 39
3.4.3 Climate Data 43
3.4.4 Structural Layers and Material Properties of the Pavement 44
3.5 Summary of Findings 47
Chapter 4 Methodology, Results and Discussion 48
4.1 Introduction 48
4.1.1 Pavement Section Selection 48
4.1.2 Preparation of the Input and Output 49
4.1.3 Calibration Examination 49
4.1.4 Calibration 50
4.1.5 Validation 50
4.2 Calibration Results 51
4.2.1 Low Traffic Volume Calibration 51
4.2.2 High Traffic Volume Calibration 55
4.2.3 Overall Network Calibration 57
4.3 Calibration Summary: 59
4.4 Validation Results 60
4.4.1 Low Traffic Volume Validation 60
4.4.2 High Traffic Volume Validation 61
4.4.3 Overall Network Validation 61
4.5 Validation Summary 62
Chapter 5 Conclusions and Recommendations 63
5.1 Conclusions 63
5.2 Future work 64
Guide for the Local Calibration of the Mechanistic-empirical Pavement Design Guide, American Association of State Highway and Transportation Officials, AASHTO, 2010 66
Appendix A 74

ASSHTOWare® 74
Appendix B 81
Output Sample from the Pavement-ME Software 81
Appendix C 110
Statistical Analysis 110

List of Figures

Figure 1-1: Observed versus Predicted IRI for onesection only [Hamdi 2012] 4
Figure 1-2: Research Plan 6
Figure 1-3: Organization of the Thesis 7
Figure 2-1: Load Transfer in Flexible Pavement [WDOT, 2011] 8
Figure 2-2: Decision-Making Framework for Asset Management [TAC, 2013] 10
Figure 2-3 Typical Pavement Performance Curve [FHWA, 2011] 11
Figure 2-6: Rutting [www.ino.ca] 13
Figure 2-5: Longitudinal Cracking 13
Figure 2-4: Fatigue Cracking 13
Figure 2-7: Flexible Pavement Survey Form for a Manual Surface Distress Survey [MTO, 1990] 15
Figure 2-8: Factors Affecting Pavement Performance [Tighe, 2007] 16
Figure 2-9: Predicted versus Measured Total Rutting Values before Calibration, for the North Carolina Study [Richard, 2007] 22
Figure 2-10: Predicted versus Measured Total Rutting Value after Calibration, for the North Carolina Study [Richard, 2007] 22
Figure 2-11: Predicted versus Measured Total Rutting Values before Calibration, for the Utah Study [UDOT, 2009] 23
Figure 2-12: Predicted versus Measured Total Rutting Values after Calibration, for the Utah Study [UDOT, 2009] 24
Figure 2-13: Predicted versus Measured Total Rutting Values before Calibration, for the Ohio Study 25
Figure 2-14: Predicted versus Measured Total Rutting Values after Calibration, for the Ohio Study 26
Figure 2-15: Predicted versus Measured Total Rutting Values before Calibration, for the Arkansas Study [Hall, 2011] 27
Figure 2-16: Predicted versus Measured Total Rutting Values after Calibration, for the Arkansas Study [Hall, 2011] 28
Figure 2-17: Predicted versus Measured IRI Values before Calibration, for the Iowa Study [Halil, 2013] 29
Figure 2-18: Predicted versus Measured IRI Values after Calibration, for the Iowa Study [Halil, 2013] 30

Figure 2-19 : Predicted versus Measured Rutting Values for Western Washington [Li, 2009] 32
Figure 2-20 : Predicted versus Measured Rutting Values for Eastern Washington [Li, 2009]..... 32
Figure 3-1: ARAN Automatic Road Analyzer (www.epc.com.hk)..... 37
Figure 3-2: Illustration of Basic AASHTOWare® Input [Waseem, 2013] 38
Figure 3-3: AASHTOWare® General Information Screen 39
Figure 3-4: AASHTOWare® Traffic Input Screen 41
Figure 3-5: AASHTOWare® Climate Data Input Screen 44
Figure 3-6: AASHTOWare® Asphalt Layer Input Screen..... 45
Figure 3-7: AASHTOWare® Base Material Input Screen 45
Figure 4-1: Uncalibrated Rutting for Low Traffic Volume Category..... 51
Figure 4-2: Calibrated Rutting for Low Traffic Volume Category..... 52
Figure 4-3: Uncalibrated IRI for Low Traffic Volume Category 53
Figure 4-4: Calibrated IRI for Low Traffic Volume Category 54
Figure 4-5: Uncalibrated Rutting for High Traffic Volume Category..... 55
Figure 4-6: Calibrated Rutting for High Traffic Volume Category..... 56
Figure 4-7: Uncalibrated Rutting for Overall Network..... 57
Figure 4-8: Calibrated Rutting for Overall Network..... 58
Figure 4-9: Rutting Validation of Low Traffic Volume Category..... 60
Figure 4-10: Rutting Validation of High Traffic Volume Category 61
Figure 4-11: Rutting Validation of Overall Network Category 62

List of Tables

Table 2-1 : Flexible Pavement Subtypes [Newcomb, 2001] 8
Table 2-2: Distress Occurring in Flexible Pavement [TAC, 2013] 9
Table 2-3: Pavement Condition Index Rating [ASTM D 6433 – 07] 14
Table 2-4: Pavement Distress and Relevent Weights [MTO, 1990] 14
Table 2-5: Input Data for Each Level in the MEPDG [FHWA, 2012] 19
Table 2-6: Recommended Local Calibration Factors for NCDOT Prediction Models [Richard, 2007] 22
Table 2-7: Final Local Calibration Coefficients for the Arkansas Study [Hall, 2011] 28
Table 2-8: Final Local Calibration Coefficients for the Iowa Study [Halil, 2013] 30
Table 2-9: Calibration Coefficients Produced by the MEPDG Flexible Pavement Distress Models for Arizona Conditions [Souliman et al, 2010] 31
Table 2-10: Final Local Calibration Coefficients for the Washington Study [Li, 2009] 33
Table 3-1: Pavement Sections Classififcation 34
Table 3-2: Summary of Traffic Input Levels Used in This Research 40
Table 3-3: Recommended Percentage of Trucks in the Design Lane for Ontario [MTO, 2012] 41
Table 3-4: FWHA System of Vehicle Classification (Source: www.fhwa.dot.gov) 42
Table 3-5: Typical Axles-per-Truck Table for Southern Ontario [MTO, 2012] 42
Table 3-6: Typical Axles-Per-Truck Table for Northern Ontario [MTO, 2012] 43
Table 3-7: Ontario Typical Superpave and SMA Asphalt Concrete Properties [MTO, 2012] 46
Table 3-8: Typical Marshall Mix Properties for Ontario [MTO, 2012] 47
Table 4-1: Statistical Analysis for Rutting in Low Traffic Volume Roads 52
Table 4-2: Local Calibration Coefficients for Rutting Model in Low Traffic Volume Roads 53
Table 4-3: Statistical Analysis of IRI Model for Low Traffic Volume Roads 54
Table 4-4: Statistical Analysis for High Traffic Volume Rutting Predictions 56
Table 4-5: Local Calibration Coefficients for the High Traffic Volume Rutting Predictions 57
Table 4-6:Statistical Analysis for Overall Network Rutting Predictions 58
Table 4-7: Local Calibration Coefficients for the Overall Network Rutting Predictions 59
Table 4-8 : Summary of Ontario Local Calibration Coefficients 59

Chapter 1
Introduction

1.1 Background

The enormous impacts of traffic and environmental loading on the performance of a pavement play a significant role in the inevitable deterioration exhibited by various types of pavement over time. As pavements deteriorate, the needs of users can no longer be met. Pavement performance models and associated Key Performance Indicators (KPIs) are important not only for monitoring current Level of Service (LOS) but also for selecting the most effective maintenance, preservation, and rehabilitation treatments for a pavement throughout its life cycle [NRC, 2003]. These KPIs and associated performance models are also helpful for determining the end of service life, at which point rehabilitation or reconstruction is required. In addition, performance models provide engineers and managers with the ability to allocate resources appropriately through the effective use of a pavement management system (PMS). The development of the new *Mechanistic-Empirical Pavement Management Design Guide* (MEPDG) presents an opportunity for the utilization of existing PMS data as a means of improving pavement performance [AASHTO, 1993].

According to the American Association of State Highway and Transportation Officials (AASHTO), pavement performance is defined as the serviceability trend of the pavement over its design period, with serviceability indicating the ability of the pavement in its existing condition to serve the demand presented by the traffic [AASHTO, 1993]. Pavement performance is managed through a PMS, which is divided into two main levels: project and network. Project-level data are used for calibrating and validating pavement performance models at the network level. Based on empirical, mechanistic, or mechanistic-empirical approaches, basic pavement performance models vary from simple linear regression models to complex Markov chain models [Ningyuan, 1997].

AASHTOWare® offers models for pavement design and analysis. The MEPDG is based on consideration of input parameters that influence pavement performance, including traffic, climate, pavement structure, and materials properties, followed by the application of engineering mechanics principles in order to predict pavement responses. Suitable for both flexible and rigid pavement, the MEPDG is divided into three main levels. Level One requires very detailed materials, traffic, and climate information for developing the pavement design; Level Two involves a moderate level of data input; and Level Three relies on the default values of the input data. The MEPDG is advancing state-

of-the-art practice by enabling the inclusion of materials characteristics in conjunction with bothtraffic and environmental data in order to provide enhanced predictions of pavement performance. It can also forecast not only roughness but also specific pavement distress performance, based on traffic and environmental data. The effective implementation of this guide will result in substantial progress in the area of pavement management because it will enable the improved prediction of deterioration and facilitate the timely implementation of improvement treatments. It should be noted that while the MEPDG was never designed to work with a PMS, many MEPDG features, with appropriate adjustments, could nonetheless be helpful for PMS managers [Ddamda, 2011].

A PMS includes KPIs, such as the International Roughness Index (IRI) or the Pavement Condition Index (PCI), as indicators of pavement age. These indicators enable a PMS to be used for improving budget allocations through the prioritizing of network needs [TAC, 2013]. The MEPDG predicts various types of distress and IRI as a function of time.

1.2 **Problem Definition**

Most North American studies of the local calibration of AASHTOWare® have concluded that national calibration coefficients fail to offer reliable accuracy or precision. The AASHTOWare® was developed based on several Long Term Pavement Performance sections (LTPP) from various regions in North America. Significant variation is noted between various LTPP sections including binder and aggregate properties, climate conditions, traffic spectrum, etc. Performance of local calibration of AASHTOWare® was reported to enhance the models' accuracy in predicting pavement performance. Landmark case studies of local calibration projects are discussed in subsequent chapters.

1.3 Research Scope and Objectives

The AASHTOWare® Design software is used as a means of providing predictions of the structural performance of pavements. The overall objective of the thesis is to evaluate the feasibility of using the current pavement management system data to improve AASHTOWare® models accuracy for Ontario flexible pavements.

The specific objectives of the thesis are to:

- Investigation of the accuracy and precision of the results.
- Obtain and evaluate the local calibration coefficients.

A statistical analysis of AASHTOWare® structural performance predictions demonstrated a serious need for the incorporation of local calibrations into the AASHTOWare® models. Furthermore AASHTOWare® model validation shows a significant improvement in pavement performance prediction, resulting in enhanced representation of the spectrum of local materials, climate, and traffic. However, the calibration coefficients that were obtained should be updated as the performance database expands and innovative materials are utilized in Ontario pavement designs.

1.4 Local Calibration Methodology

1.4.1 Introduction

Reducing the difference between the observed and predicted values and minimizing the sum of squared errors (RMSE) is the goal of calibration [Williams, 2013]. Calibration process is designed in steps in order to eliminate bias and minimize any discrepancies between the observed performance of actual pavements and the results predicted by an empirical or mechanistic model [von Quintus, 2007]. In this study, AASHTOWare® has been run using the national calibration and the default calibration coefficients, which show an overestimate with respect to pavement structure because materials, environmental conditions, and construction practices in the United States differ from those in Canada. To enhance performance predictions and minimize bias (systematic errors) in the model, additional calibration is therefore required through changes to the calibration coefficients built into the prediction models (transfer functions). For the current study, asphalt concrete (AC) was the focus of the recalibration, which was conducted with consideration of the IRI and rutting prediction models included in the current AASHTOWare® and a comparison of their results with actual in-field performance observations of Ontario pavement sections. In this study, bias correction factors were established by minimizing the root mean square errors (RMSE) between the observed and predicted pavement distress for specific Ontario sections. For a sample section, Figure 1-1 shows a comparison of the IRI values predicted by the AASHTOWare® software using the national calibration and the observed IRI measurements obtained from PMS2 for one section only [Hamdi, 2012] representing general trend in all sections. The AASHTOWare® model may show the same trend as the observed

measurements but have higher IRI values, which will result in failure to allocate sufficient budget for preservation and maintenance.

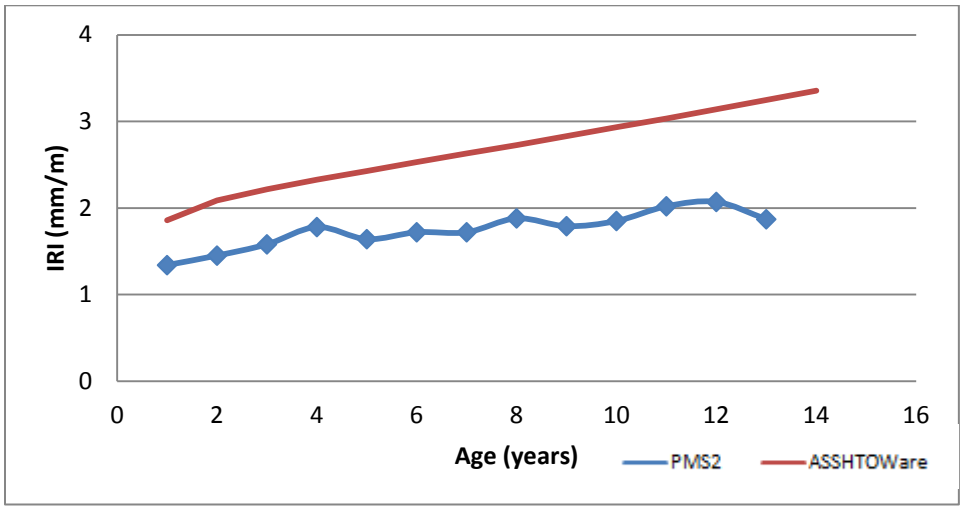

Figure 1-1: Observed versus Predicted IRI for onesection only [Hamdi 2012]

1.4.2 Research Plan

For this research, the iteration method was chosen as the calibration methodology, as many researches and Department of Transportation followed. This method included three major stages: checking the need for calibration, calibration, and validation. The following research plan was followed:

1. Selection of Ontario pavement sections as will be presented in section 4.1.1.
2. Preparation of the AASHTOWare® input database and performance data for the pavement sections selected from PMS2
3. Determine whether calibration is needed will be presented in section 4.1.3
4. Calibration
5. Validation of the calibration coefficients

Figure 1-2 provides a flowchart of these steps.

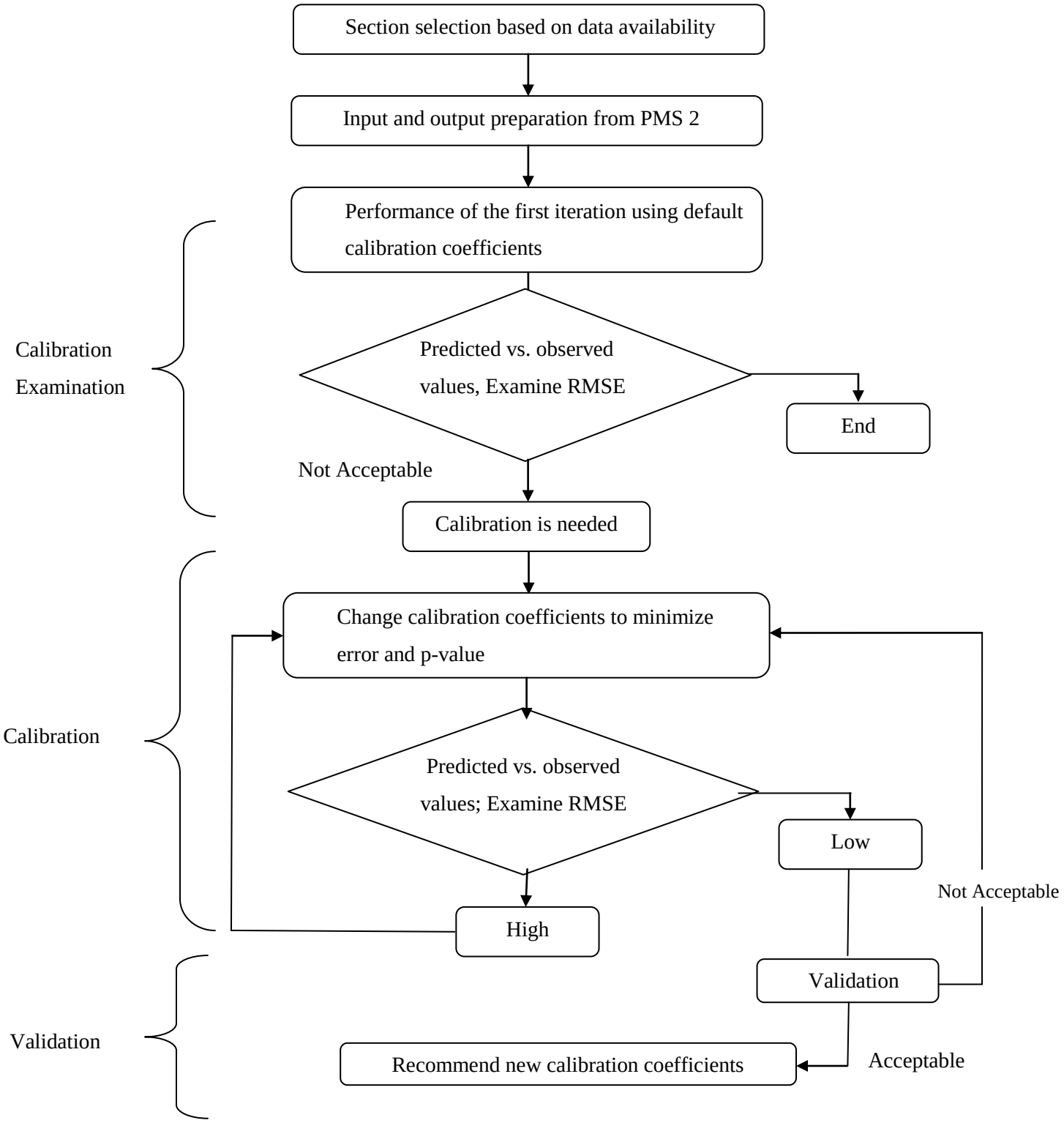
Section selection based on data availability
Input and output preparation from PMS 2
Performance of the first iteration using default calibration coefficients
Calibration Examination
Predicted vs. observed values, Examine RMSE
End
Not Acceptable
Calibration is needed
Calibration
Change calibration coefficients to minimize error and p-value
Predicted vs. observed values; Examine RMSE
Low
Not Acceptable
High
Validation
Validation
Recommend new calibration coefficients
Acceptable

Figure 1-2: Research Plan

1.5 Organization of the Thesis

The thesis contains six chapters, with supporting tables and figures that illustrate the information conveyed in the text. To demonstrate specific trends in the data, the figures provide visual representations of the data presented in the corresponding tables.

Chapter 1 gives a brief background and general idea of the topic and sets out the research hypothesis, scope and objectives of the research, and the research methodology followed for obtaining and validating the local calibration coefficients.

Chapter 2 provides an extensive literature review related to the main thesis topics, as a means of providing a solid background for readers from other majors or disciplines. This chapter discusses the basic types of pavements, pavement distress, key performance indicators, and design methods and also includes a review of pavement management systems, the AASHTOWare® Mechanistic, and pertinent studies of local calibration of the AASHTOWare®.

Chapter 3 presents the data provided by the PMS along with an indication of their importance. The experimental program is also introduced through an explanation of the development of the overall evaluation of the feasibility of using the MEPDG for improving pavement management.

Chapter 4 presents the results obtained from AASHTOWare® both before and after calibration as well as the outcomes of the validation process that was conducted with the use of a variety of statistical tools.

Chapter 5 includes the conclusions drawn and recommendations made as a result of this research and also highlights its main contributions.

Figure 1-3 provides a flowchart that illustrates the relationships among the thesis chapters.

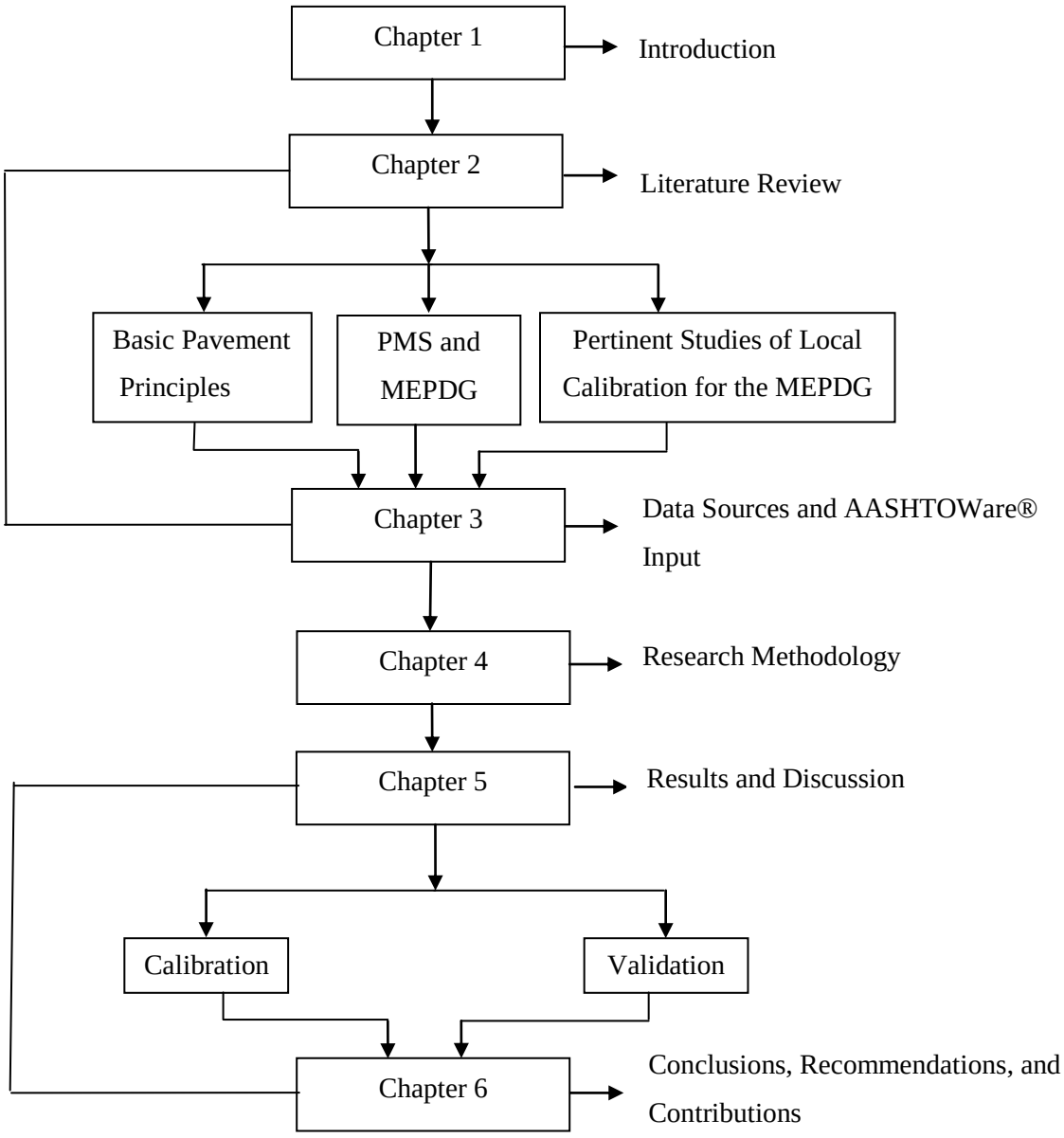

Figure 1-3: Organization of the Thesis

Chapter 2

Literature Review

2.1 Introduction

Many types of pavement are available, including flexible, rigid, surface treated, and gravel surfaced. In Canada, the pavement on most major arterial roads and highways is categorized as rigid or flexible. A flexible pavement is defined as "a pavement comprised of a wearing surface of asphalt concrete on a granular base" [TAC, 2013]. Flexible pavement comprised of fine aggregate (FA) and coarse aggregate (CA). However, their mechanisms for load transfer vary. Figure 2-1 illustrates the load transfer on flexible pavements. Flexible pavement includes several subtypes, as listed in Table 2-1 [Newcomb, 2001].

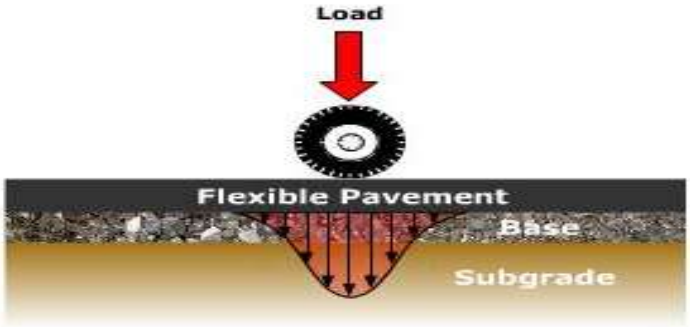

Figure 2-1: Load Transfer in Flexible Pavement [WDOT, 2011]

Table 2-1 : Flexible Pavement Subtypes [Newcomb, 2001]

Flexible Pavement Subtypes	**Explanation**
Conventional Flexible Pavement	150 mm of asphalt over granular base and subbase
Deep Strength	asphalt surface and asphalt base over a minimal aggregate base above subgrade
Full Depth pavement	asphalt courses used for all layers above

Distresses in flexible pavement are classified into cracking, Surface defects, and Surface deformation. The common types of distress are shown in Table 2-2.

Table 2-2: Distress Occurring in Flexible Pavement [TAC, 2013]

Category	Distress Type
Cracking	Fatigue Cracking
	Block Cracking
	Edge Cracking
	Longitudinal Cracking
	Reflection Cracking at Joints
	Transverse Cracking
Surface Defects	Bleeding
	Polished Aggregate
	Ravelling
Surface Deformation	Rutting
	Shoving
	Distortion

2.2 Pavement Management Systems

A pavement management system (PMS) can be defined as a tool that assists decision makers in determining optimum strategies for providing and maintaining pavements in serviceable condition over a given period of time [Haas, 1994]. In response to recent increases in the number of roads, the PMS was developed to help engineers and decision makers monitor and evaluate pavement condition [MTO, 2013]. PMS utilize time-series data to create a variety of pavement performance models, and traditional PMS tools were designed to achieve performance prediction objectives using the most cost-effective data collection methodology [Prakash, 1988]. As shown in Figure 2-2, a PMS operates at two levels: network and project. The network-level perspective is based on a top-down approach, which includes consideration of the overall network performance goal in relation to the available budget. It addresses the question of what should be done in order to maintain an overall satisfactory network condition while maximizing benefit and/or minimizing cost. The project-level

perspective entails a bottom-up approach, which takes into account each segment of the network and evaluates the point at which it reaches a specified failure threshold. It addresses the question of what action should be taken and then provides recommendations for the application of rehabilitation tactics for those projects, or segments, in order to restore them to nearly new condition.

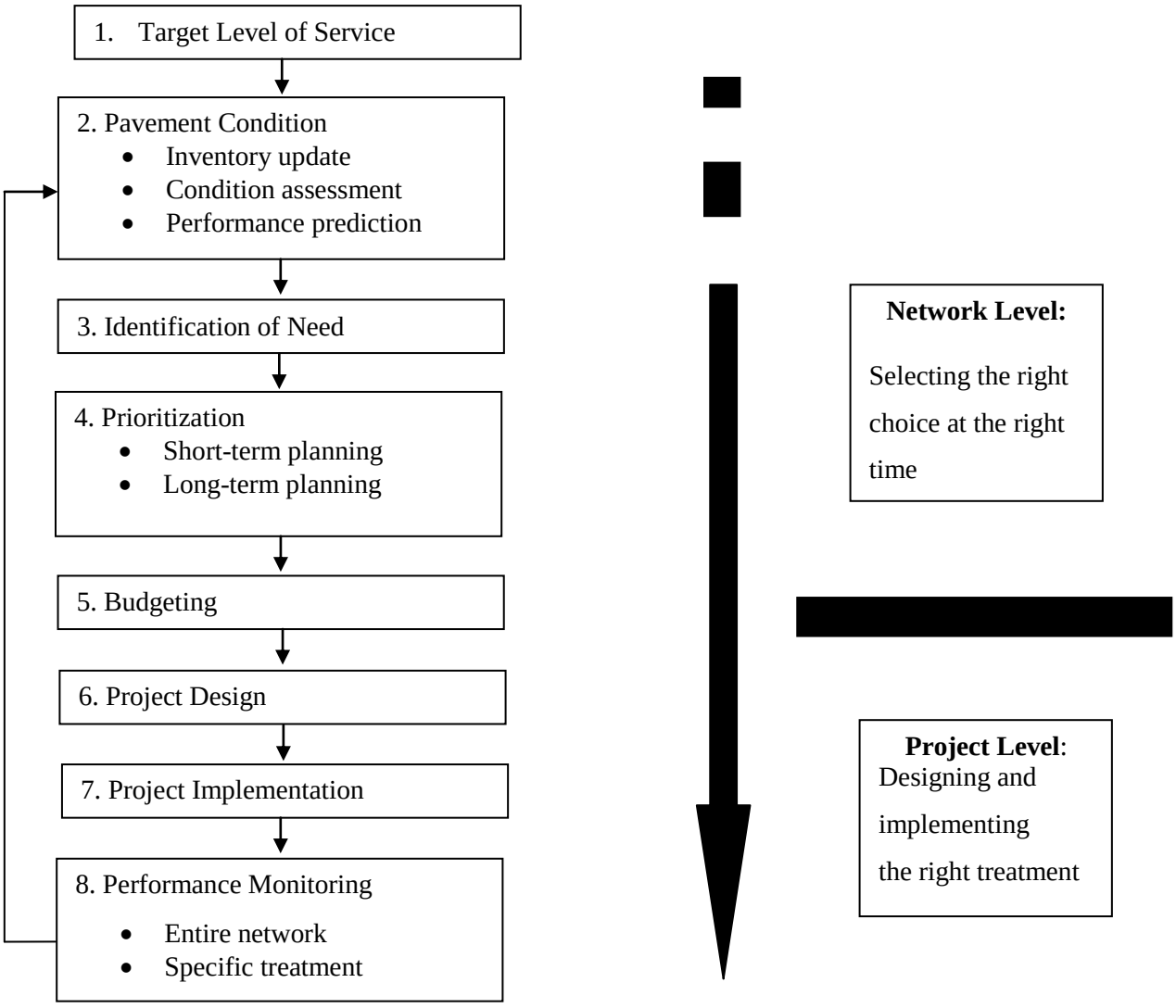

Figure 2-2: Decision-Making Framework for Asset Management [TAC, 2013]

The Ministry of Transportation of Ontario (MTO) employs an advanced PMS tool called PMS2, which is the second generation of PMS, an enhancement of the original one developed in 1985. Some of the most important features of PMS2 include its ability to archive pavement condition data; evaluate pavement condition; predict the long-term performance of a pavement; identify pavement repair needs; and recommend a cost-effective, prioritized list of projects [MTO, 2013]. The goal of pavement management is to facilitate the application of the appropriate treatment to the appropriate pavement at the appropriate time [Ningyuan, 2014]. PMS components include inventory data, pavement condition assessment, criteria establishment, prediction models of pavement performance deterioration, rehabilitation and maintenance strategies, priority programming of rehabilitation and maintenance, economic evaluation of alternative pavement design strategies, and program implementation [Farashah, 2012]. Figure 2-3 shows a typical pavement performance curve. On the y-axis pavement Condition Index (PCI) represent the pavement condition while on the x-axis is the pavement age in years. Normally a new pavement will be constructed in excellent condition and deteriorate over time due to deferent factor. By applying the goal of pavement management, a great impact on pavement service life and budget allocation will accrue.

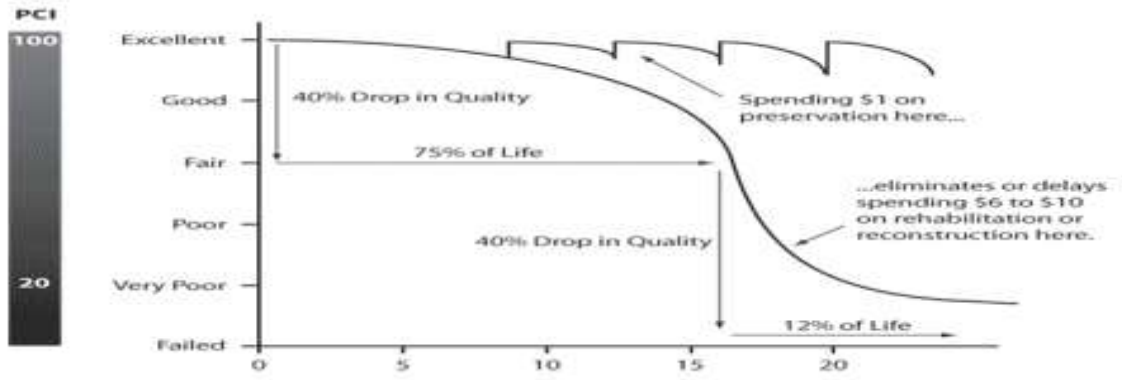

Figure 2-3 Typical Pavement Performance Curve [FHWA, 2011]

2.3 PMS Key Performance Indicators

Key performance indicators (KPIs) represent an important element of a PMS. They are quantifiable measurements that designate current pavement condition. For monitoring the level of service of a pavement, two basic KPIs are suggested: the International Roughness Index (IRI) and the Pavement Condition Index (PCI).

2.3.1 International Roughness Index

Roughness is defined according to the American Society for Testing and Materials (ASTM) as "the deviation of a surface from a true planar surface with characteristic dimensions that affect vehicle dynamics and ride quality" [ASTM, 2008]. The IRI represents pavement roughness and is known as a key indicator of pavement quality. It can be calculated based on the measurement of a single longitudinal profile on the inside and outside wheel paths for each 0.1 km of the pavement section, based on a road profile. The average of these two IRI measurements provides a value that indicates the roughness of the pavement, and this estimation of roughness can be used in both network and project-level pavement management [AASHTO, 1993].

2.3.2 Cracking

Cracking is considered a major concern in pavement performance and is a significant factor in determination of pavement maintenance time. Most pavements develop cracks as they age in service due to the recurring traffic load and the impact of the climate. Cracking appears in a variety of manifestations: fatigue cracking, block cracking, edge cracking, longitudinal cracking, and transverse cracking. The goal of good pavement design is to reduce the incidence of cracking and extend the service life of the road. Figures 2-4 and 2-5 represent two types of pavement cracking [Tri Technologies, 2014].

Figure 2-4: Longitudinal Cracking

Figure 2-5: Fatigue Cracking

[www.pavementinteractive.org]

2.3.3 Rutting

Rutting, or permanent deformation, has a significant effect on the performance of flexible pavements. Rutting can be defined as "longitudinal depressions left in the wheel paths after repeated loadings, combined with a sideways shoving of the pavement material" [BCMoT, 2012]. Optimal pavement structure design can delay the appearance of rutting. Figure 2-6 shows an example of severe pavement rutting.

Figure 2-6: Rutting [www.ino.ca]

2.3.4 Pavement Condition Index

The Pavement Condition Index (PCI) a numerical rating of the pavement condition that ranges from 0 to 100 with 0 being the worst possible condition and 100 being the best possible condition [ASTM D 6433 – 07]. However, it is not allowable for a road to have a zero PCI value because, realistically, once a road reaches 30 it would be impassable for vehicles. Table 2-3 shows PCI rating.

Table 2-3: Pavement Condition Index Rating [ASTM D 6433 – 07]

Pavement Condition Index	
Good	86-100
Satisfactory	71-85
Fair	56-70
Poor	41-55
Very Poor	26-40
Serious	11-25
Failed	0-10

MTO practice for monitoring pavement performance specifies annual or biannual PCI measurement as a means of assessing severity of pavement distress, smoothness and ride comfort of the road. Each type of distress is individually weighted based on its overall impact on performance, as shown in Table 2-4, and is then recorded on a distress survey sheet, as depicted in Figures 2-7 for flexible pavements. The PCI can be calculated manually or with the use of a pavement management program [MTO, 1990].

Table 2-4: Pavement Distress and Relevent Weights [MTO, 1990]

Types of Distress	**Weight**
Ravelling and Coarse Aggregate Loss	3.0
Flushing	0.5
Rippling and Shoving	1.0
Wheel Track Rutting	3.0
Distortion	3.0
Long Wheel Track – Single/Multiple	1.0
Long Wheel Track – Alligator	3.0
Centerline – Single/Multiple	0.5
Centerline – Alligator	2.0
Pavement Edge – Single Multiple	0.5
Pavement Edge – Alligator	1.0
Transverses – Single/Multiple	3.0
Transverse – Alligator	1.0

Long Meander Midlane Map	0.5

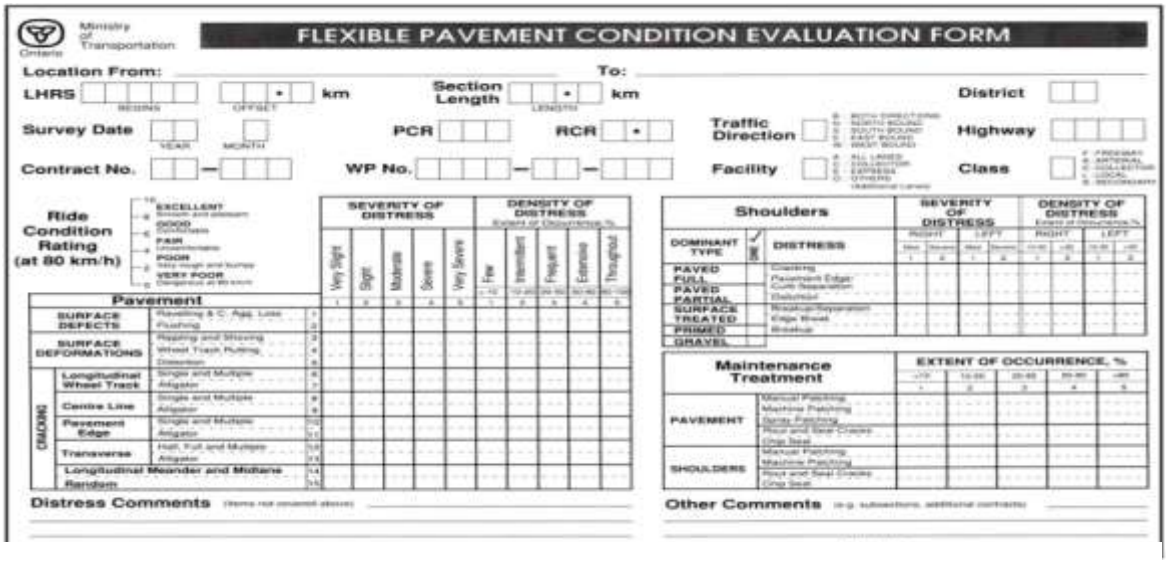

Figure 2-7: Flexible Pavement Survey Form for a Manual Surface Distress Survey [MTO, 1990]

Accurate prediction of pavement deterioration is the most important factor in the ability to enhance pavement performance [Ningyuan, 1999]. Pavement design methods incorporate a variety of models for predicting performance, with each method including a number of models. For example, the overall PCI of a road can be predicted. Pavement performance prediction models can be classified as deterministic, which rely on a single point value estimator, or probabilistic, which include consideration of variability through an examination of probabilities [TAC, 2013]. Both types of models are employed for the estimation of pavement performance over time. Pavement design approaches include four broad categories: experience based, empirical, mechanistic, and mechanistic-empirical.

2.4.1 Pavement Design Approaches

2.4.1.1 Empirical

This method is based on the use of experimental or test results as a means of predicting performance. The observed variable, or measured amount of distress, is related to one or more independent variables such as age, distress condition, or the thickness of the pavement layer [TAC, 2013].

2.4.1.2 Mechanistic

A mechanistic pavement design approach relies on measurements of the response of the pavement to the loads created by the traffic, such as stress and strain [TAC, 2013].

2.4.1.3 Mechanistic-Empirical Based

With mechanistic-empirical methods, the structural or functional deterioration measured is related to stress or strain through a transfer function or regression equation such as that used in the AASHTO *Mechanistic-Empirical Pavement Design Guide* (MEPDG). This approach was also used for the development of OPAC 2000 [AASHTO, 2008].

2.4.2 Mechanistic-Empirical Pavement Design Guide

The method set out in the MEPDG was introduced as a means of filling the gaps in mechanistic and empirical design methods. The MEPDG merges the finest elements of both design methods: mechanistic models were used for calculating mechanistic properties such as tensile strain, stress, and deflection, while empirical models were used for determining transfer functions. Transfer functions are employed for converting mechanistic properties into performance indices such as the rutting depth, the IRI, and the percentage of longitudinal and alligator cracking. A number of additional factors, such as environmental impact, traffic growth and loading, and the accuracy of the transfer function, also affect predictions of the structural deterioration of pavement. Figure 2-8 indicates the factors that affect pavement performance [Williams, 2013], [Halil, 2013], [Pierce, 2014].

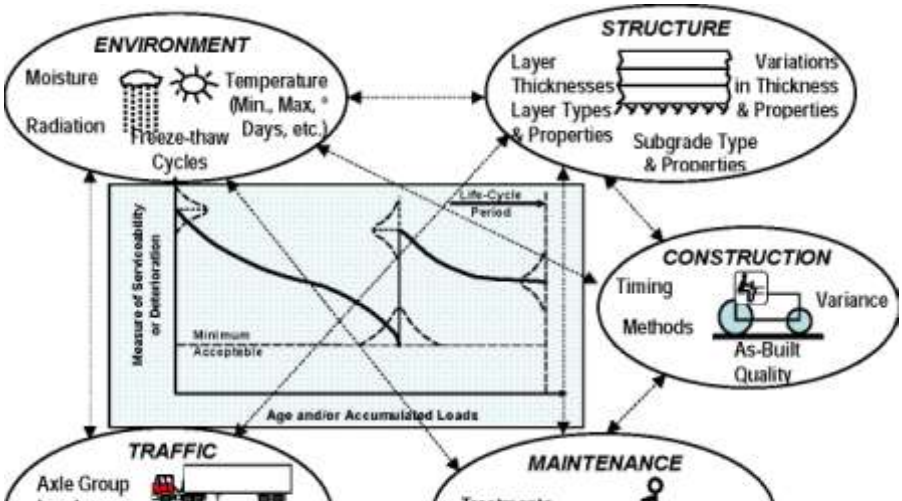

In 2002, the MEPDG was released by the National Cooperative Highway Research Program (NCHRP) as Project 1-37A [NCHRP, 2004a]. Since then, the MEPDG has been investigated by several municipalities and departments of transportation (DOTs) in North America and worldwide [Schwartz, 2007]. DOTs for several states have been involved in examining MEPDG results with respect to local calibration in order to develop MEPDG models that represent the actual structural deterioration in those states [El-Hakim, 2013]. However, a number of technical deficiencies were noted in regard to the accuracy of the transfer functions, specifically in the thermal cracking model [Zborowski, 2007]. In 2011, the second version of the MEPDG was issued under the name of DARWin-ME. It has since become known as AASHTOWare® pavement design software, and its use requires annual fees and licensing. The Transportation Association of Canada (TAC) has established a working group comprised of provincial agencies to explore how the new software can be calibrated and implemented [Tighe, 2012]. AASHTOWare® involved using state-of-the practice tools and methods for enhanced prediction of pavement performance. The enhancement is achieved through the inclusion traffic loading, materials characterization, climate, and construction procedures. AASHTOWare® calculates the mechanistic responses of pavement section as a result of the traffic loading. Prediction of pavement distresses is performed through transfer functions correlating the mechanistic pavement responses to expected distresses over the design period. This pavement design philosophy would enable practitioners to develop a maintenance and rehabilitation program to mitigate the expected distresses. AASHTOWare® was also aimed at improving the pavement design process by offering three levels of performance analysis based on the available data.

2.4.2.1 AASHTOWare® General Design Approach

AASHTOWare® could be used in design of new pavement sections or rehabilitation of in-service pavements, the design tool could be utilized to incorporate a wide range of engineering creativity in design and material selection. It consists of three major stages [Williams, 2013; Jannat, 2012]:

Stage 1 – Development of input values and evaluation

Stage 2 – Structural analysis of trial designs, including performance modeling

Stage3 –Evaluation of viable alternatives, such as engineering analysis and Life Cycle Cost Analysis (LCCA)

2.4.2.2 Levels of Input

AASHTOWare® contains three levels of types of performance analysis [FHWA, 2010] whose use is dependent on the amount of data. Table 2-5 lists the specific data required for running the MEPDG at each level:

Level 1 – The input incorporates detailed mechanistic properties of pavement layers and entails the least amount of uncertainty. This level requires laboratory testing of the materials to be used in the pavement layers.

Level 2 – The input data are less comprehensive than in Level 1 and may be selected from a database, extrapolated from limited testing, or estimated through correlations.

Level 3 – This level represents the lowest degree of accuracy and is usually employed when the results of laboratory or field testing of the materials are unavailable. Local agencies recommend default values for the materials characterization used for this input level. Regardless of which input level (or mixture of input levels) is used, in the MEPDG software, the computational methodology for predicting distress remains the same [NCHRP, 2004b].

Table 2-5: Input Data for Each Level in the MEPDG [FHWA, 2012]

Input Group		Input Variable	How to acquire and measure	Level
Traffic		**AADT and Truck %**	**Calculated from reality**	**All**
Climate		Temperature, participation, wind speed, and humidity	Weather station provided by the MEPDG	All
Material properties	Hot Mix Asphalt	Dynamic modulus	Detailed material testing required	1
			Based on calculations	2
			Available data or typical values	3
		Aggregate gradation	Detailed material testing required	1
			N/A	2
			N/A	3
		Binder content	Detailed material testing required	1
			N/A	2
			Available data or typical values	3
		Air voids	Detailed material testing required	1
			N/A	2
			Available data or typical values	3
		Unit weight	Detailed material testing required	1
			N/A	2
			Available data or typical values	3
		Dynamic modulus	Detailed material testing required	1
			Correlation based on CBR, R-value, a_i, and DCP	2
			Available data or typical values	3
	Unbounded	Dynamic modulus	Detailed material testing required	1
			Correlation based on CBR, R-value, a_i, and DCP	2
			Available data or typical values	3
		California bearing ratio (CBR)	Detailed material testing required	1
			N/A	2
			Available data or typical values	3
		Classification and volumetric Properties	Detailed material testing required	1
			N/A	2
			N/A	3
	All other layers	Unit weight	Detailed material testing required	1
			N/A	2
			Available data or typical values	3
		Poisson's ratio	N/A	1
			N/A	2

			Available data or typical values	3
		Elastic/resilient modulus HMA (surface)	Detailed material testing required	1
			Correlation based on strength	2
			Available data or typical values	3

2.4.2.3 Performance Prediction Equations for Flexible Pavement

This subsection provides a brief description of the MEPDG models used for predicting performance. The equations specify the MEPDG computational steps for calculating distress, as taken from the *Mechanistic-Empirical Pavement Design Guide, a Manual of Practice, Interim Edition* [AASHTO, 2008]. Detailed descriptions of these models and the entire MEPDG design procedure have been presented in several publications, including AASHTO's *MEPDG Manual of Practice* [AASHTO 2008], as well as in MEPDG reports developed as part of NCHRP Projects 1-37A [ARA, 2004] and 1-40D [AASHTO, 2008], [Darter et al. 2007] [Guo, 2013].

The equations were nationally calibrated from field testing using Long-Term Pavement Performance (LTPP) data and indicate which calibration coefficients are required for the local calibration of distress predictions. More information about theses equation can be found in Appendex A.

2.5 Pertinent Studies of Local Calibration of the MEPDG

In a recent *Pavement Management Roadmap* [FHWA, 2011], the Federal Highway Administration (FHWA) initiated discussions about the eventual use of the MEPDG performance models in network-level pavement management. Numerous departments of transportation have been questioning whether either the PMS or the MEPDG will exist in the future. Most agencies and DOTs in the United States and Canada are moving toward the use of the MEPDG within a pavement management context. However, the differences between these two resources make it uncertain how they can be combined to provide technical and economic cost savings. If they are to be combined, then calibration, validation, and amalgamation will be required. Over the past few years, a variety of research studies have been conducted in the United States and Canada with respect to the development of a database for the MEPDG. LTPP data, which contain records about more than 2500 pavement sections across the two countries are under consideration and are believed to be an important source of information because they include detailed distress statistics that will help with model calibration. Currently, an increasing number of United States studies related to the calibration of the MEPDG are based on the use of LTPP data, and a limited number are employing PMS data for the calibration of the MEPDG [FHWA, 2011].

North Carolina study involved an evaluation of local calibration of the MEPDG for flexible pavement design, based on the LTPP data in the DOT. The researchers evaluated the requirements related to input data and how they could be used for calibrating and validating the MEPDG. Two performance models, rutting and alligator cracking, focusing on rutting only as it part of my thesis, were developed using local climate and materials data. This study employed 53 LTPP sections that contained more detailed data, which were used for calibration, as well as non-LTPP data, which were used for validation. One of the findings of this work was that more data sections are needed for calibration and validation. Also discovered during this study were discrepancies between the data collection methods carried out by the North Carolina Department of Transportation (NCDOT) and the LTPP program; those differences affected the calibration, In short, an LTPP experiment collects data in a manner that differs from that employed by the DOT.[Richard, 2007]. Figures 2-9 and 2-10 show the predicted versus the measured values before and after local calibration for rutting, and Table 2.6 shows the local calibration factors for rutting that were recommended as a result of the two approaches that were applied in this study. The calibration coefficients show that the rut depth values predicted by the locally-calibrated model are matching well with the observed rut depth values in LTPP sections.

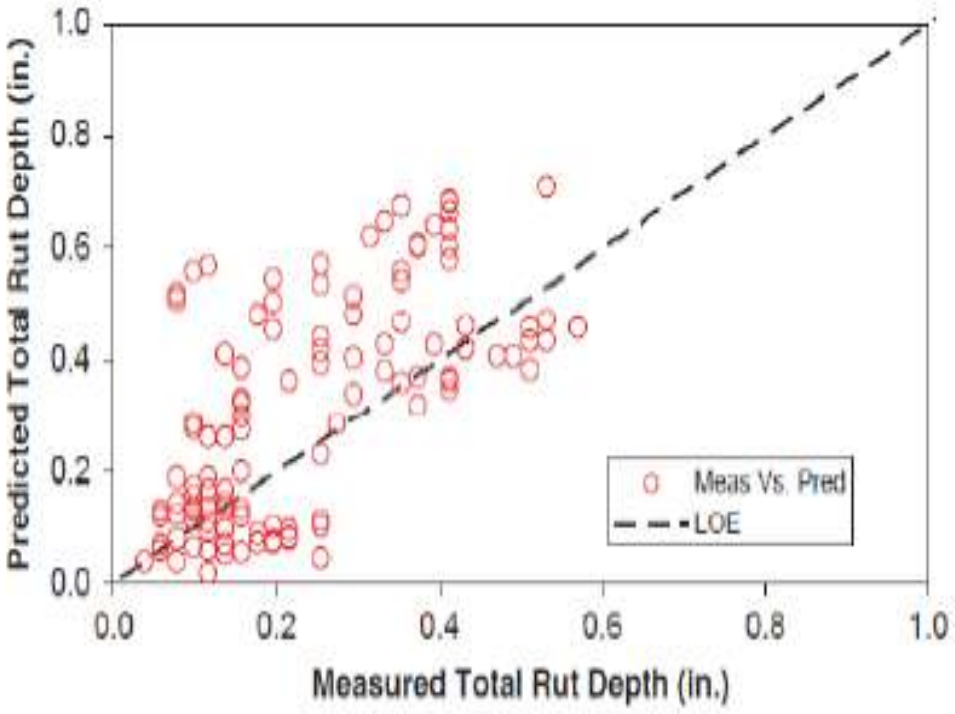

Figure 2-9: Predicted versus Measured Total Rutting Values before Calibration, for the North Carolina Study [Richard, 2007]

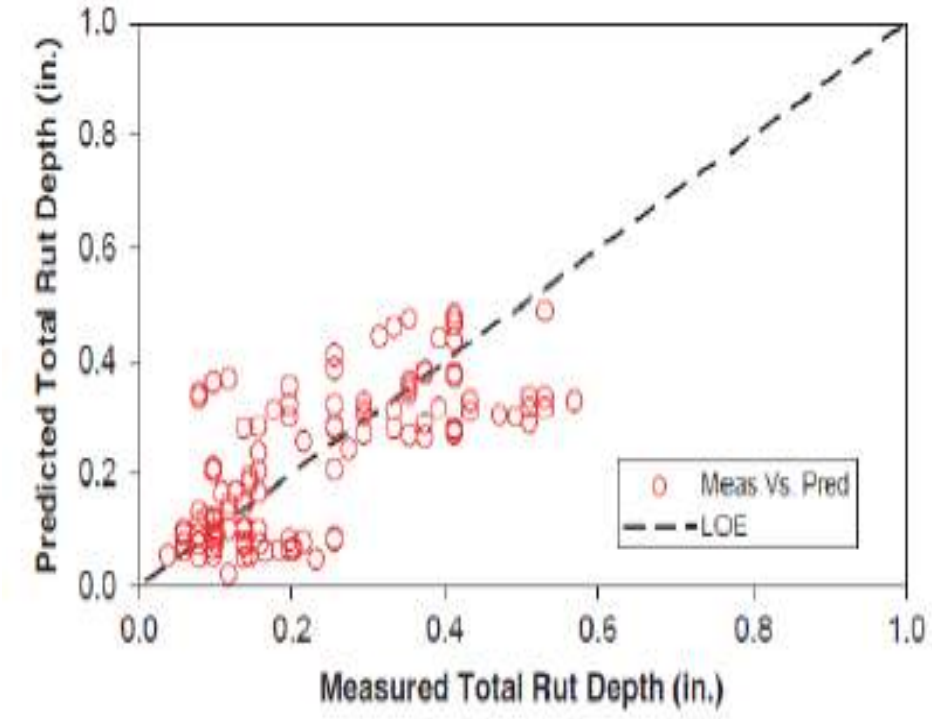

Figure 2-10: Predicted versus Measured Total Rutting Value after Calibration, for the North Carolina Study [Richard, 2007]

Table 2-6: Recommended Local Calibration Factors for NCDOT Prediction Models [Richard, 2007]

Recalibration		Calibration Factors	National Calibration	Local Calibration
Rutting	AC	k_1	-3.4488	-3.41273
		k_2	1.5606	1.5606
		k_3	0.479244	0.479244
	GB	β_{GB}	1.673	1.5803
	SG	β_{SG}	1.35	1.10491

The Utah Department of Transportation (UDOT) published a report about the implementation of the MEPDG in Utah: Validation, Calibration, and Development of the UDOT MEPDG User's Guide. This report assessed asphalt pavement and jointed plain concrete pavement (JPCP). The calibration of the HMA was based on LTPP data projects in Utah and UDOT PMS data. All of the MEDPG models were evaluated except for the HMA total rutting model because previous researchers had concluded that this model was inaccurate. Instead, the local Utah rutting models were calibrated based on experience. The study concluded that further calibration models based on IRI should be developed in the MEPDG, taking into account the impact of pavement design, materials, and construction methods [UDOT, 2009]. Figures 2-11 and 2-12 show the predicted versus measured values for UDOT total rutting before and after calibration. It is obvious that there is poor correlation between measured and AASHTOWare® predicted rutting before calibration. According to the report this was due to data availability in the UDOT PMS database. While after calibration there was reduction in the SSE from before calibration.

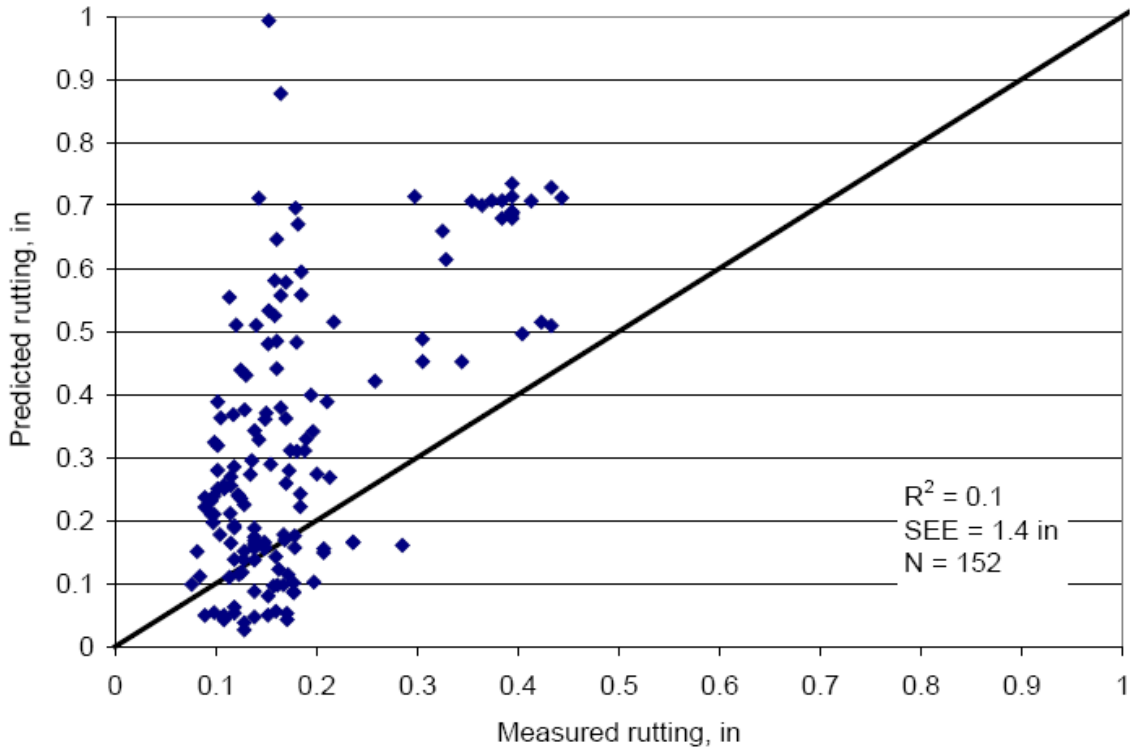

Figure 2-11: Predicted versus Measured Total Rutting Values before Calibration, for the Utah Study [UDOT, 2009]

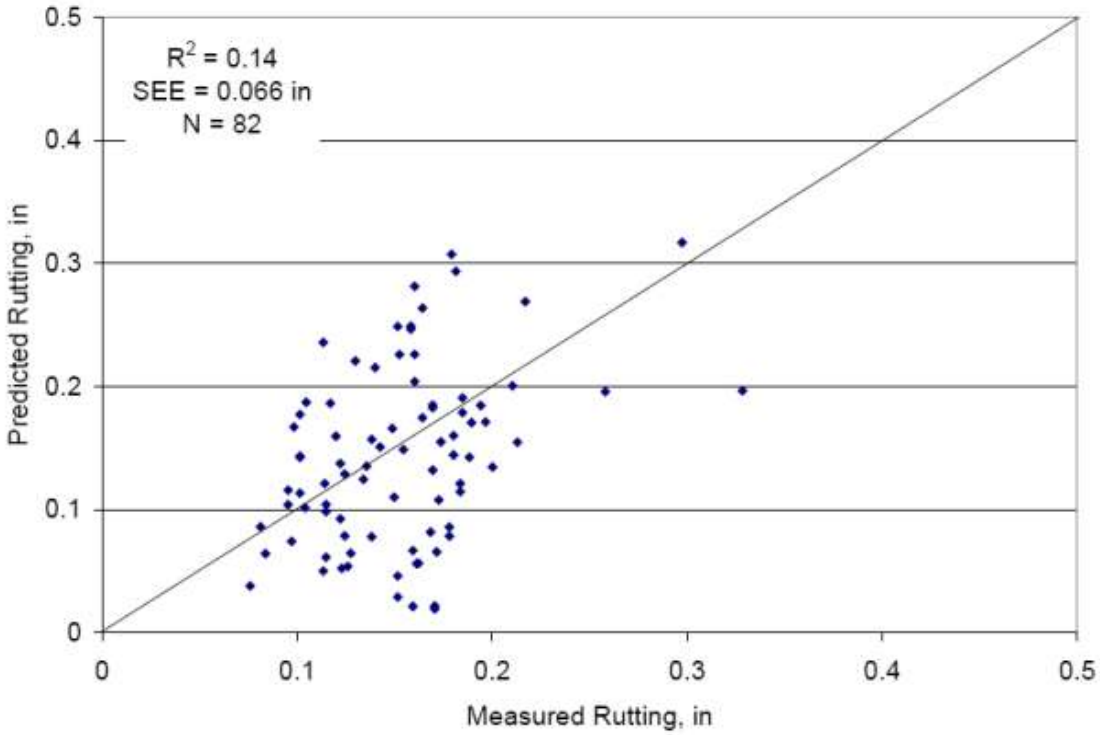

Figure 2-12: Predicted versus Measured Total Rutting Values after Calibration, for the Utah Study [UDOT, 2009]

FHWA produced a technical report about the development of the Texas flexible pavements database. The primary objective of the work presented in this report was to develop guidelines for the local calibration of the MEPDG. The data used in the report were taken from the Texas Flexible Pavement Database (TFPD), which includes data from the LTPP database. The objective was to reduce the sum of squares error between the available and predicted models. The researchers concluded that, to date, no accurate mechanistic models for estimating roughness have been created and that the Texas Department of Transportation must continue their detailed monitoring of rutting, roughness, and cracking so that site-specific models can be developed [FHWA, 2010].

The FHWA technical report provided guidance with respect to performing local calibration of the MEPDG using PMS, which involved eight DOTs. The DOTs were selected according to criteria related to the availability of data, the quality of the data, and the format of the data with respect to suitability for the state's plan to implement the MEPDG. After selection, the states involved employed a framework in order to implement local calibration. They used both LTPP and local PMS

data for both asphalt and concrete pavement sections. Some of the recommendations of this study focused on subjectivity in PMS and LTPP data collection. It was concluded that a substantial data sample is needed in order to develop accurate models; however, the evaluation and analysis of a large number of data will make calibrating the MEPDG a challenge.

Local calibration for Ohio was executed through the collection of relevant input data for the MEPDG, followed by the development of time series data. Statistical analysis was conducted as a means of checking the adequacy of the results predicted from by MEPDG models [Ohio, 2009]. The standard error of the estimate (SSE) was used in order to determine the accuracy of the model. To establish the presence of bias in the model, three statistical t-tests were executed for each model. Models that passed all three tests were considered unbiased. The biased models were deemed unsatisfactory, and recalibration was performed using modified HMA, base, and subgrade coefficients derived from LTPP data [Ohio, 2009]. Figures 2-13and 2-14 displays Ohio's predicted versus measured total rutting values before and after calibration. It is noticed that the same number of sections has been used however the R^2 after calibration is lower, which conclude that local calibration improve the prediction only not the R^2.

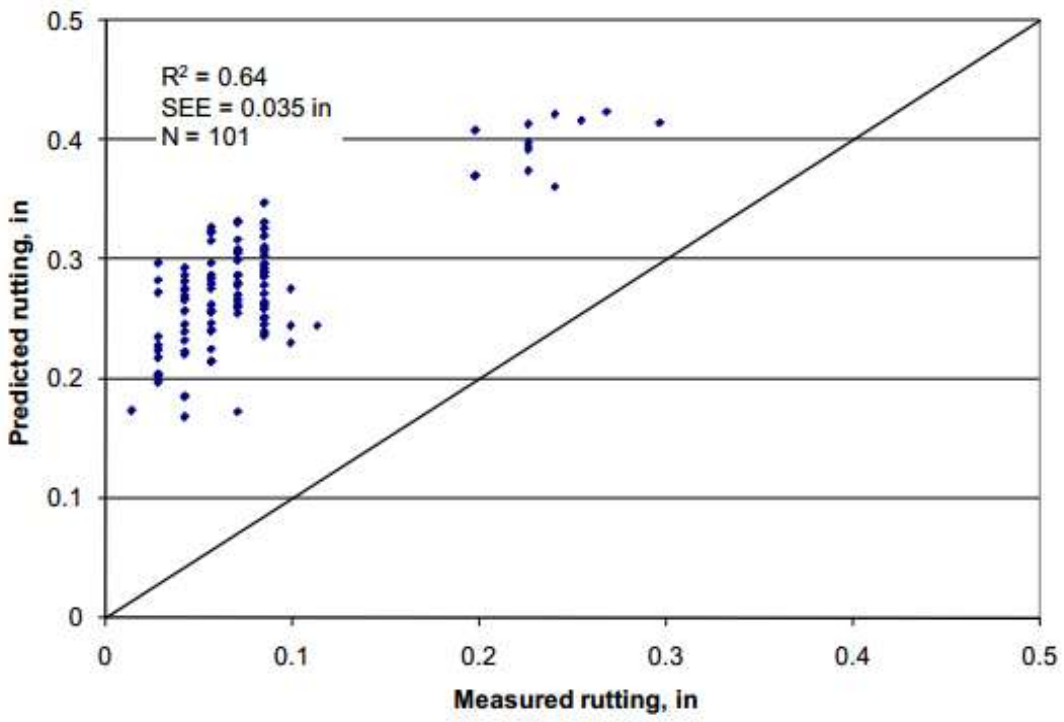

Figure 2-13: Predicted versus Measured Total Rutting Values before Calibration, for the Ohio Study

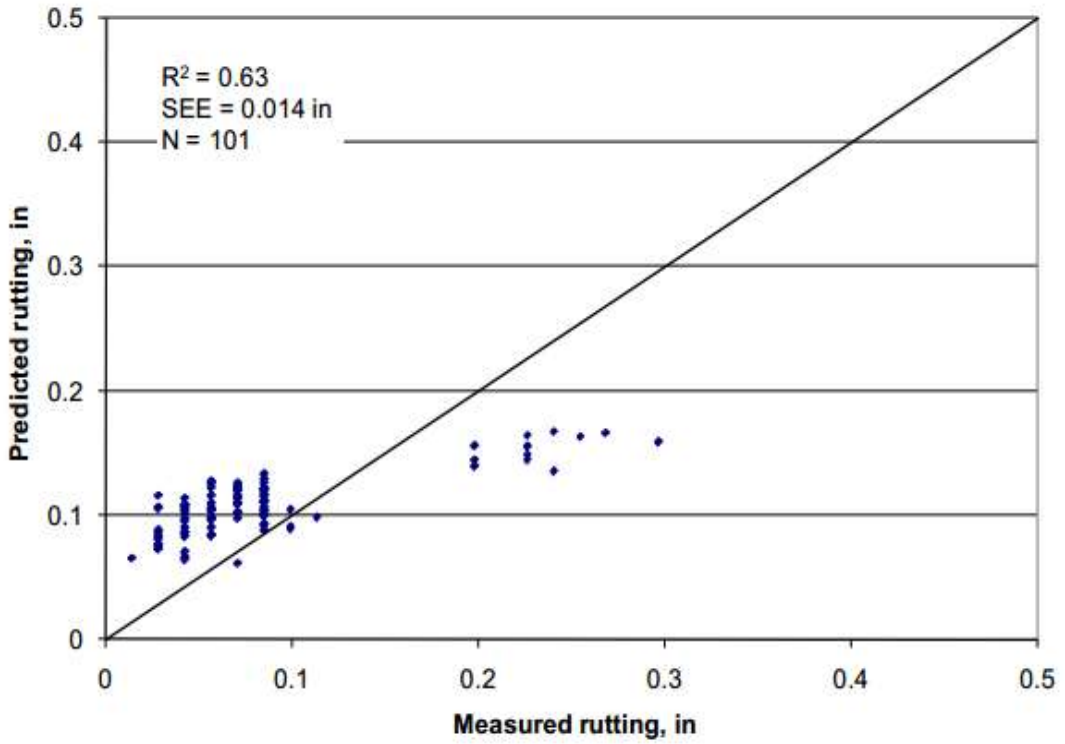

Figure 2-14: Predicted versus Measured Total Rutting Values after Calibration, for the Ohio Study

MnROAD, a pavement test track owned and operated by the Minnesota Department of Transportation, was used for developing MEPDG local calibrations in Minnesota. Rutting measurements were collected from 31 test sections constructed on Highway 94, which represents the main line of MnROAD. MEPDG runs were executed as a means of comparing the simulated and measured rutting depths for these sections. The MEPDG runs used actual traffic input data acquired from traffic sensors installed on site [MNROAD, 2010]. MnROAD research findings proved that the MEPDG overestimate base and subgrade rutting depth. While the analysis of the asphalt concrete (AC) layer data indicated that the rutting model is accurate with respect to predicting actual AC rutting. However, the primary sources of error in the total rutting model were the granular base and subgrade rutting models [MNROAD, 2010].

The Arkansas Highway and Transportation Department used LTPP and PMS data as their two sources of input for performing the initial calibration of flexible pavement models in the MEPDG [Hall, 2011]. This study involved 26 sections, 80 % of which were included in the calibration, with

the remaining 20 % being employed in the validation. All required input such as traffic, climate, and materials data were available; any missing data were replaced with the default values. In the calibration section, for the rutting model, repeated MEPDG runs were used for optimizing the rutting model, with a different coefficient for each run. Because the rutting occurs primarily in the HMA layer and the subbase, the rutting model for the granular base is assumed to be identical. The study concluded that additional calibration sites must be established and the IRI model was not calibrated as it is a function of other predicted distress. LTPP data and the MEPDG define transverse cracking differently, which creates problems with respect to data collection [Hall, 2011]. Figures 2-15 and 2-16 show the predicted versus measured total rutting values before and after calibration for Arkansas. Table 2-7 lists the final rutting local calibration results for this study. Rutting mainly occurs in the HMA layers and subgrade therefore the coefficients of rutting in the subgrade was not changed. And all other coefficients were calibrated.

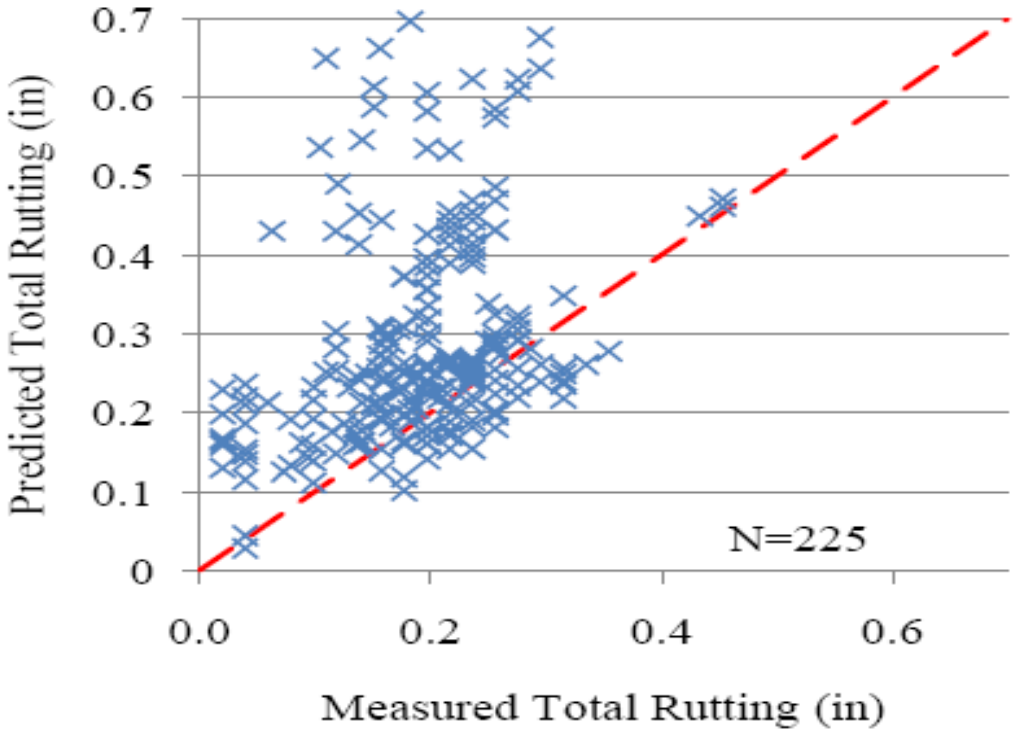

Figure 2-15: Predicted versus Measured Total Rutting Values before Calibration, for the Arkansas Study [Hall, 2011]

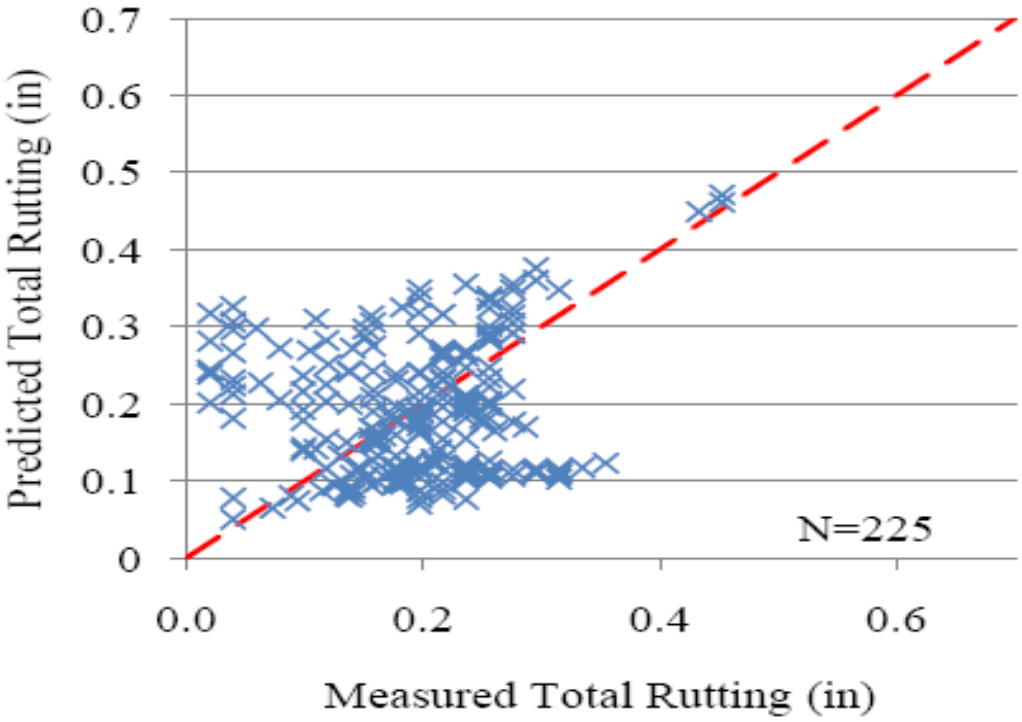

Figure 2-16: Predicted versus Measured Total Rutting Values after Calibration, for the Arkansas Study [Hall, 2011]

Table 2-7: Final Local Calibration Coefficients for the Arkansas Study [Hall, 2011]

Calibration Factor	MEPDG Default	After Local Calibration
AC rutting		
β_{r1}	1	1.20
β_{r2}	1	1
β_{r3}	1	0.80
Base rutting		
β_{s1}	1	1
Subgrade rutting		
β_{s1}	1	0.50

The Iowa Department of Transportation (IDOT) selected 130 sections representing rigid, flexible, and composite pavements. Thirty-five flexible pavements were considered, and the input for running the MEPDG was extracted from the Iowa Pavement Management Information System (PMIS). The calibration was performed for rutting, longitudinal cracking, alligator cracking, and IRI as a means of improving the accuracy of MEPDG pavement performance predictions. Linear and nonlinear statistical models were used for enhancing the accuracy of the model predictions. The study found that global calibration for rutting and longitudinal cracking provides good predictions but that local calibration provides better predictions with less bias and standard error [Halil, 2013]. Figures 2-17 and 2-18 show the predicted versus measured IRI values before and after calibration for Iowa. Table 2-8 indicates the final local calibration results for this study.

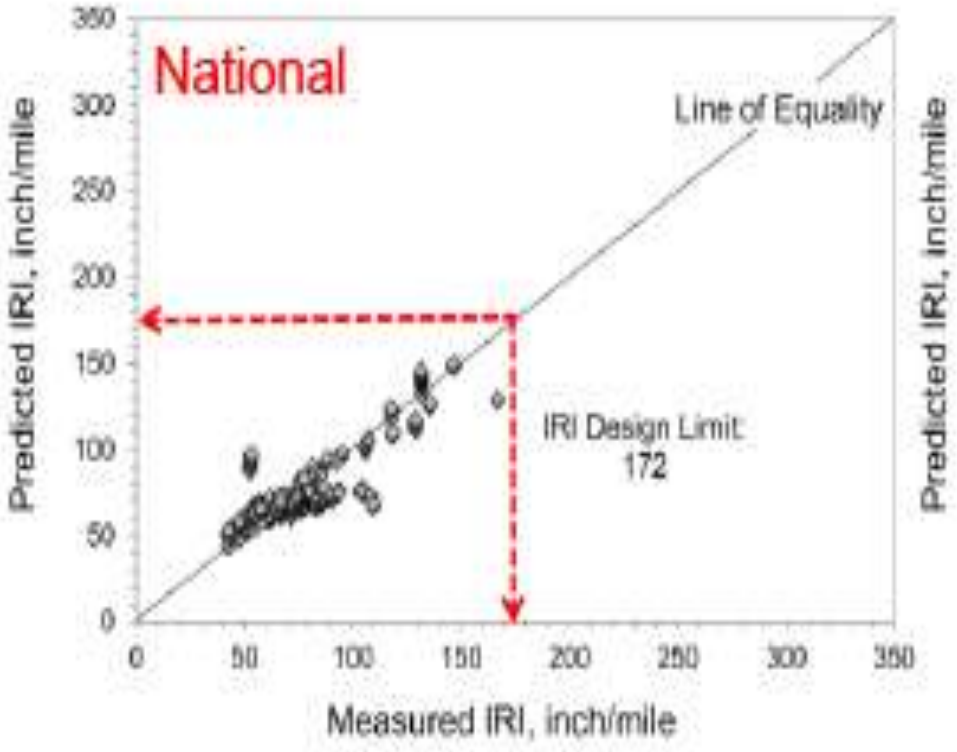

Figure 2-17: Predicted versus Measured IRI Values before Calibration, for the Iowa Study [Halil, 2013]

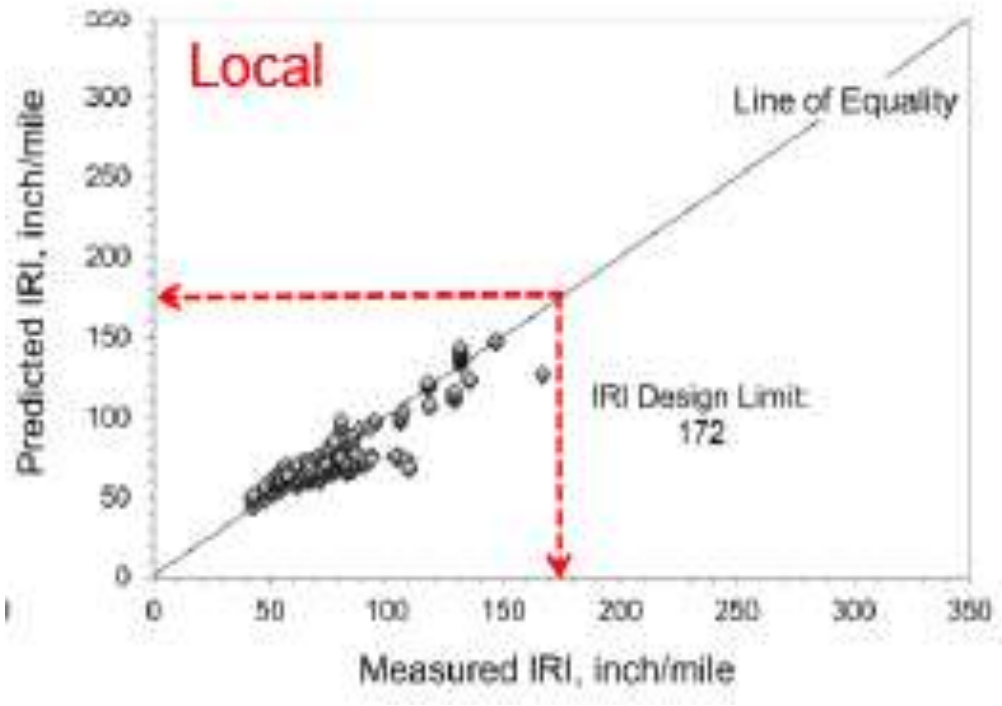

Figure 2-18: Predicted versus Measured IRI Values after Calibration, for the Iowa Study [Halil, 2013]

Table 2-8: Final Local Calibration Coefficients for the Iowa Study [Halil, 2013]

Model	Calibration Factors	National	Local
HMA Rut	β_{r1}	1	1
	β_{r2}	1	1.15
	β_{r3}	1	1
	GB Rut B_1_Granular	1	0
	SG Rut B_1_Fine-grain	1	0
IRI	C_1	40	40
	C_2	0.4	0.4
	C_3	0.008	0.008
	C4	0.015	0.015

In an Arizona study, 39 sections were selected for the local calibration of fatigue cracking, rutting, and IRI. LTPP data were used for the calibration, the goal of which was to reduce the sum of squared errors (SSE) between the predicted values and the observed values through repeated runs

with the MEPDG, using different coefficients for each distress mode [Souliman et al., 2010]. Table 2-9 lists the final local calibration results for this study.

Table 2-9: Calibration Coefficients Produced by the MEPDG Flexible Pavement Distress Models for Arizona Conditions [Souliman et al, 2010]

MEPDG Model	Global Calibration	Local Calibration	Effect on calibration
AC Rutting Model	β_{r1} =1	β_{r1} =3.63	Increased prediction
	β_{r2} =1	β_{r2} =1.1	
	β_{r3} =1	β_{r3} =0.7	
Granular Base Rutting Model	β_{gb} =1	β_{gb} =0.111	Increased prediction
Subgrade Rutting Model	β_{sb} =1	β_{sb} =1.38	Decreased prediction
Roughness Model	C_1 =40	C_1 =1.38	Decreased prediction
	C_2 =0.4	C_2 =5.45	
	C_3 =0.008	C_3 =0.008	
	C_4=0.015	C_4=0.015	

Studies involving eight United States DOTs used state PMS data in order to validate the new MEPDG. The objective of this research was to calibrate the MEPDG using long-term pavement management data. Surveys and questionnaires were distributed to the DOTs as a means of assessing any current or future difficulties the DOTs may face in adopting the MEPDG. The study concluded that databases should be updated and that each state DOT should have a satellite pavement management/pavement design database that includes as-built data with accurate information about traffic, climate, distress, and deflections [Hudson, 2008].

The Washington State Department of Transportation (WSDOT) undertook a project involving local calibration of the MEPDG using split-sample and jackknife testing approaches. In the split-sample approach, half of the selected sections are used for calibration and the other half for validation. In the jackknife approach, each selected section is withheld for prediction measurements; with the other sections being employed for calibration [Li, 2009].The reason for using a combination of the two approaches is to produce stable and accurate predictions with a limited sample size. The MEPDG transverse cracking results matched those measured, as documented in the WSDOT database [Baus, 2010]. The default calibration factors from the transverse cracking model therefore resulted in sufficient accuracy. Other MEPDG models were subsequently calibrated: the fatigue model and the longitudinal cracking and alligator cracking models, followed by the roughness model [Guo, 2013]. The final calibration factors were chosen based on the least root-mean-square error (RMSE) method.

The local calibration process was finalized through model validation with the use of an independent dataset that had not been included in the calibration process [Li, 2009]. Figures 2-19 and 2-20 below show the consistency and the match in the rutting prediction and the data from Washington state PMS in the western and eastern regions respectively. Table 2-10 lists the final local calibration results for this study, that shows that rutting is predicted rutting is almost the same with the measured rutting in Washington PMS while the IRI calibrations coefficients were not provided.

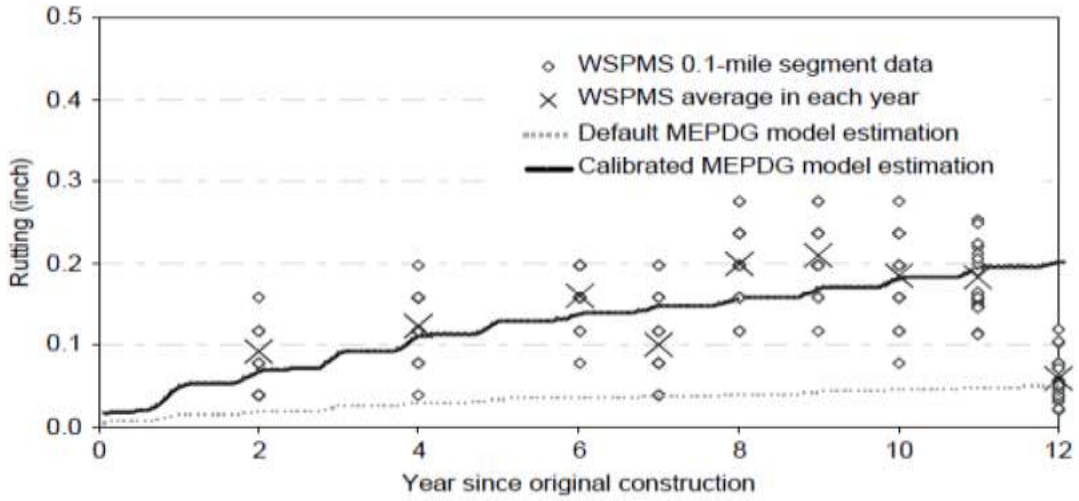

Figure 2-19 : Predicted versus Measured Rutting Values for Western Washington [Li, 2009]

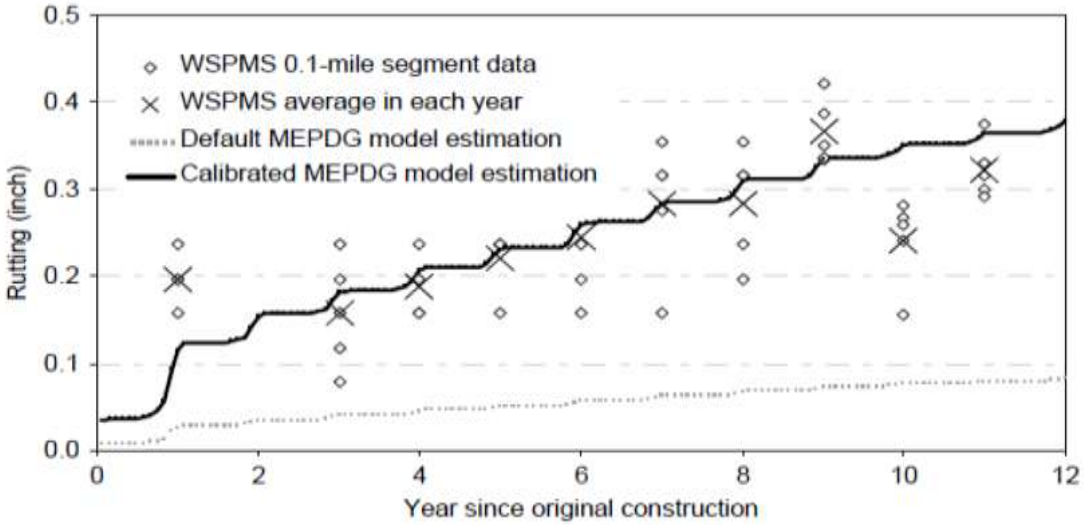

Figure 2-20 : Predicted versus Measured Rutting Values for Eastern Washington [Li, 2009]

Table 2-10: Final Local Calibration Coefficients for the Washington Study [Li, 2009]

Calibration Factor	MEPDG Default	After Local Calibration
AC rutting		
β_{r1}	1	1.05
β_{r2}	1	1.109
β_{r3}	1	1.1
Subgrade rutting		
	1	0
IRI		
C_1	40	N/A
C_2	0.4	N/A
C_3	0.008	N/A
C_4	0.015	N/A

2.6 Summary of Findings

This chapter has provided a review of the literature relevant to the research presented in this thesis. The first section explained the concepts of a variety of basic design methods. The second section introduced the history and goals of the Pavement Management System. The literature review highlighted the investigations performed by multiple municipalities, US DOTs and Canadian Ministries of Transportation to develop locally calibrated AASHTOWare® models. The literature review derived the research motivation of assessment of default AASHTOWare ® model accuracy for Ontario. The evaluation of default model accuracy would lead to determination of the need to develop local calibration coefficients for Ontario or not. The predicted pavement distress using AASHTOWare® would be compared to measured pavement distresses archived in Ontario's PMS. Research is needed on the input parameters related to local calibration of the AASHTOWare® based on the gaps identified in the literature review.

Chapter 3
Data Sources and AASHTOWare® Input

3.1 Introduction

This chapter describes the research data sources that were used in this research. Using data from the MTOPMS2 for a period of 20 years, from 1990 to 2010, two types of data were collected: historical data and survey data. The historical data included equivalent total thickness, subgrade type, climate zone, and pavement type. The survey data included Average Annual Daily Traffic (AADT), Equivalent Single Axle Load (ESAL), International Roughness Index (IRI), Pavement Condition Index (PCI), and Distress Magnification Index (DMI) [Hamdi, 2012]. The data represent a total of 870 pavement sections; however, when sections are broken down into treatment cycles (i.e., pavement preservation and rehabilitation cycles), the result is 17,868 cycles. After a thorough analysis, 870 sections were selected for analysis in this research. Thus, only 10% of the original sections were used in this research. The selected sections were classified in according with pavement type and annual AADT, as summarized in Table 3-1 It should be noted that the total number of sections within each class is 90. These were based on available data but more importantly these 870 section contained high quality and reliable data per MTO. Access to high quality data can be a challenge to this research.

The majority of the available data in the PMS2 is for asphalt pavement because there are relatively few concrete roads, with most having been constructed only during the last ten years. Very few treatment cycles for these roads are thus available for analysis purposes. Although information about surface-treated pavement is included in the database, this type of pavement was removed for the purpose of this research due to the shortage of information.

Table 3-1: Pavement Sections Classififcation

Pavement Type	AADT	Sec
AC	<10,000	39
	>10,000	51
Total		90

3.2 Data Collection

Data for Pavement management use should be reliable, consistent, and of high quality. The quality of the data stems from both frequency of collection and accuracy. Pavement data and information about distress can be collected manually, semi-automated, or using automated methods [TAC, 2013].

To ensure high-quality pavement management system (PMS) data, a three-phase process should be followed. First, before data are collected, each evaluator should be trained and certified, and the equipment calibrated. Second, during the data collection process, environmental conditions should be recorded, and readings for any previous year should be compared to the current data to ensure that no major changes have occurred. The third phase involves an evaluation of data quality and accuracy by reviewing current previous year data [Gonzalo, 2009].

Manual data collection includes a visual distress survey and is a subjective collection method. Evaluators are trained and certified either by their own organization or by an external agency. Although measurements vary from person to person, they have been found to be reliable in the past. Field distress forms or electronic devices can be used for conducting the surveys. Each type of pavement distress is recorded in terms of density and severity, and the results are then incorporated into the PCI calculation. The roughness value is also measured subjectively.

Semi-automated data collection involves a process of capturing pavement images with the use of a camera or video recorder, mounted on a van that drives over the pavement. During the drive, a trained evaluator in the vehicle also records his or her evaluation. The type, density, and severity of the distress are recorded, but in this case, manual and automated measurements are combined to yield a semi-automated evaluation [FHWA, 2006].

Automated data collection is similar to semi-automated; however, a portion of the semi-automated task is completed automatically by distress-detection software. The longitudinal profile of a section can also be measured automatically using lasers and other devices mounted on the vehicles. To evaluate the road user's ride quality, the vertical displacement between the vehicle and the road is measured by means of noncontact sensors [Tighe, 2008, NCHRP, 2004].

Overall, automated data collection results in superior consistency of distress measurements and also offers safety benefits because evaluators are not required to leave their vehicles, which is especially relevant on busy roads. For their network-level PMS, most transportation agencies are moving away from the manual method toward automated data collection. However, it should be noted

that at the project level, manual surveys can be a very important element in the design and construction of future preservation and rehabilitation treatments [Tighe, 2008, Chamorro, 2010].

3.3 Collection of Performance Data

Pavement performance refers to the assessment of two aspects of pavement condition: for structural condition and road condition. Structural condition, as indicated by pavement distress, is assessed visually and subjectively by MTO's highly trained pavement engineers. Road condition, the functional serviceability of the pavement, denotes the amount of contact or friction between the pavement surface and the vehicles for different climate conditions. It is designated as ride quality, or roughness, and skid resistance, or safety. At present, MTO uses fully automated data collection equipment for almost all types of pavement distress, including roughness (IRI), cracking-related surface distress (longitudinal, transverse, and alligator cracks), and wheel path rutting, and employs GPS and video imaging of right-of-way and geometric road information and conditions. However, past performance data used in the research were collected by manual and semi-automated methods. The next subsections provide a brief description of the MTO data collection methods used for obtaining the data acquired over the 20-year period examined: from 1990 to 2010 [Tighe, 2014].

3.3.1 IRI

Since its introduction in 1986, the IRI has become the most common pavement performance index used in almost all PMSs in the world. The IRI value of a pavement section provides information about its riding serviceability level and vehicle operating costs [Ningyuan, 2013]. The IRI values used in the MTO PMS are calculated from a longitudinal profile measured along a road, which reflects pavement ride quality. While the version of IRI used in Ontario has an open-ended scale, it typically ranges from 0 (m/km) to 4 (m/km), with zero implying an absolutely perfect road.

3.3.2 Rutting

The MTO computes pavement rutting using the Automatic Road Analyzer (ARAN) vehicle, which has a computer-controlled roadway data-collection system that takes measurements at 100 m intervals and summarizes the data at each 100 m interval. To measure pavement ruts at highway speed, the ARAN uses 4000 points of laser to collect rut depth and lateral profile information. Rutting directly affects public safety and driving comfort, as many research suggested wet weather in with the present of rutting can affect the vehicle skid resistance [Fwa,T.,2012]. The IRI and longitudinal profile are

measured at the same time the rutting data are collected [Ningyuan, 2004]. Figure 3-1 is a photograph of an ARAN Automatic Road Analyzer.

Figure 3-1: ARAN Automatic Road Analyzer (www.epc.com.hk)

3.4 AASHTOWare® Input

The following subsections include a brief description of the input from PMS2 required for the local calibration of AASHTOWare® for Ontario. Information about design life, traffic, climate, pavement structural layers, materials properties, and asphalt binders is important to calibrate the coefficients. The AASHTOWare® input is divided into two groups: design parameters, which indicate parameters that are dependent on project specifications, and default values, which denote input that is available, assumed, or derived from the default values in AASHTOWare®. As mentioned in Chapter 2, AASHTOWare® allows the user to choose the level at which the analysis will be run [Velasquez, 2009]. Figure 3-2 provides a visual representation of the required AASHTOWare® input, and the

following section gives more detailed information about the input values. More input data can be found in appendix A

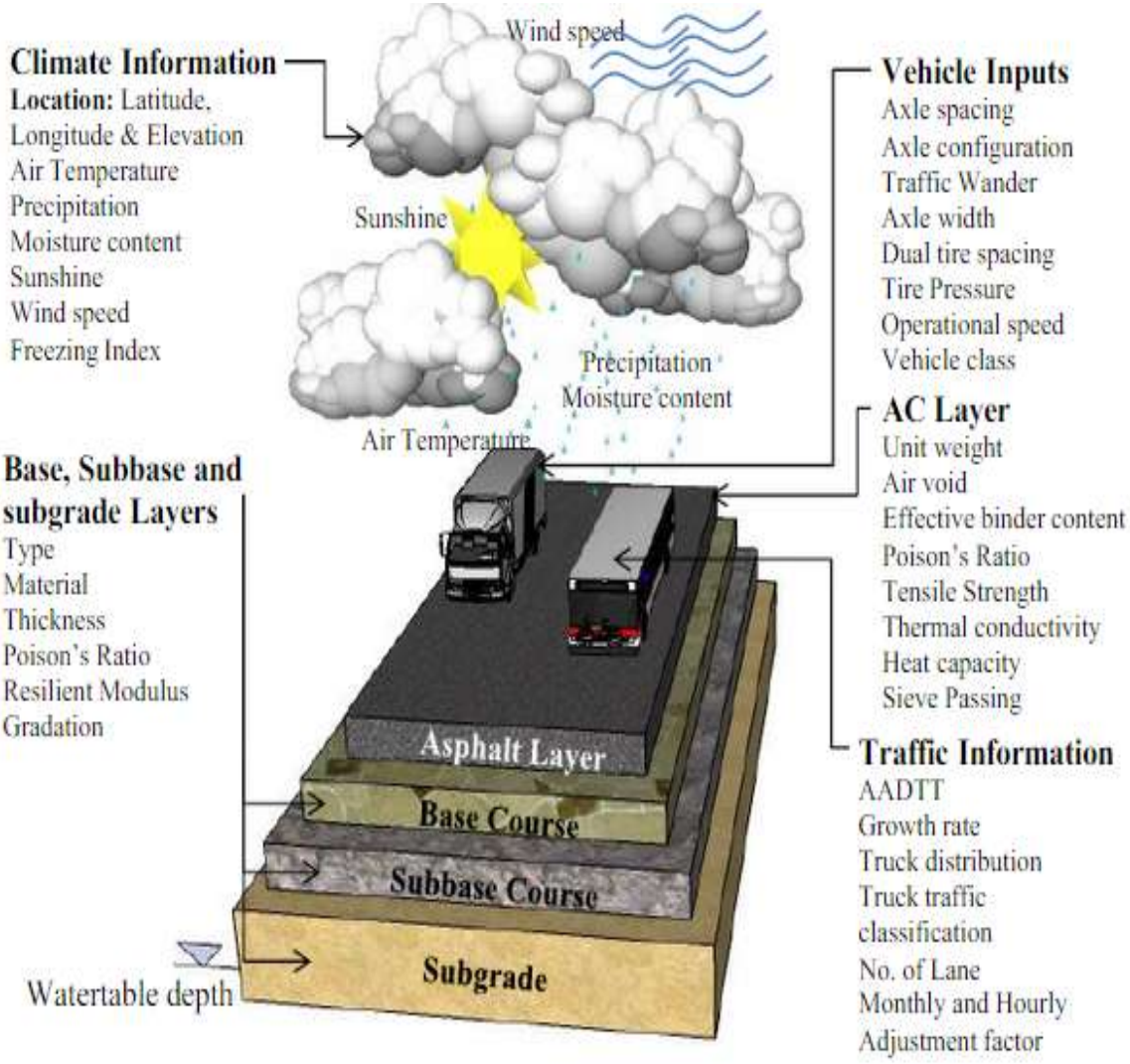

Figure 3-2: Illustration of Basic AASHTOWare® Input [Waseem, 2013]

3.4.1 General Site Information

General information about a pavement section includes highway name, a clear description of the start and end stations of the location, direction of the traffic flow, design type, pavement type, design life, base construction, pavement construction, and date of opening for traffic. Figure 3-3 shows sample input screen for providing general information.

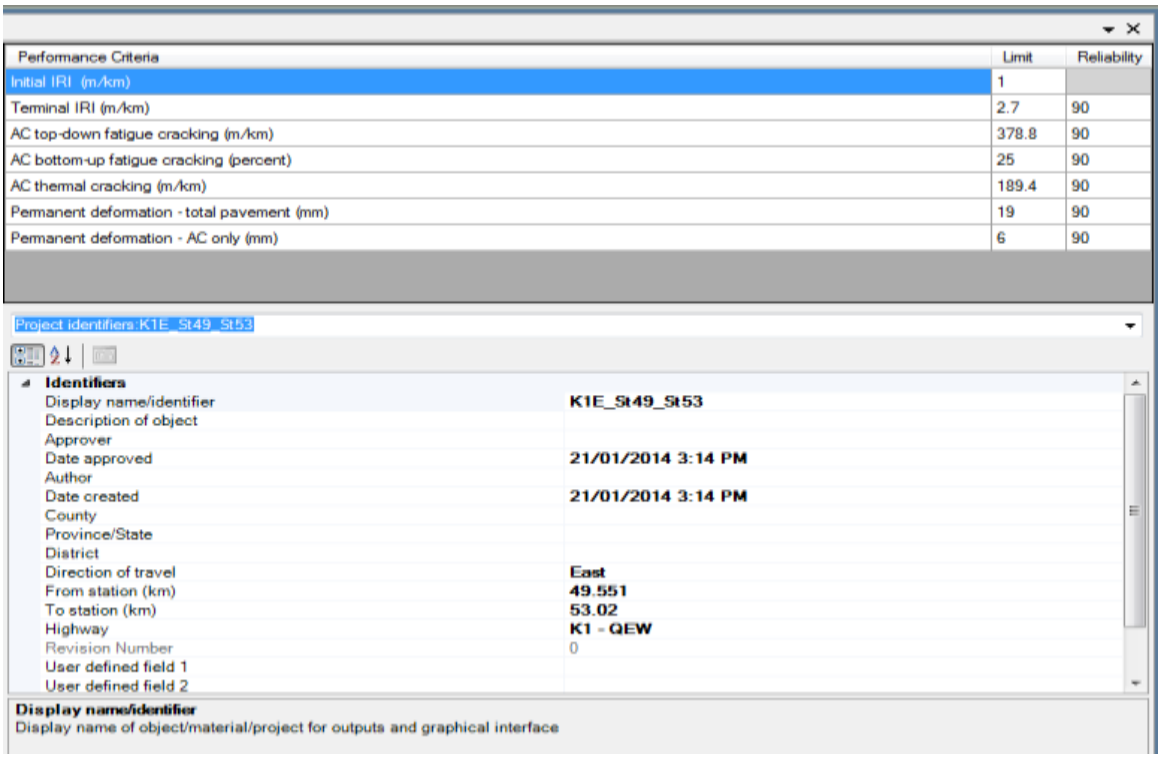

Figure 3-3: AASHTOWare® General Information Screen

3.4.2 Traffic Information

AASHTOWare® uses axle load spectra, a histogram, or the distribution of axle loads for a specific axle type (single, tandem, tridem, quad), in other words, the number of axle applications within a specific axle load range [Manual of Practice for the ME Pavement Design Guide, 2007].

For this research, traffic information was entered based on all three levels of accuracy. Table 3-2 summarizes which input level has been used for each type of traffic input, along with its corresponding value. Traffic input includes traffic volume adjustment factors, axle load distribution factors, and general traffic input. The Average Annual Daily Truck Traffic (AADTT) quantity is used as the primary traffic input rather than the Equivalent Single Axle Load (ESAL) value. Figure 3-4 shows a sample input screen for entering traffic information. Additional input, such as geometric factors, truck traffic classification, traffic growth factor, monthly adjustment factor, hourly distribution, and axle load distribution, are entered based on availability in PMS2 and according to Ontario's Default Parameters for AASHTOWare Pavement ME Design [MTO, 2012], which was

prepared by the MTO to provide information missing from PMS2. The values used are listed in Tables 3-3 to 3-6.

Table 3-2: Summary of Traffic Input Levels Used in This Research

Input Level	Input	Input value
1	Two-way AADT and Percentage of Trucks	Site-specific values are used.
	Number of Lanes	Site-specific values are used.
	Traffic Wander Standard Deviation	Site-specific values are used.
	Traffic Growth Factor	Site-specific values are used.
2	Percentage of Trucks in Design Lane	Table 3.3 shows the Ontario AADT standard value for percentage of trucks in design lane.
	Directional Speed	Table 3.5 shows the Ontario standard speed for different highway classes.
	Average Axle Width	Ontario standard value 2.6 m
	Dual Tire Spacing	Ontario standard value 300 mm
	Tire Pressure	Ontario standard value 830 kPa
	Tandem Axle Spacing	Ontario standard value 1.45m
	Tridem Axle Spacing	Ontario standard value 1.68m
	Quad Axle Spacing	Ontario standard value 1.32m
	Mean Wheel Location	Ontario standard value 460 mm
	Traffic Wander Standard Deviation	Ontario standard value 254 mm
	Average Spacing for Short Axles	Ontario standard value is 5.1 m
	Average Spacing for Medium Axles	Ontario standard value is 4.6 m
	Average Spacing for Long Axles	Ontario standard value is 4.7 m
	Percentage of Trucks with Short Axles	Ontario standard value is 33
	Percentage of Trucks with Medium Axles	Ontario standard value is 33
	Percentage of Trucks with Long Axles	Ontario standard value is 34
	Truck Traffic Classification	Table 3.4 shows the vehicle classification from FWHA.
	Axles per Truck	Tables 3.5 and 3.6 show the Ontario axles-per-truck values
	Axle Distribution	Two different load spectra are used for Northern and Southern Ontario.
3	Monthly Adjustment Factor and Hourly Distribution	Software default value is used.

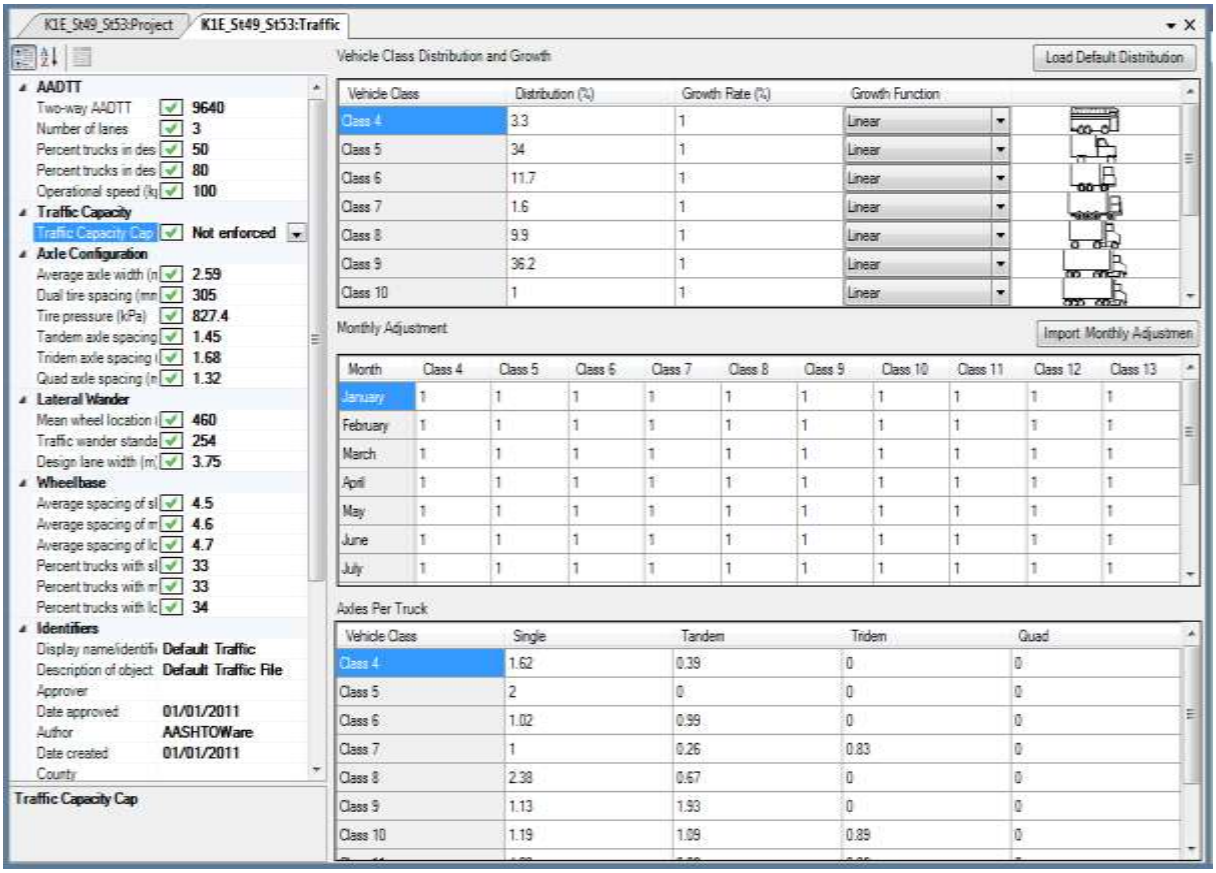

Figure 3-4: AASHTOWare® Traffic Input Screen

Table 3-3: Recommended Percentage of Trucks in the Design Lane for Ontario [MTO, 2012]

Number of Lanes in One Direction	AADT (both directions)	Percentage of Trucks in Design Lane (%)
1	All	100
2	<15,000 >15,000	90 80
3	<25,000 25,000 to 40,000 >40,000	80 70 60
4	<40,000 >40,000	70 60
5	<50,000 >50,000	60 60

Table 3-4: FWHA System of Vehicle Classification (Source: www.fhwa.dot.gov)

Vehicle Class	Vehicle Type	Description
Class 4	Buses	All vehicles manufactured as traditional passenger-carrying buses with two axles and six tires or three or more axles
Class 5	Two-Axle, Six-Tire, Single-Unit Trucks	All vehicles on a single frame, including trucks, camping and recreational vehicles, motor homes, etc., with two axles and dual rear wheels
Class 6	Three-Axle Single-Unit Trucks	All vehicles on a single frame, including trucks, camping recreational vehicles, motor homes, etc., with three axles
Class 7	Single-Unit Trucks with Four or More Axles	All trucks on a single frame with four or more axles
Class 8	Single-Trailer Trucks with Four or Fewer Axles	All vehicles with four or fewer axles consisting of two units, one of which is a tractor or straight truck power unit
Class 9	Five-Axle Single-Trailer Trucks	All five-axle vehicles consisting of a tractor or straight truck power unit
Class 10	Single-Trailer Trucks with Six or More Axles	All vehicles with six or more axles consisting of two units, one of which is a tractor or straight truck power unit
Class 11	Multi-Trailer Trucks with Five or Fewer Axles	All vehicles with five or fewer axles consisting of three or more units, one of which is a tractor or straight truck power unit
Class 12	Six-Axle Multi-Trailer Trucks	All six-axle vehicles consisting of three or more units, one of which is a tractor or straight truck power unit
Class 13	Multi-Trailer Trucks with Seven or More Axles	All vehicles with seven or more axles consisting of three or more units, one of which is a tractor or straight truck power unit

Table 3-5: Typical Axles-per-Truck Table for Southern Ontario [MTO, 2012]

Class	Single	Tandem	Tridem	Quad	Total
Class 4	1.62	0.39	0	0	2.4
Class 5	2	0	0	0	2
Class 6	1.001	1	0	0	2.996
Class 7	1.783	1.056	0.036	0	3.382
Class 8	2.171	0.842	0	0	3.853
Class 9	1.128	1.932	0.003	0	5
Class 10	2.087	1.459	0.465	0.032	6.366
Class 11	4.589	0.185	0	0	4.882
Class 12	3.336	1.332	0.06	0	5.909
Class 13	1.536	2.038	0.797	0.004	7.957

Table 3-6: Typical Axles-Per-Truck Table for Northern Ontario [MTO, 2012]

Class	Singles	Tandems	Tridems	Quads	Total
4	1.62	0.39	0	0	2.4
5	2	0	0	0	2
6	1.014	0.993	0	0	3
7	1.244	0.962	0.043	0	3.297
8	2.414	0.674	0	0	3.762
9	1.048	1.955	0.014	0	5
10	1.358	1.165	0.84	0.044	6.384
11	3.849	0.538	0	0	4.925
12	2.91	1.514	0.021	0	6.001
13	1.1	2.012	0.945	0.011	8.003

3.4.3 Climate Data

The AASHTOWare® software contains a climate database, which provides historical hourly data such as temperature, rainfall, wind speed, and humidity from numerous weather stations across the United States and Canada. A site location form is used for entering site information, and then a Google map is employed for identifying the longitude and latitude. This information is input into the software as a means of simplifying the multitude of climate input data. A linear interpolation within the software produces an estimate of the climate details for the selected zone, such as precipitation and air temperature. The AASHTOWare® software can then simulate temperature and moisture profiles in the pavement structure and subgrade over the design life of a pavement based on the longitude, latitude (level 1 input accuracy), elevation, and depth of the water table (Level 2 input accuracy, from Ontario Standard 6.1 m). Figure 3-5 shows a sample climate input screen.

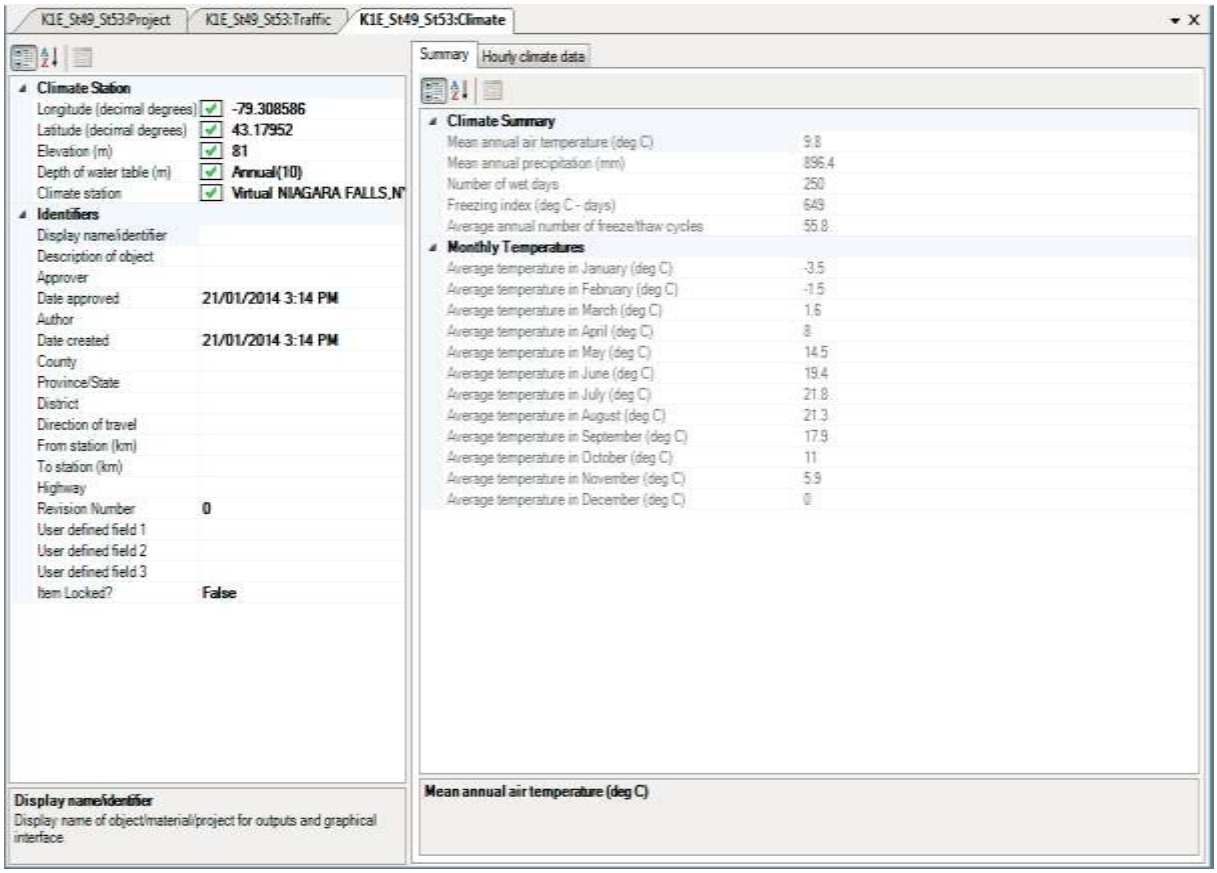

Figure 3-5: AASHTOWare® Climate Data Input Screen

3.4.4 Structural Layers and Material Properties of the Pavement

In AASHTOWare®, one required input for the mechanistic analysis of pavement responses is materials properties of the pavement layers. The input includes the dynamic modulus of the asphalt mixtures, the rheological properties of the asphalt binder, creep compliance and indirect tensile strength, and the mix properties. Figures 3-6 and 3-7 show sample input screens for materials properties. For this study, only flexible pavement is considered; therefore, any of the following surface layers are considered to be asphalt concrete (AC) layers: hot mix asphalt (HMA), dense graded asphalt, open graded asphalt, asphalt stabilized base mixes, sand asphalt mixtures, stone matrix asphalt (SMA), cold mix asphalt, central plant processed, and cold in-place recycling. Tables 3-7 and 3-8 indicate the properties of typical Ontario pavements.

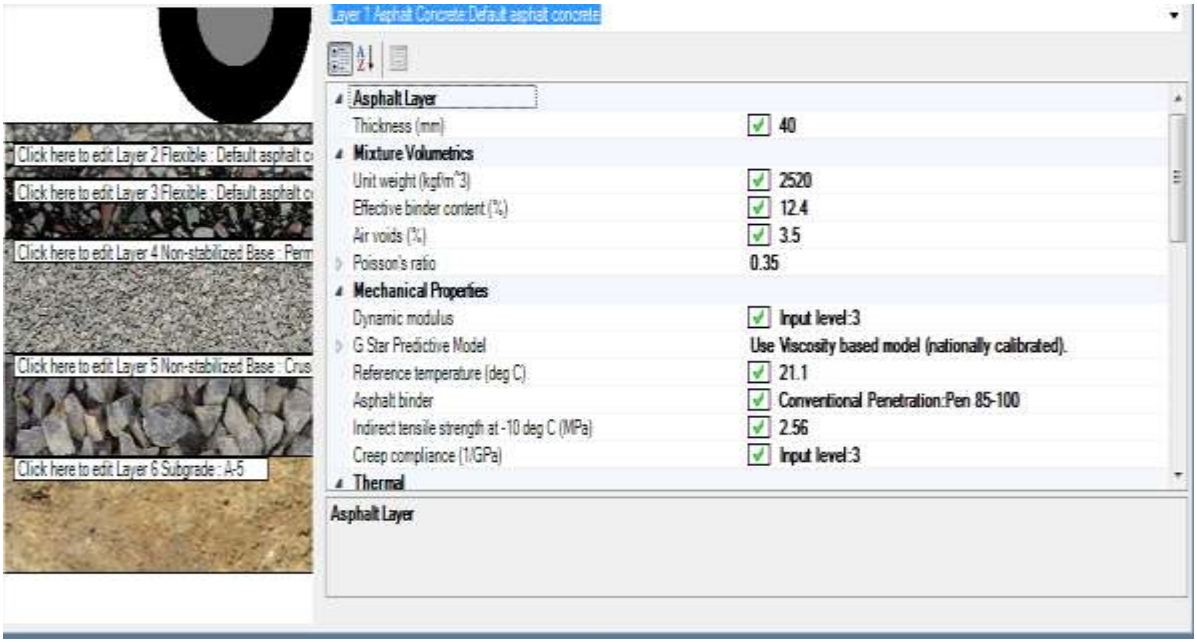

Figure 3-6: AASHTOWare® Asphalt Layer Input Screen

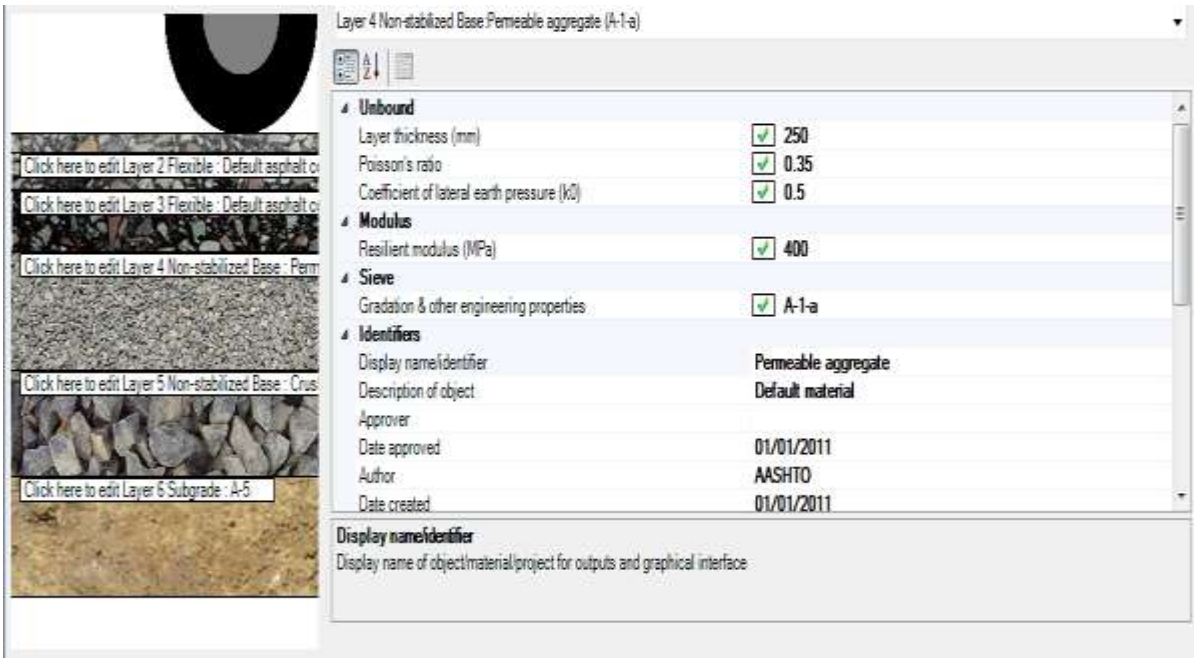

Figure 3-7: AASHTOWare® Base Material Input Screen

Table 3-7: Ontario Typical Superpave and SMA Asphalt Concrete Properties [MTO, 2012]

Asphalt Layers		**SP 12.5**	**SP 19.0**	**SP 25.0**	**SMA 12.5**
Thickness (mm)		Project specific			
Mixture Volumetric					
Unit Weight (kg/m3)		See Note 1	2460	2469	See Note 1
Effective Binder Content - by Volume (%)		11.8	11.2	10.4	14.6
Air Voids (%)[2]		4.0			
Poisson's Ratio[3]		0.35			
Mechanical Properties					
Dynamic Modulus		"Input level: 3" selected			
Aggregate Gradation	% Passing the 19 mm Sieve	100 %	96.9 %	89.1 %	100.0 %
	% Passing the 9.5 mm Sieve	83.2 %	72.5 %	63.3 %	73.1 %
	% Passing the 4.75 mm Sieve	54 %	52.8 %	49.3 %	29.7 %
	% Passing the 75 µm Sieve	4 %	3.9 %	3.8 %	9.3 %
G Star Predictive Model		"Use viscosity based model (nationally calibrated)" selected			
Reference Temperature		21.1 ºC			
Asphalt Binder[4]		PG 64-28	PG 58-28	PG 58-28	PG 70-28
Indirect Tensile Strength – 10 °C (MPa)		Calculated			
Creep Compliance (1/GPa)		"Input level: 3" selected			
Thermal					
Thermal Conductivity (watt/meter-Kelvin)		1.16			
Heat Capacity (joule/kg-Kelvin)		963			
Thermal Contraction		Calculated			

Note 1: For SP 12.5, the unit weight is 2,460 kg/m3. For SP 12.5 FC1, FC2 and SMA 12.5, unit weight varies from different regions: Central and North regions – 2,520 kg/m3; East region – 2,390 kg/m3; West region – 2,530 kg/m3

Note 2: For existing HMA layers, measured in situ air voids should be used.

Note 3: For new HMA mixtures, the calculated Poisson's ratio is used by expanding the row on 'Poisson's ratio' and setting to 'true.' For the row on 'Is Poisson's Ratio calculated?' refer to MEPDG Table 11-3 for other reference temperatures and open-graded HMA Poisson ratios.

Note 4: PGAC varies based on locations and traffic loading conditions. Refer to MTO Superpave Guide to select the proper PGAC grade.

Table 3-8: Typical Marshall Mix Properties for Ontario [MTO, 2012]

Asphalt Layers		DFC	HDBC	MDBC	HL1	HL2	HL3	HL4	HL6	HL8
Thickness (mm)		Project specific								
Mixture Volumetric										
Unit Weight (kg/m3)		2520	2460	2500	2520	2410	2520	2480	2460	2460
Effective Binder Content - by Volume (%)		12.4	10.9	12.3	12.4	14.2	12.4	12.2	10.9	10.9
Air Voids (%) [1]		3.5	4	4	4	5	4	4	4	4
Poisson's Ratio		0.35								
Mechanical Properties										
Dynamic Modulus		Calculated								
Aggregate Gradation	% Passing the 19 mm Sieve	100	97	97	100	100	100	100	97	97
	% Passing the 9.5 mm Sieve	82.5	63	63	82.5	100	82.5	72	72	63
	% Passing the 4.75 mm Sieve	52.5	43.5	40	55	92.5	55	53.5	53.5	42.5
	% Passing the 75 μm Sieve	2.5	3	3	2.5	5.5	2.5	3	3	3
G Star Predictive Model		"Use viscosity based model (nationally calibrated)" selected								
Reference Temperature		21.1 ºC								
Asphalt Binder		Penetration Grade[2]								
Indirect Tensile Strength – 10 °C (MPa)		Calculated								
Creep Compliance (1/GPa)		"Input level: 3" selected								
Thermal										
Thermal Conductivity (watt/meter-Kelvin)		1.16								
Heat Capacity (joule/kg-Kelvin)		963								
Thermal Contraction		Calculated								

Note 1: For existing HMA layers measured in situ air voids should be used.
Note 2: For Southern Ontario, pen. grade 85-100 is used; for NE Ontario, pen. grade 120-150; for NW Ontario, pen. grade 200-300.

3.5 Summary of Findings

This chapter has described the data collection methods and data sources have been used in this research. Ontario's default Values were used in the setup process of the software. Ontario Traffic information replaced the build in traffic information. This chapter, a detailed explanation on inputs parameters required to run the AASHTOWare® is defined and described. Understanding the data and the input levels were key elements in this research and have been presented. The details provided in this chapter may benefit other researchers who wish to locally calibrate AASHTOWare®. Sample of AASHTOWare® report can be found in appendix B.

Chapter 4

Methodology, Results and Discussion

4.1 Introduction

The literature review revealed that two approaches are commonly used in the field to conduct calibration in general : iteration, which involves calibrating prediction models by varying the calibration coefficients, and adjustment, which entails direct modifications to the results the model predictions through the subtraction of a specified constant value from the prediction results produced by the nationally calibrated models [Li., 2009] [Muthadi, 2008] [Schram & Abdelrahman, 2010] [Banerjee et al., 2009] [Hoegh et al., 2010]. The availability of the data for this research enabled the calibration of one distress and one performance measure rutting and IRI respectively. In ASSHTOWare®, distress is predicted by means of a mechanistic model. The first step was sites selection based on data availability followed by preparation inputs and outputs files and then run AASHTOWare® using the default calibration coefficients to predict rutting and IRI and then to examine the accuracy of the predicted values by comparing them with the observed values from the PMS2. The predictions were plotted against the measurements on the line of equality, and the average bias and standard error values were also calculated and compared. Insignificant correlation between predicted and measured distresses indicated a need for the local calibration of ASSHTOWare®. The calibration was performed by adjusting the calibration coefficients so that the bias and the RMSE between the predicted and measured distress values would be reduced. The precision of the data points and the variations from their average were represented based on standard error. Prediction accuracy was evaluated based on the root-mean-square error (RMSE). A minimum RMSE result denotes a maximum accuracy. The p-value, the smallest level of significance at which the null hypothesis will be rejected, [Donnelly, 2007] was also used for rejecting the null hypothesis: H_0: $\mu_o \neq \mu_{p.}$

4.1.1 Pavement Section Selection

Data quantity and quality were the key elements that influenced the selection of pavement sites for this research. Sections included in the local calibration process should include sufficient traffic data, basic pavement material identification and documented rutting and IRI records. AASHTOWare® can

be used at three different levels of accuracy based on data availability. The visual method of collecting pavement distress data, which is consistent with MTO practice, is subjective, and the ratings differ from one person to another even if both have had the same training at the same time. Recording data into the PMS can be affected by issues related to data accuracy and human error. At least ten years of distress data were available for the selected sections.

4.1.2 Preparation of the Input and Output

Data extraction is a critical step in successful calibration and validation work. For this research, Excel spreadsheets that included all of the required AASHTOWare® input were merged with data available from PMS2 and *Ontario's Default Parameters for AASHTOWare® Design Interim Report*. Intensive effort was required in order to find and merge the input data, which include traffic, structural, materials, and climate information. Performance data were considered to be the output. A project template was generated as a default section, and the template file was updated for each new section so that it included all of the required input, such as the climate, traffic, and materials details.

4.1.3 Calibration Examination

After section selection and data file preparation, the next step was to determine whether calibration is required. Running the software with the default calibration coefficient gives a clear idea of the need for calibration based on the calculation of the root-mean-square error (RMSE) as set out in equation (4.1). The RMSE, also called the root-mean-square deviation (RMSD), is used in statistics as a measure of the difference between the values predicted by a model and the values observed in the field, which provides an indication of the accuracy of the model. The RMSE was therefore employed in this research for measuring the difference between the predicted and observed distress values. A low RMSE indicates that the AASHTOWare® prediction values are close to the observed values, with no need for calibration, and a high RMSE signifies the opposite result.

$$RMSE = \sqrt{\frac{\sum (f(x_i) - y_i)^2}{n}} \tag{4.1}$$

where

RMSE = root-mean-square error
$f(X)$ = predicted AASHTOWare® output
y_i = measured distress according to PMS2

n = number of data points

4.1.4 Calibration

The next step was to establish the Ontario calibration coefficients for the sites selected. For this research, 78 sections were considered in the calibration process, representing 85 % [AASHTO, 2010] of the sections available for the study. The alterations to the default coefficient followed a specific trend: changes were made to one coefficient in each model at a time. The model outcome was compared to the measured IRI or rutting documented in the PMS2 for the identical year. RMSE was calculated as presented in equation 4.1 to determine the accuracy of model including modified calibration coefficient. Iterations of coefficient changes were performed to determine the minimum RMSE.

For example, the rutting model includes three coefficients where ($\beta 1r = \beta 2r = \beta 3r = 1$) as default values. During the first trial, $\beta 1r$ was changed to $\beta 1r = 0.8$. The other two coefficients ($\beta 2r$, $\beta 3r$) were fixed as 1 in this iteration. The predicted rutting was compared to PMS2 rutting in order to calculate the RMSE. Reduction in RMSE indicates increase in model accuracy. Further modifications on the $\beta 1r$ are applied in subsequent iterations until reaching the minimum RMSE. The subsequent iterations would examine the ability of other coefficients to further reduce the RMSE. The final calibration results –presented at the end of this chapter- represent the combination of calibration coefficients that produced the minimum RMSEs for rutting, and IRI models.

4.1.5 Validation

Validation is an important component of the acceptance of model accuracy. Model validation is the process of determining whether the model produces an accurate prediction compared to real-world data. If the proposed calibration coefficients can be validated, they can be adopted by the MTO. For the validation process, the remaining 15% [AASHTO, 2010] of the sections, which were not used for calibration, were employed for validation purposes. AASHTOWare® was used to predict the distresses in the calibration sections. The RMSE is calculated to examine the model accuracy. Statistical t-test was performed as well to compare the predicted and measured distresses. The null hypothesis examined was "the predicted values and measured values were not significantly different". T-test was performed assuming significance level (α) of 0.05. The P-value is used in this study as a means of determining whether the null hypothesis can be accepted based on the following guideline:

- If the p-value $\leq \alpha$, then reject the null hypothesis.
- If the p-value > α , then accept the null hypothesis.

A statistical conclusion or decision about the calibration of the prediction model can be determined from the results of the p-value, bias, and RMSE.

4.2 Calibration Results

In this research, calibration coefficients were obtained for the three data categories: low traffic volume (AADT < 10,000), high traffic volume (AADT => 10,000), and overall network.

4.2.1 Low Traffic Volume Calibration

Rutting

All pavement sections that have an Average Annual Daily Traffic (AADT) value less than 10,000 were included in the Low volume category. A total of 24 pavement sections were examined for the calibration, which translated into 204 data points. Figure 4-1 shows that the predictions obtained with the default calibration coefficients overestimate the rutting depth for the low traffic volume category.

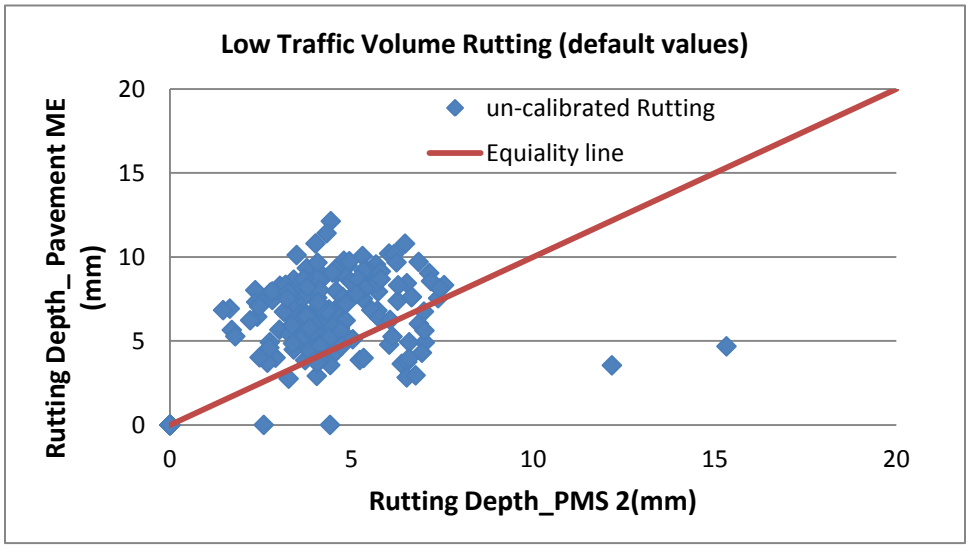

Figure 4-1: Uncalibrated Rutting for Low Traffic Volume Category

After the calibration had been performed and the default calibration coefficients had been changed several times, the locally calibrated model predicted lower rutting depth values. Figure 4-2 shows the low traffic volume rutting results obtained with the locally calibrated coefficients.

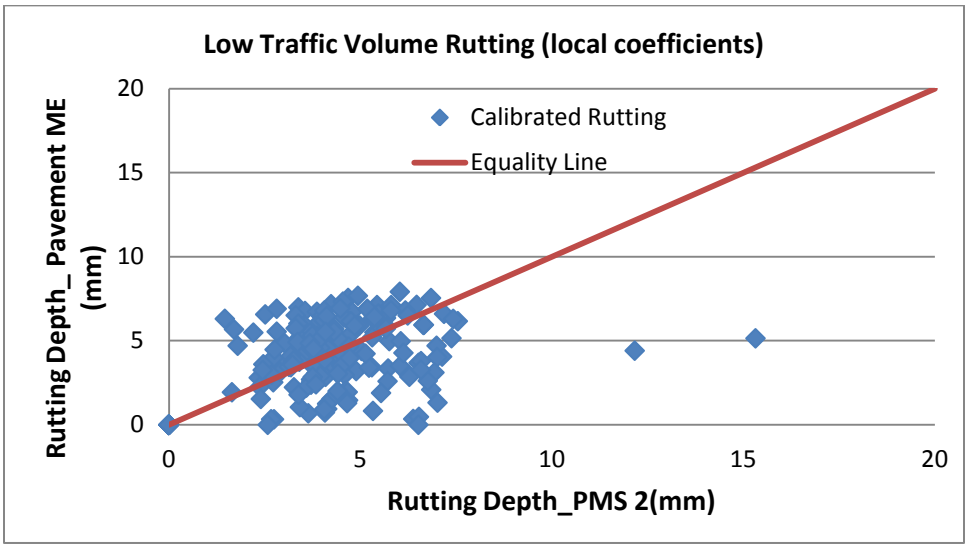

Figure 4-2: Calibrated Rutting for Low Traffic Volume Category

The local calibration based on the PMS2 data reduced the RMSE of the rutting model for low traffic volume category. Table 4-1 summarizes the statistical analysis for low traffic volume rutting prediction, the RMSE was reduced by 30% and the variance was reduced by 21%, after the local calibration. The Student's *t*-test indicates insignificant difference between the AASHTOWare® rutting predictions and the measured rutting, after performing the local calibration. Table 4-2 presents the local calibration coefficients for the low traffic volume rutting predictions.

Table 4-1: Statistical Analysis for Rutting in Low Traffic Volume Roads

	Default Values	Local Calibration	Reduction in Error
Standard error	0.199	0.154	-21.67
RMSE	3.179	2.200	-30.47
N	204	204	
p-value	6.46E-23 =0	0.1874 > 0.05(∝)	

Table 4-2: Local Calibration Coefficients for Rutting Model in Low Traffic Volume Roads

Distress	Coefficients	Default Values	Local Calibration
Rutting	β_1	1	1
	β_2	1	0.6
	β_3	1	0.6

IRI

Pavement sections with AADT below 10,000 were included in the low traffic volume category. A total of 31 pavement sections were used in the calibration which included 361 data points. Figure 4-3 shows the relation between predicted IRI using default AASHTOWare® model and measured IRI in low traffic volume road category. No correlation between the predicted IRI and the measured IRI was observed during the analysis of the default AASHTOWare® model.

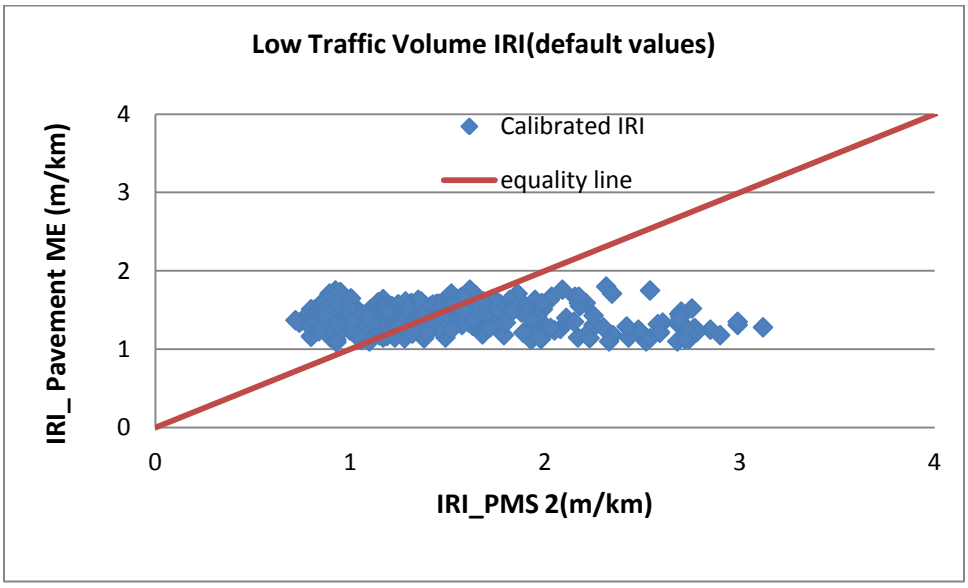

Figure 4-3: Uncalibrated IRI for Low Traffic Volume Category

Several attempts were performed to develop a correlation between predicted and measured IRI through calibration iterations. The attempts to develop a statistically significant correlation were not

successful. Figure 4-4 shows the relation between predicted and measure IRI for low traffic volume road category the generated the least RMSE.

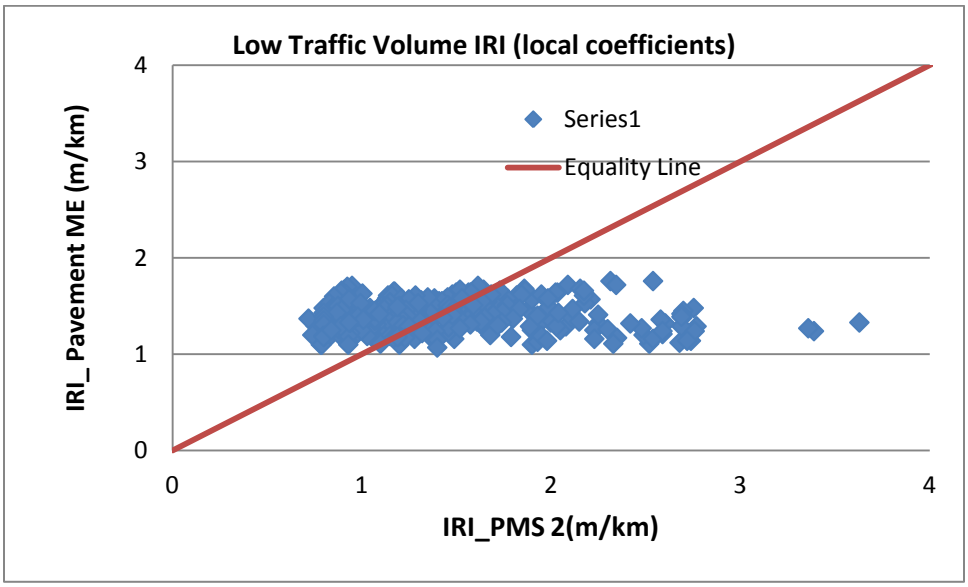

Figure 4-4: Calibrated IRI for Low Traffic Volume Category

Insignificant reduction in RMSE was observed as a result of calibration iterations. Table 4-3 presents the RMSE and P-value comparing the default model with the model associated with minimum RMSE determined during the calibration iterations.

Table 4-3: Statistical Analysis of IRI Model for Low Traffic Volume Roads

	Default Values	Local Calibration	Reduction in Error
Standard error	0.00799	0.007881	-1.425
RMSE	0.5660	0.5392	-4.722
N	361	361	
p-value	0.3790 > 0.05(∝)	0.802 > 0.05(∝)	

4.2.2 High Traffic Volume Calibration

Rutting

Pavement sections characterized with AADT exceeding 10,000 are classified as high traffic volume roads. A total of 39 pavement sections were used in the calibration which included 343 data points. Figure 4-5 shows that prediction using default calibration coefficients is over estimating the rutting depth for high traffic volume category.

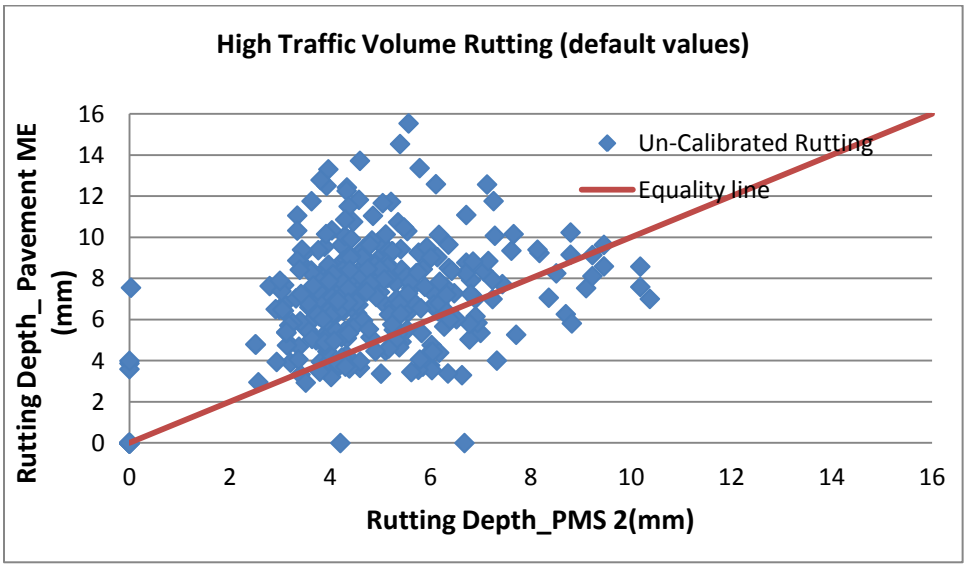

Figure 4-5: Uncalibrated Rutting for High Traffic Volume Category

The local calibration iterations were performed to reduce the RMSE. Figure 4-6 presents the predicted high traffic volume rutting associated with the minimum RMSE versus measured rutting depth for high traffic volume roads.

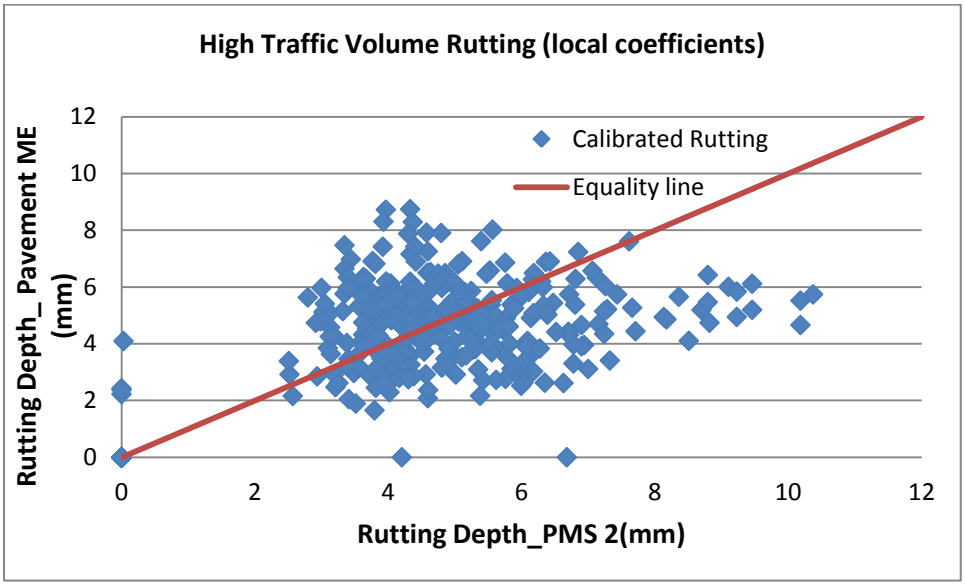

Figure 4-6: Calibrated Rutting for High Traffic Volume Category

The local calibration using the PMS2 data reduced the RMSE of the rutting model for the high traffic volume category. Table 4-4 summarizes the statistical analysis for high traffic volume rutting prediction, the RMSE was reduced by 43% and the variance was reduced by 37%, after the local calibration iterations. The Student's *t*-test concludes insignificant difference between calibrated AASHTOWare® rutting prediction and the measured rutting. Table 4-5 presents the local calibration coefficients for the high volume roads rutting predictions.

Table 4-4: Statistical Analysis for High Traffic Volume Rutting Predictions

	Default Values	Local Calibration	Reduction in Error
Standard error	0.17	0.11	-36.98
RMSE	3.297	1.862	-43.53
N	343	343	
P-value	7.55E-39 =0	0.0667 > 0.05(∝)	

Table 4-5: Local Calibration Coefficients for the High Traffic Volume Rutting Predictions

Distress	Coefficients	Default Values	Local Calibration
Rutting	β_1	1	1
	β_2	1	0.7
	β_3	1	1

IRI

Attempts to perform local calibration of IRI model were unsuccessful for high traffic volume roads. No correlation was identified between measured and predicted IRI using the default AASHTOWare® model.

4.2.3 Overall Network Calibration

Rutting

A dataset was developed including highways with various AADTs including low and high traffic volume roads. A total of 66 pavement sections were used in the calibration of the overall network calibration which included 589 data points. Figure 4-7 presents the measured and predicted rutting depths using default AASHTOWare® model for the entire network.

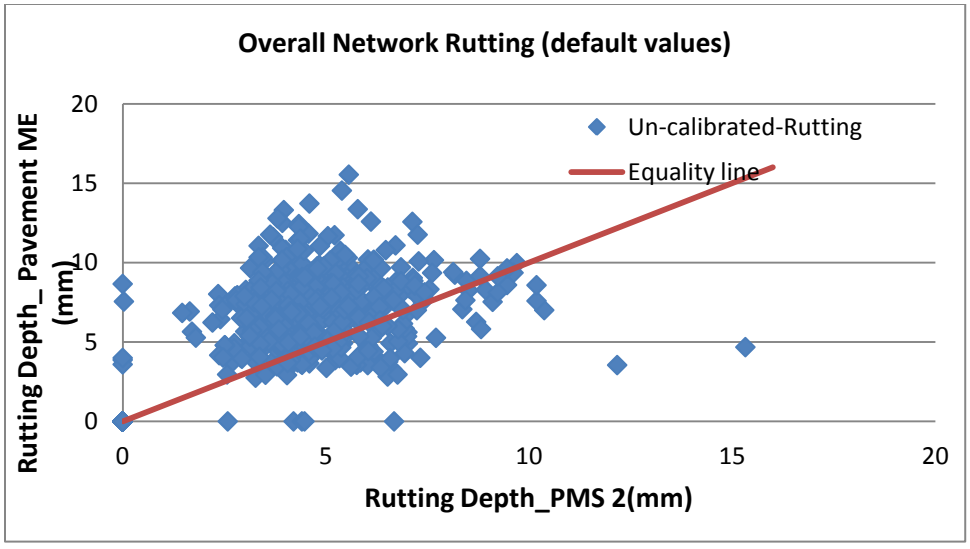

Figure 4-7: Uncalibrated Rutting for Overall Network

Local calibration iterations were performed to reduce the RMSE for the entire network. The comparison between measured and predicted rutting depth using AASHTOWare® model is presented in Figure 4-8.

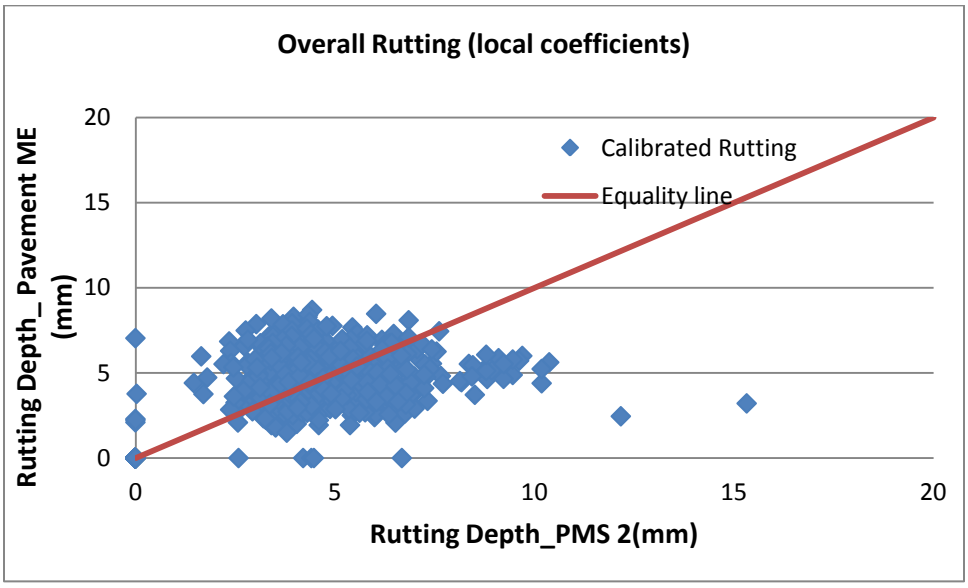

Figure 4-8: Calibrated Rutting for Overall Network

The local calibration using the PMS2 data reduced the RMSE of the rutting model for the overall network. Table 4-6 summarizes the statistical analysis for high traffic volume rutting prediction, the RMSE was reduced by 37% and the variance was reduced by 33%, after the local calibration. No significant difference is identified between AASHTOWare® rutting predictions after calibration and measured rutting. Table 4-7 presents the local calibration coefficients for the overall network rutting predictions.

Table 4-6:Statistical Analysis for Overall Network Rutting Predictions

	Default Values	Local Calibration	Reduction in Error
Standard error	0.126	0.084	-33.10
RMSE	0.422	0.370	-37.48
N	589	589	
p-value	1.21957E-64 =0	0.716 > 0.05(∝)	

Table 4-7: Local Calibration Coefficients for the Overall Network Rutting Predictions

Distress	Coefficients	Default Values	Local Calibration
Rutting	β_1	1	0.7
	β_2	1	0.6
	β_3	1	1

IRI

No correlation was identified between measured and predicted IRI using the default AASHTOWare® model. Attempts to develop a significant enhancement on the IRI model were not successful for the entire network.

4.3 Calibration Summary:

MTO PMS2 data were used in this study to perform Ontario local calibration. The AASHTOWare® default values showed that there is a significant difference in the means between predict and observed values for both distress, rutting and IRI. For the rutting model, by changing to the local calibration coefficients there was significant improvement in the prediction, lower RMSE and there was no significant difference in the means between the two values. For the IRI model, no correlation was observed between the measured and predicted IRI. Attempts to develop a significant improvement in the IRI model accuracy were not successful. Table 4-8 presents the locally calibrated coefficients for the rutting model in low traffic volume roads, high traffic volume roads and the entire network classes.

Table 4-8 : Summary of Ontario Local Calibration Coefficients

Distress Model	Coefficients	Default Value	Low Traffic Volume	High Traffic Volume	Overall Network
Rutting	β_{f1}	1	1	1	0.7
	β_{f2}	1	0.6	0.7	0.6
	β_{f3}	1	0.6	1	1

4.4 Validation Results

The validation was conducted using the remaining 15 % [AASHTO, 2010] sections that were not used in the calibration process. The validation for each category was performed using local calibration coefficients. In terms of the rutting model, the validation indicated that the local calibration did greatly improve the accuracy of rutting prediction. In addition, the IRI model was validated to have no remarkable improvement on the prediction accuracy after the adoption of local calibration for the rutting model.

4.4.1 Low Traffic Volume Validation

Using the calibrated coefficients found from this research from the prediction process, on validation sections in low traffic volume category for the rutting validation, these sections provide the results, as shown in Figure 4-9.

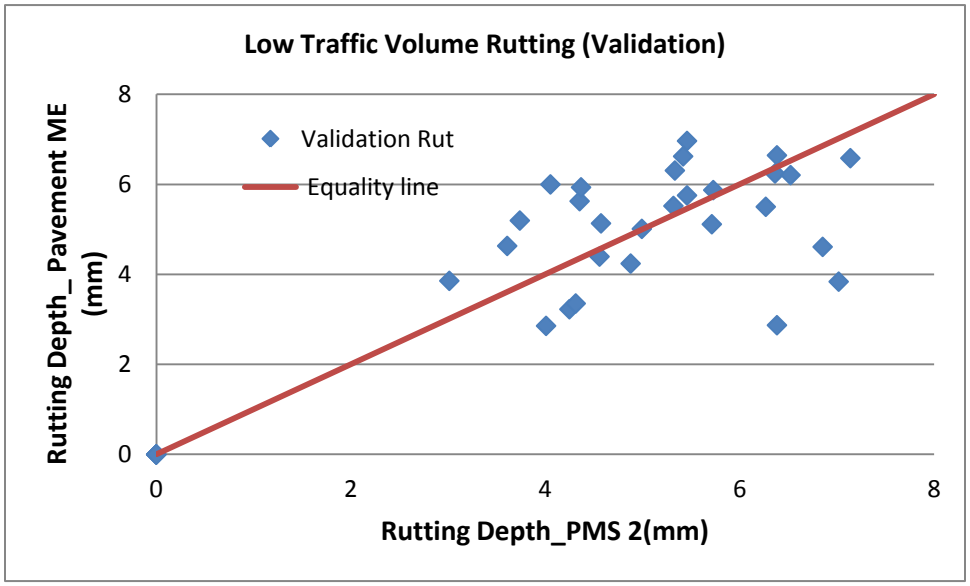

Figure 4-9: Rutting Validation of Low Traffic Volume Category

The p = 0.786> ∝, providing evidence that the predicted values shows no significant difference in the means with the measured values for rutting of low traffic volume category.

4.4.2 High Traffic Volume Validation

Using the calibrated coefficients found from this research from the prediction process, on validation sections in high traffic volume category for the rutting validation, these sections provide the results,, as shown in Figure 4-10.

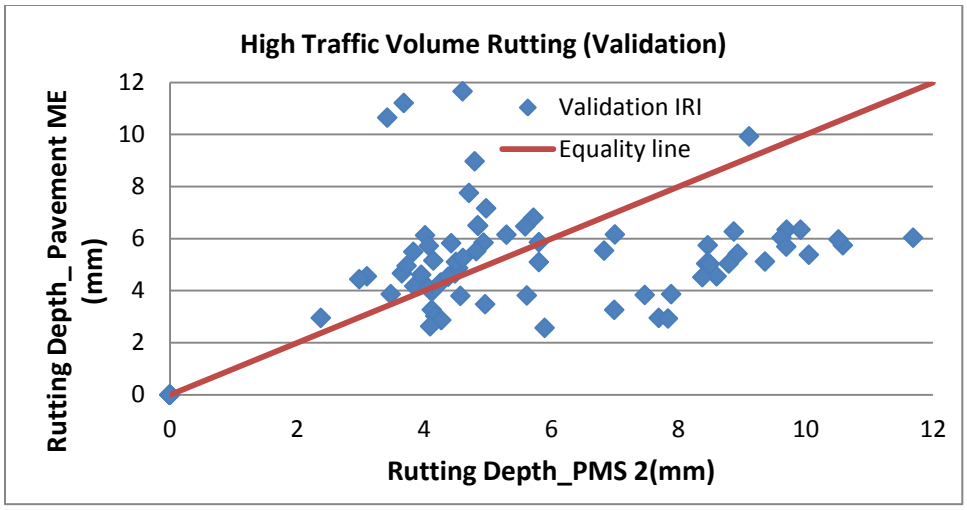

Figure 4-10: Rutting Validation of High Traffic Volume Category

The p = 0.2624> ∝, providing evidence that the predicted values shows no significant different in the means with the measured values for rutting of high traffic volume category.

4.4.3 Overall Network Validation

Rutting

Using the calibrated coefficients found from this research from the prediction process, on validation sections in overall network traffic volume category for the rutting validation, these sections provide the results,, as shown in Figure 4-11.

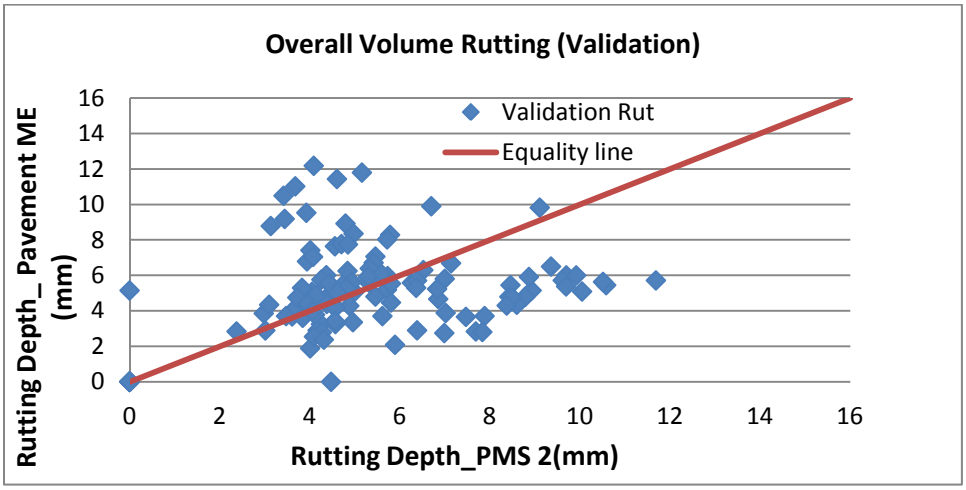

Figure 4-11: Rutting Validation of Overall Network Category

The p = 0.570> ∝, providing evidence that the predicted values shows no significant different in the means with the measured values for rutting of overall network category.

4.5 Validation Summary

The validation for each category was performed independently. The validation of rutting model indicated the local calibration reduced the RMSE of rutting prediction. Detailed t-test outcomes and further information is presented in appendix C.

Chapter 5
Conclusions and Recommendations

5.1 Conclusions

The research presented in this thesis identified an urgent need based on an assessment of pavement performance prediction developed by AASHTOWare® to carry out local calibration for various distresses. However, rutting and IRI prediction models were the only distresses considered in the study with Ontario pavements selected as the case study. The results of the initial analysis showed that the predicted distress values for both the rutting and IRI levels did not correlate well with the measured pavement distresses documented in PMS2. This preliminary conclusion provided the motivation for the investigation of local calibration coefficients to improve the accuracy of AASHTOWare® performance predictions for Ontario. It is concluded that local calibration coefficients should be developed and utilized in AASHTOWare® pavement design. Furthermore, this thesis emphasized the need to achieve further calibration for other types of distress models such as fatigue cracking and thermal cracking.

The following results of this research support the main conclusions of the research:

1. Ontario locally calibrated coefficients for the AASHTOWare® rutting model are 0.7, 0.6, and 1 for $\beta 1$, $\beta 2$, and $\beta 3$, respectively. Using the locally calibrated coefficients for Ontario would result in a reduction in Root Mean Square Error (RMSE) of 37.48 % compared to default AASHTOWare® model.
2. Ontario local calibration coefficients for rutting in low-volume roads (AADT < 10,000) were determined to be: 1, 0.6, and 0.6 for $\beta 1$, $\beta 2$, and $\beta 3$, respectively. The locally calibrated RMSE was reduced by 30 % compared to the default AASHTOWare® model for low traffic volume roads.
3. Ontario local calibration coefficients were determined for rutting in high traffic volume roads (AADT > 10,000): 1, 0.7, and 1 for $\beta 1$, $\beta 2$, and $\beta 3$, respectively. The locally calibrated RMSE was reduced by 43% compared to default AASHTOWare® model for high-volume roads.

In general, the developed models which are presented in this thesis resulted in noticeable improvement with respect to the prediction of pavement rutting, while the analysis of the IRI data did not show any significant correlation. In fact, the results of the calibration of the IRI showed that IRI variable should not be considered in any future local calibration.

This thesis was undertaken in order to evaluate and calibrate the default AASHTOWare® models in predicting accurate pavement performance in Ontario as a case study. Moreover, one of the important conclusions is the fact that improving the prediction abilities of the local models will provide a cost-effective pavement design tool that accounts for expected pavement performance, and associated pavement preservation/treatment activities.

While the local calibration procedure employed in this thesis relied on the default mechanistic properties of asphalt mixes used in Ontario. The incorporation of in-situ mechanistic properties into PMS2 will offer researchers a valuable resource for enhancing the AASHTOWare® calibration process.

Both public and private partners working in the pavement industry will benefit from the results of this thesis. For the Private sector corporate involved in Public-Private Partnerships (PPP), would benefit from the development of accurate pavement performance prediction. This would lead to design of cost-effective maintenance program and benefit the private sector especially on performance-based contracts.

The research methodology and analytical approaches followed in this thesis offer a roadmap that can be used by other researchers not only in Ontario but anywhere when PMS is implemented along the adoption of ASSHTOWare®.

5.2 Future work

The research scope of this thesis had few constrains which need to be addressed in future work. It is recommended that further detailed mechanical properties of asphalt mixes to be included in the PMS2 database. Also, more data related to material, traffic, and pavement distresses should be collected and utilized.

On the other hand, PMS2 documentation of top-down cracking and fatigue cracking does not match the AASHTOWare® output. As cracking distresses is documented in terms of two ratings that represent the severity and extent of cracks in PMS2, while AASHTOWare® performance

predictions reporting cracking percentages, which will facilitate the local calibration of cracking models.

The recycling and reuse of innovative materials in asphalt pavement encouraged through the LEED, GreenRoads and GreenPave programs. The ability to obtain accurate predictions of pavement performance relies on knowledge of the mechanistic properties associated with such innovative mix designs. Contractors should determine the mechanistic properties of innovative mix designs in order to facilitate performance predictions for these mixes through ASSHTOWare®. The experimental matrix required for an innovative mix design should satisfy the AASHTOWare® input requirements with respect to mechanistic properties.

Local calibration should be updated on a regular basis in order to accommodate modifications in materials properties, changes in the traffic spectrum, and the impact of global warming.

An individual research project should be pursued with the goal of correlating the PMS2 crack-rating system with the cracking percentage method. The development of a reliable technique for converting the distress measurement systems from one to the other will enable researchers to utilize PMS2 data for the local calibration of top-down and fatigue cracking models.

Bibliography

[AASHTO, 1993] American Association of State Highway, & Transportation Officials. (1993).AASHTO Guide for Design of Pavement Structures, 1993 (Vol. 1). AASHTO.

[AASHTO, 2008] "Guide, M. E. P. D. (2008). A Manual of Practice. American Association of State Highway and Transportation Officials.

[AASHTO, 2010] Guide for the Local Calibration of the Mechanistic-empirical Pavement Design Guide, American Association of State Highway and Transportation Officials, AASHTO, 2010

[ARA, 2004] Applied Research Associates, Inc. Development of the 2002 Guide for the Design of New and Rehabilitated Pavement Structures, Final Report and Software (Version 0.70) NCHRP Project 1-37A, Transportation Research Board, Washington, D.C., April 2004.

[ASTM, 2008] ASTM E1926 - 08 "Standard Practice for Computing International Roughness Index of Roads from Longitudinal Profile Measurements", ASTM International, West Conshohocken, PA, 2003, DOI: 10.1520/E1926-08

[Banerjee,2009] Banerjee, A., Aguiar-Moya, J. P., & Prozzi, J. A. (2009). Calibration of mechanistic-empirical pavement design guide permanent deformation models.Transportation Research Record: Journal of the Transportation Research Board, 2094(1), 12-20.

[Baus, 2010] Baus, R. L., & Stires, N. R. (2010). Mechanistic-empirical pavement design guide implementation (No. FHWA-SC-10-01).

[BCMoT, 2012] Pavement Surface Condition Rating Manual, British Columbia Ministry of Transportation, Canada, Fourth Edition, 2012.

[Chamorro, 2010] Chamorro, A. Validation and Implementation of Ontario Network Level Distress Guidelines and Condition Rating. Transportation Research Record, (2153), 49-57.

[Darter et al. 2007] Darter, M. I., Mallela, J., Titus-Glover, L., Rao, C., Larson, G., Gotlif, A., ... & Zapata, C. E. (2006). Changes to the" Mechanistic-empirical Pavement Design Guide" Software Through Version 0.900, July 2006. NCHRP Research Results Digest, (308).

[Ddamda 2011] Ddamba, S. J. (2011). Evaluation of the Effect of Recycled Asphalt Shingles on Ontario Hot Mix Pavement.

[Donnelly, 2007] Donnelly, R. A. (2007). The complete idiot's guide to statistics. Penguin.

[El-Assaly, 2002] El-Assaly, A., Ariaratnam, S., & Hempsey, L. (2002). Development of Deterioration Models for the Primary Highway Network in Alberta, Canada. InAnnual Conference of the Canadian Society for Civil Engineering, Montréal, Québec, Canada.

[El Hakim, 2011] El Hakim, M." Evaluation of Field Strain in Asphalt Perpetual Pavements using Laboratory Testing "PhD Proposal. Civil Engineering, University of Waterloo, Waterloo, Ontario, 2011.

[El-Hakim, 2013] El-Hakim, M. (2013). A Structural and Economic Evaluation of Perpetual Pavements: A Canadian Perspective (Doctoral dissertation, University of Waterloo).

[Farashah, 2012] Kafi Farashah, M. (2012). Development Practices for Municipal Pavement Management Systems Application.

[FHWA, 2003] Miller, J. S., & Bellinger, W. Y. (2003). Distress identification manual for the long-term pavement performance program (No. FHWA-RD-03-031).

[FHWA, 2006] J.Arellano, M.M. de Farias, R.O. de Souza, V.P.K. Ganesan, M.P. McDonald, D. Morian, S.D. Neto, J.T. Smith, S.M. Stoffels, S.L. Tighe "Improving Pavements With Long-Term Pavement Performance: Products for Today and Tomorrow", technical report, FHWA, 2006.

[FHWA, 2010] Banerjee, A. Aguiar-Moya, J. Smit, A, and Prozzi, A" Development of a Flexible Pavements Database", Technical Report, FHWA, 2010

[FHWA, 2011] "Impact of Design Features on Pavement Response and Performance in Rehabilitated Flexible and Rigid Pavements" Technical Report,2011

[FHWA, 2011] FHWH."Federal Highway Administration website" Retrieved Feb 2011, from:http://www.fhwa.dot.gov/asset/hif11011/map02.cfm

[FHWA, 2012] Local Calibration of The MEPDG Using Pavement Management Systems, Final report, volume one , 2012

[Fwa,T.,2012] Fwa, T., Pasindu, H., and Ong, G. (2012). "Critical Rut Depth for Pavement Maintenance Based on Vehicle Skidding and Hydroplaning Consideration." J. Transp. Eng., 138(4), 423–429.

[Gonzalo, 2009] Rada, G. R., Simpson, A., Engineer, P. P., López Jr, A., & Leader, P. L. T. (2008). High-Quality Pavement Performance Data: Meeting Research and Management Needs. In Seventh International Conference on Managing Pavement Assets.

[Guo, 2013] Guo, X. (2013). Local Calibration of the MEPDG Using Test Track Data (Doctoral dissertation, Auburn University).

[Haas, 1994] Haas, R., Hudson, W. R., & Zaniewski, J. P. (1994). Modern pavement management.

[Halil, 2013] Ceylan, H., Kim, S., Gopalakrishnan, K., & Ma, D. (2013). Iowa calibration of MEPDG performance prediction models.

[Hall, 2011] Hall, K. D., Xiao, D. X., & Wang, K. C. (2011). Calibration of the mechanistic-empirical pavement design guide for flexible pavement design in Arkansas. Transportation Research Record: Journal of the Transportation Research Board, 2226(1), 135-141.

[Hamdi, 2012] Hamdi, A. S., Alyami, Z., Zhou, T., & Tighe, S. (2012). Improving Ontario Pavement Management through Long Term Monitoring. In Proceedings of the 91st Transportation Research Board Annual Meeting (pp. 1-16). Transportation Research Board.

[Hamdi, 2013] Hamdi,A. Tabassum, A. Tighe,S. (2013) Evaluation of Ontario's Pavement Design Methodology, Transportation Association of Canada,2013

[Hamdi, 2014] Hamdi, A. S., Tighe, S. L., & Li, N. Y. (2014). Canadian Calibration on Mechanistic-Empirical Pavement Design Guide to Estimate International Roughness Index (IRI) Using MTO Data. International Journal of Pavement Research and Technology, 7(2), 101-108.

[Hudson, 2008] Hudson, W. R., Visser, W., Monismith, C. L., & Dougan, C. (2008). Using state PMS data to validate the new mechanistic/empirical pavement design

guide (MEPDG). In 7th international conference on managing pavement assets, Calgary, Alberta, Canada

[ICT,2014] Pavement condition Index,(2014). Retrieved May 25, 2013, Illinois Center for Transportation: http://128.174.2.147/Spotlights/PMS_local_agency.aspx

[Jannat,2012] Jannat, G. E. (2012). Database Development For Ontario's Local Calibration Of Mechanistic–Empirical Pavement Design Guide (MEPDG) Distress Models. Database, 1, 1-2012.

[Li, 2009] Li, J., Pierce, L. M., & Uhlmeyer, J. (2009). Calibration of flexible pavement in mechanistic-empirical pavement design guide for Washington state. Transportation Research Record: Journal of the Transportation Research Board, 2095(1), 73-83.

[MNROAD, 2010] Hoegh, K., Khazanovich, L., & Jense, M. (2010). Local calibration of mechanistic-empirical pavement design guide rutting model. Transportation Research Record: Journal of the Transportation Research Board, 2180(1), 130-141.

[MTO, 1990] Chong, G. J., Phang, W. A., & Wrong, G. A. (1982). Manual for Condition Rating of Flexible Pavements-Distress Manifestations (No. Monograph).

[MTO,2012] MTO. Ontario’s Default Parameters for AASHTOWare Pavement ME Design Interim Report, Ministry of Transportation, Ontario, Canada, 2012

[MTO, 2013] Pavement Design and Rehabilitation Manual, Ministry of Transportation Ontario ,2013

[Muthadi, 2007] Muthadi, N. R. (2007). Local Calibration of the MEPDG for Flexible Pavement Design.

[NCHRP, 2004a] “Guide for Mechanistic-Empirical Design of New and Rehabilitated Pavement Structures”, Final Document, National Cooperative Highway Research Program Transportation Research Board National Research Council, 1-37A Report.

[NCHRP, 2004b] McGhee, K. H. (2004). Automated pavement distress collection techniques (Vol. 334). Transportation Research Board.

[Ningyuan, 1997] Li, N. (1997). Development of a probabilistic based, integrated pavement management system.

[Ningyuan ,1999] Li, N., Xie, W. C., & Haas, R. (1996). Reliability-based processing of Markov chains for modeling pavement network deterioration. Transportation Research Record: Journal of the Transportation Research Board, 1524(1), 203-213.

[Ningyuan ,2006] Ningyuan, L., Eng, P., Kazmierowski, T., & Lane, B. (2006). Long-Term Monitoring of Low-Volume Road Performance in Ontario. In 2006 annual conference and exhibition of the transportation association of canada: transportation without boundaries; held 17-20 september, charlottetown, prince edward island.

[Ningyuan, 2001] Ningyuan, L., Kazmierowski, T., Tighe, S., & Haas, R. (2001, August). Integrating dynamic performance prediction models into pavement management maintenance and rehabilitation programs. In Proceedings of the 5th International Conference on Managing Pavements, Seattle, Wash (pp. 11-14).

[Ningyuan, 2013] Ningyuan, L., Tighe, S., & Hamdi, A. (2013). IMPACTS OF USING ALTERNATIVE PERFORMANCE INDICIES ON ROAD ASSET VALUE ASSESSMENT.

[NRC,2003] "Developing Level of Service" a best practice by the national guide to sustainable municipal infrastructure,2003

[Ohio, 2009] Glover, L. T., & Mallela, J. (2009). Guidelines for Implementing NCHRP 1-37A ME Design Procedures in Ohio: Volume 4-MEPDG Models Validation & Recalibration. Rep. No. FHWA/OH-2009/9D.

[OHMPA, 1999] The ABCs of PGAC, Ontario Hot Mix Producers Association, 1999

[Pavementinteractive, 2014] Pavementinteractive,(2014) Retrieved July 15, 2014, from Pavementinteractivehttp://www.pavementinteractive.org/category/pavement

[Prakash, 1988] Prakash, A. Design and Development of a Pavement Management System for Large Network; Proceedings of Problems, India, 1988.the International Conference on Roads and Road Transport

[Pierce, 2014] Pierce, L. M., & McGovern, G. (2014). Implementation of the AASHTO Mechanistic-Empirical Pavement Design Guide and Software (No. Project 20-05, Topic 44-06).

[Schram & Abdelrahman, 2010] Schram, S. A., & Abdelrahman, M. (2010). Integration of mechanistic-empirical pavement design guide distresses with local performance indices.Transportation Research Record: Journal of the Transportation Research Board, 2153(1), 13-23.

[Schwartz,2007] Charles W. Schwartz, and Regis L. Carvalho. Implementation of NCHRP 1-37A Design Guide, Final Project, Volume 2: Evaluation of Mechanistic-Empirical Design Procedure, Department of Civil and Environmental Engineering, The University of Maryland, Prepared for Maryland State Highway Administration, Lutherville, MD, February, 2007.

[Souliman, 2010] Souliman, M. I., Mamlouk, M. S., El-Basyouny, M. M., & Zapata, C. E. (2010). Calibration of the AASHTO MEPDG for flexible pavement for Arizona conditions. In Transportation Research Board 89th Annual Meeting (No. 10-1817).

[TAC, 1997] Transportation Association of Canada. (1997). Pavement design and management guide. Transportation Association of Canada.

[TAC, 2013] Transportation Association of Canada. (2013). Pavement design and management guide. Transportation Association of Canada

[Tighe 2007] Tighe, S., Huen, K., & Haas, R. (2007). Environmental and traffic deterioration with mechanistic-empirical pavement design model: Canadian example.Transportation Research Record: Journal of the Transportation Research Board, 1989(1), 336-343.

[Tighe, 2008] Tighe, S. L., Ningyuan, L., & Kazmierowski, T. (2008). Evaluation of semiautomated and automated pavement distress collection for network-level pavement management. Transportation Research Record: Journal of the Transportation Research Board, 2084(1), 11-17.

[Tighe 2014] Tighe, S. Ningyuan, L "Practical Data collection and Evaluation for Pavement Management" Ontario Green Road Association ,2014

[Tri Technologies,2014] Tri Technologies, (2014). Retrieved July 15, 2014, from Tri Technologies:http://www.tritechasphalt.com/our-services/asphalt-crack-sealing

[UDOT, 2009] Darter, M. I., Titus-Glover, L., & Von Quintus, H. L.

(2009). Implementation of the Mechanistic-Empirical Pavement Design Guide in Utah: validation, calibration, and development of the UDOT MEPDG User's Guide (No. UT-09.11).

[UL-Islam, 2011] Islam, R. U. (2011). Performance Evaluation of Recycled Asphalt Shingles (RAS) in Hot Mix Asphalt (HMA): An Ontario Perspective.

[Uzarowski, 2006] Uzarowski, L. (2006). The development of asphalt mix creep parameters and finite element modeling of asphalt rutting (Doctoral dissertation, University of Waterloo).

[Van Dam, 1996] Van Dam, T. J., Chesher, A. D., & Peshkin, D. G. (1997). Evaluation of LTPP Data Using HDM-III Probabilistic Failure-Time Models for Crack Initiation in Bituminous Pavements. Transportation Research Record, 1592.

[Velasquez, 2009] Velasquez, R., Hoegh, K., Yut, I., Funk, N., Cochran, G., Marasteanu, M., & Khazanovich, L. (2009). Implementation of the MEPDG for new and rehabilitated pavement structures for design of concrete and asphalt pavements in Minnesota.

[von Quintus , 2007] Von Quintus, H., Darter, M., & Mallela, J. (2007). Manual of Practice - Interim Mechanistic Empirical Pavement Design Guide. NCHRP Project 1-40B

[Wassem, 2013] Afzal Waseem,"Methodology Development and Local Calibration of MEPDG Permanent Deformation Models "for Ontario's Flexible Pavements Master Thesis, Department of Civil Engineering, Ryerson University, Toronto, Ontario, 2013.

[WDOT, 201] WDOT" Washington Department of Transportation websit" Retrieved July 15, 2011, from http://training.ce.washington.edu/WSDOT/Modules/02_pavement_types/02-5_body.htm

[Williams, 2013] Williams, R. C., & Shaidur, R. (2013). Mechanistic-Empirical Pavement Design Guide Calibration for Pavement Rehabilitation.

[Zborowski, 2007] Zborowski, A., Kaloush, K., "Predictive equations to evaluate thermal fracture of asphalt rubber mixtures." Road Materials and Pavement Design 8.4: 819-833, 2007.

LIST OF ACRONYMS

AADT	Annual Average Daily Traffic
AASHTO	American Association of State Highway and Officials Transportation
DMI	Distress Manifestation Index
ESALs	Equivalent Single-Axle Loads
HMA	Hot Mix Asphalt
IRI	International Roughness Index
LTPP	Long Term Pavement Performance
ME	Mechanistic-Empirical
MEPDG	Mechanistic-Empirical Pavement Design Guide
MnDOT	Minnesota Department of Transportation
MnRoad	Minnesota Road
MTO	Ministry of Transportation, Ontario
NCHRP	National Cooperative Highway Research Program
PCI	Pavement Condition Index
PCR	Pavement Condition Rating
PMS	Pavement Management Systems
RCI	Riding Comfort Index
RCR	Ride Comfort Rating

Appendix A

ASSHTOWare®

5.2.1.1.1 Rutting

As specified in the MEPDG, rutting is calculated for Hot Mix Asphalt (HMA) layers as follows:

$$\Delta_{p(HMA)} = \varepsilon_{p(HMA)} h_{HMA} = \beta_{1r} k_2 \varepsilon_{r(HMA)} 10^{k1r} n^{k_{2r}\beta_{2r}} T^{k_{3r}\beta_{3r}}$$

where

$\Delta_{p(HMA)}$ = Accumulated permanent or plastic vertical deformation in the HMA layer/sub layer, in inches

$\varepsilon_{p(HMA)}$ = Accumulated permanent or plastic axial strain in the HMA layer/sublayer, in inches/inch

$\varepsilon_{r(HMA)}$ = Resilient or elastic strain calculated by the structural response model at the mid-depth of each HMA sublayer, in inches/inch

$h_{(HMA)}$ = Thickness of the HMA layer/sublayer, in inches

n = Number of axle load repetitions

T = Mix or pavement temperature, in °F

k_z = Depth confinement factor

$k_{1r,2r,3r}$ = Global field calibration parameters (from the NCHRP 1-40D recalibration: k1r = -3.35412, k2r = 1.5606, k3r = 0.4791)

β_{1r}, β_{2r}, β_{3r}, = Local or mixture field calibration constants, all set to 1.0 for the global calibration

$$k_z = (C_1 + C_2 D)0.328196^D$$

$$C_1 = -0.1039(H_{HMA})^2 + 2.4868 H_{HMA} - 17.342$$

$$C_2 = 0.0172(H_{HMA})^2 - 1.7331 H_{HMA} + 27.428$$

where

D = Depth below the surface, in inches

H_{HMA} = Total HMA thickness, in inches

Rutting in the foundation and in all unbound pavement layers is calculated based on the following:

$$\Delta_{p(soil)} = \beta_{s1} k_{s1} \varepsilon_v h_{soil} \left(\frac{\varepsilon_0}{\varepsilon_r}\right) e^{-\left(\frac{p}{n}\right)^{\beta}}$$

where

$\Delta_{p\,(Soil)}$ = Permanent or plastic deformation for the layer/sublayer, in inches
n = Number of axle load applications
ε_o = Intercept determined from laboratory repeated-load permanent deformation tests, in inches/inch
ε_r = Resilient strain imposed in laboratory tests to obtain material properties εo, β, and ρ, in inches/inch
ε_v = Average vertical resilient or elastic strain in the layer/sublayer and calculated by the structural response model, in inches/inch
h_{Soil} = Thickness of the unbound layer/sublayer, in inches
k_{s1} = Global calibration coefficients: ks1 = 2.03 for granular materials, and ks1 = 1.35 for fine-grained materials
β_{s1} = Local calibration constant for the rutting in the unbound layers (base or subgrade), set to 1.0 for the global calibration effort, with βs1 representing the subgrade layer and $\beta_B 1$ representing the base layer

$$Log\beta = -0.61119 - 0.017638(W_c)$$

$$\rho = 10^{9\left(\frac{C0}{(1-(10^9)^{\beta}}\right)^{\frac{1}{\beta}}}$$

$$C_0 = Ln\left(\frac{a_1 M_r^{b_1}}{a_9 M_r^{b_9}}\right) = 0.0075$$

where

Wc = Water content, in %
Mr = Resilient modulus of the unbound layer or sublayer, in psi
$a_{1,9}$ = Regression constants: a1 = 0.15 and a9 = 20.0
$b_{1,9}$ = Regression constants: b1 = 0.0 and b9 = 0.0

5.2.1.1.2 Smoothness

In the MEPDG, smoothness (IRI) is affected by all of the other distress models based on the assumption that any surface distress leads to an increase in roughness. The MEPDG specifies the following equations for calculating the predicted IRI for flexible pavement designs over time:

$$IRI = IRI_0 + 0.0150(\text{SF}) = 0.400(\text{FC}_{\text{Total}}) + 0.0080(\text{TC}) + 40.0(RD)$$

where

IRI_o = Initial IRI after construction, in inches/mi
SF = Site factor
FC_{Total} = Area of fatigue cracking (combined alligator, longitudinal, and reflection cracking in the wheel path), in % of total lane area, with all load-related cracks being combined on an area basis, with the length of cracks multiplied by 1 ft to convert length into an area basis, 18
TC = Length of transverse cracking (including the reflection of transverse cracks in existing HMA pavements), in ft/mi
RD = Average rut depth, in inches

$$SF = FROSTH + SWELLP * AGE^{1.5}$$

where

FROSTH = LN([PRECIP+1]*FINES*[FI+1])
SWELLP = LN([PRECIP+1]*CLAY*[PI+1])
FINES = FSAND + SILT
AGE = pavement age, in years
PI = subgrade soil plasticity index
PRECIP = mean annual precipitation, in inches
FI = mean annual freezing index, in °F days
FSAND = amount of fine sand particles in subgrade (% of particles between 0.074 mm and 0.42 mm)
SILT = amount of silt particles in subgrade (% of particles between 0.074 mm and 0.002 mm)
CLAY = amount of clay-sized particles in subgrade (% of particles less than 0.002 mm)

General Information Inputs

HWY_ID_A	From	To	REGION	DISTRICT	Year
K 1 E	49.551	53.02	2	20	1993
K 1 E	54.384	57.547	2	20	1994
K 1 E	56.643	59.943	2	20	1997
K 1 E	72.399	76.099	2	20	1994
K 1 E	74.799	82.999	2	20	1995
K 1 E	82.026	86.826	2	20	1993
K 1 E	118.883	122.983	2	20	2000
K 1 E	129.876	131.276	2	20	1998
K 1 N	99.861	101.661	2	20	1991
K 1 S	101.411	101.611	2	20	1998
K 1 W	48.551	51.051	2	20	1993
K 1 W	56.643	59.943	2	20	1997
K 1 W	118.883	123.033	2	20	1999
K 101 B	337.855	345.459	4	53	2000
K 101 B	345.459	372.259	4	62	2000
K 102 B	6.89	32.94	5	61	1995
K 11 B	1072.065	1096.309	4	53	1992
K 11 B	1096.309	1097.765	4	54	1992
K 11 B	1201.395	1228.895	4	53	1999
K 11 B	1228.895	1249.979	4	54	1995
K 11 B	1281.145	1330.375	4	53	1996
K 11 B	1366.305	1368.055	4	53	2006
K 11 B	1428.775	1431.299	5	61	1994
K 12 B	48.994	58.757	2	20	1998
K 129 B	0.9	30.8	4	62	2000
K 130 B	9.2	13.4	5	61	2000
K 137 B	0	2.3	3	41	2003
K 17 B	61.15	65.15	4	54	1991
K 17 B	629.1	662.39	4	54	1999
K 17 B	675.92	677.52	4	62	1997
K 17 B	677.52	694.79	4	62	1996
K 17 B	765.95	783.05	4	62	1998
K 17 B	976.14	1001.89	5	61	1999

Traffic Information

HWY_ID_A	From	To	AADT	Trk%	AADTT	Growth	Lane/direction
K 1 E	49.551	53.02	76508.4	12.6%	9640.058	1%	3
K 1 E	54.384	57.547	66602.9	15.2%	10123.64	2.2%	3
K 1 E	56.643	59.943	30222.8	13.1%	3959.187	6.6%	3
K 1 E	72.399	76.099	66100	13.5%	8923.5	1.75%	3
K 1 E	74.799	82.999	40200	12.3%	4944.6	5.6%	3
K 1 E	82.026	86.826	67832.2	14.0%	9496.508	2.1%	3
K 1 E	118.883	122.983	136000	15.0%	20400	3.0%	5
K 1 E	129.876	131.276	16867	12.5%	2108.375	6.0%	4
K 1 N	99.861	101.661	80108	25%	20027	2.7%	3
K 1 S	101.411	101.611	120451	25%	30112.75	2.0%	3
K 1 W	48.551	51.051	66166	13.40%	8866.244	1.6%	3
K 1 W	56.643	59.943	66603	15.20%	10123.66	2.20%	3
K 1 W	118.883	123.033	130900	15%	19635	3%	3
K 101 B	337.855	345.459	1264	16.30%	206.032	1.30%	1
K 101 B	345.459	372.259	347	19.10%	66.277	1.70%	1
K 102 B	6.89	32.94	2450	33.60%	823.2	0	2
K 11 B	1072.065	1096.309	650	73%	474.5	2.10%	1
K 11 B	1096.309	1097.765	650	73%	474.5	2.10%	1
K 11 B	1201.395	1228.895	1145	55%	629.75	1.30%	1
K 11 B	1228.895	1249.979	1072	55%	589.6	1.30%	1
K 11 B	1281.145	1330.375	306	52.40%	160.344	7.70%	1
K 11 B	1366.305	1368.055	3367	26.50%	892.255	8.10%	1
K 11 B	1428.775	1431.299	6597	17%	1121.49	0.50%	1
K 12 B	48.994	58.757	4531	18%	815.58	4.30%	1
K 129 B	0.9	30.8	508	15%	76.2	3.10%	1
K 130 B	9.2	13.4	2314	8%	185.12	0.70%	1
K 137 B	0	2.3	4290	27.30%	1171.17	5%	2
K 17 B	61.15	65.15	6750	17%	1147.5	1.20%	1
K 17 B	629.1	662.39	3745	15%	561.75	0.40%	1
K 17 B	675.92	677.52	4800	19.50%	936	0.90%	1
K 17 B	677.52	694.79	3783	14.40%	544.752	2.80%	1
K 17 B	765.95	783.05	1516	23%	348.68	6.80%	1
K 17 B	976.14	1001.89	2000	26.70%	534	0%	1

Climate Information

HWY_ID_A	From	To	Longitude	Latitude
K 1 E	49.551	53.02	-79.308586	43.17952
K 1 E	54.384	57.547	-79.378624	43.186248
K 1 E	56.643	59.943	-79.378624	43.186248
K 1 E	72.399	76.099	-79.617319	43.212339
K 1 E	74.799	82.999	-79.650235	43.220408
K 1 E	82.026	86.826	-79.725337	43.238294
K 1 E	118.883	122.983	-79.674911	43.469989
K 1 E	129.876	131.276	-79.617963	43.550041
K 1 N	99.861	101.661	-79.828806	43.333606
K 1 S	101.411	101.611	-79.828806	43.333606
K 1 W	48.551	51.051	-79.308586	43.17952
K 1 W	56.643	59.943	-79.378624	43.186248
K 1 W	118.883	123.033	-79.674911	43.469989
K 101 B	337.855	345.459	-83.296967	47.873065
K 101 B	345.459	372.259	-83.296967	47.873065
K 102 B	6.89	32.94	-89.427767	48.496872
K 11 B	1072.065	1096.309	-84.672318	49.771952
K 11 B	1096.309	1097.765	-84.672318	49.771952
K 11 B	1201.395	1228.895	-84.672318	49.771952
K 11 B	1228.895	1249.979	-84.672318	49.771952
K 11 B	1281.145	1330.375	-84.672318	49.771952
K 11 B	1366.305	1368.055	-84.672318	49.771952
K 11 B	1428.775	1431.299	-84.672318	49.771952
K 12 B	48.994	58.757	-78.991871	44.100037
K 129 B	0.9	30.8	-83.440475	46.36695
K 130 B	9.2	13.4	-89.41618	48.370392
K 137 B	0	2.3	-75.978527	44.355769
K 17 B	61.15	65.15	-76.450253	45.437129
K 17 B	629.1	662.39	-83.323059	46.293104
K 17 B	675.92	677.52	-83.323059	46.293104
K 17 B	677.52	694.79	-83.323059	46.293104
K 17 B	765.95	783.05	-83.806801	46.306031
K 17 B	976.14	1001.89	-85.273347	48.592704

Materials Input

HWY	From	To	Layer					
			1	2	3	4	5	6
K 1 E	49.551	53.02	DFC/40	HDB/80	HL 8/130	OGDL/250	GrA/225	
K 1 E	54.384	57.547	DFC/40	HDB/40	PCC/250	OGDL/100	GrA/300	
K 1 E	56.643	59.943	DFC/40	HDB/90	HL 8/130	OGDL/100	GrA/300	
K 1 E	72.399	76.099	DFC/40	HDB/40	PCC/250	OGDL/100	GrA/300	
K 1 E	74.799	82.999	DFC/40	HDB/40	PCC/25	OGDL/100	GrA/300	
K 1 E	82.026	86.826	DFC/40	HDB/40	PCC/250	OGDL/100	GrA/150	
K 1 E	118.88	122.98	DFC/40	DFC/40	HDB/120	HL 8/80	GrA/150.	GrB1/60
K 1 E	129.87	131.27	OFC/25	HDB/90	HL 8/70	GrA/150	GrB1/700	
K 1 N	99.861	101.66	DFC/40	HDB/80	HL 8/270	GrA/150		
K 1 S	101.41	101.61	DFC/40	HDB/80	HL 8/100	GrA/150	GrB1/450	
K 1 W	48.551	51.051	DFC/40	HDB/80	HL 8/130	OGDL/250	GrA/225	
K 1 W	56.643	59.943	DFC/40	HDB/90	HL 8/130	OGDL/100	GrA/300	
K 1 W	118.88	123.03	DFC/40	HDB/190	GrA/400			
K 101 B	337.855	345.459	HL 4S/50	HL 4B/50	GrA/50.0	GrA/100	HL 4S/50	GrA/50
K 101 B	345.459	372.259	HL 4S/50	HL 4B/40	GrA/100	HL 4S/50	GrA/50	
K 102 B	6.89	32.94	HL 4S/40	RHL/40	RHL/40	GrA/120	Unk/80	GrA/60
K 11 B	1072.065	1096.309	HL 4S/40	HL 4B/40	GrA/100	GrA/100	HL 4S/40	HL 4B/80
K 11 B	1096.309	1097.765	HL 4S/40	HL 4B/40	GrA/100	GrA/160	HL 4S/40	HL 4B/80
K 11 B	1201.395	1228.895	HL 4S/50	HL 4B/40	GrA/50	GrA/160	Unk/80	GrA/80
K 11 B	1228.895	1249.979	RHL/40	RHL/50	GrA/100	GrA/100	Unk/80	GrA/60
K 11 B	1281.145	1330.375	RHL/40	RHL/40	HL 4S/40	Unk/120	GrA/60	
K 11 B	1366.305	1368.055	SP 12.5/55	SP 19.0/75.00	GrA/200.00	GrB1/650.00		
K 11 B	1428.775	1431.299	RHL/40	RHL/40.00	RHL/40.00	GrA/160.00	Unk/14	GrA/80
K 12 B	48.994	58.757	HL 1/40	MDB/40	HL 1/40	GrA/152	GrB2/381	
K 129 B	0.9	30.8	HL 4S/60	GrA/80	HL 4S/40	GrA/40		
K 130 B	9.2	13.4	HL 4S/50	GrA/50	GrA/100	HL 4S/50	GrA/50	
K 137 B	0	2.3	HL 1/50	HDB/100	GrA/175	HL 1/50	HDB/100	GrA/175
K 17 B	61.15	65.15	HL 3/40	HL 4B/100	GrA/250			
K 17 B	629.1	662.39	RHL/50	RHL/40	RHL/40	GrA/180	Unk/140	GrA/90
K 17 B	675.92	677.52	RHL/40	RHL/40	RHL/40	GrA/120	Unk/100	GrA/60
K 17 B	677.52	694.79	HL 4S/40	RHL/40	RHL/40	GrA/140	Unk/130	GrA/70
K 17 B	765.95	783.05	RHL/40	RHL/50	GrA/100	Unk/130	GrA/50	
K 17 B	976.14	1001.89	RHL/40	RHL/40	RHL/40	GrA/160	Unk/80	GrA/80

Appendix B

Output Sample from the Pavement-ME Software

K1E_St49_St53

File Name: C:\Users\admin\Desktop\Amin's Final Dataset\AASHTOWARE RUNS\Round16\AC\Calibration\K1E_St49_St53.dgpx

Design Inputs

Design Life: 20 years
Design Type: Flexible Pavement

Base construction: May, 1992
Pavement construction: June, 1992
Traffic opening: September, 1993

Climate Data Sources (Lat/Lon): 43.107, -78.945; 42.941, -78.736; 42.493, -79.272

Design Structure

Layer type	Material Type	Thickness(mm):
Flexible	Default asphalt concrete	40.0
Flexible	Default asphalt concrete	80.0
Flexible	Default asphalt concrete	130.0
NonStabilized	Permeable aggregate	250.0
NonStabilized	Crushed stone	225.0
Subgrade	A-5	Semi-infinite

Volumetric at Construction:	
Effective binder content (%)	12.4
Air voids (%)	3.5

Traffic

Age (year)	Heavy Trucks (cumulative)
1993 (initial)	9,640
2003 (10 years)	14,717,800
2013 (20 years)	30,844,000

Design Outputs

Distress Prediction Summary

Distress Type	Distress @ Specified Reliability		Reliability (%)		Criterion Satisfied?
	Target	Predicted	Target	Achieved	
Terminal IRI (m/km)	2.70	2.27	90.00	98.64	Pass
Permanent deformation - total pavement (mm)	19.00	13.68	90.00	100.00	Pass
AC bottom-up fatigue cracking (percent)	25.00	1.56	90.00	100.00	Pass
AC thermal cracking (m/km)	189.40	4.96	90.00	100.00	Pass
AC top-down fatigue cracking (m/km)	378.80	48.83	90.00	100.00	Pass
Permanent deformation - AC only (mm)	6.00	0.71	90.00	100.00	Pass

K1E_St49_St53

File Name: C:\Users\admin\Desktop\Amin's Final Dataset\AASHTOWARE RUNS\Round16\AC\Calibration\K1E_St49_St53.dgpx

Distress Charts

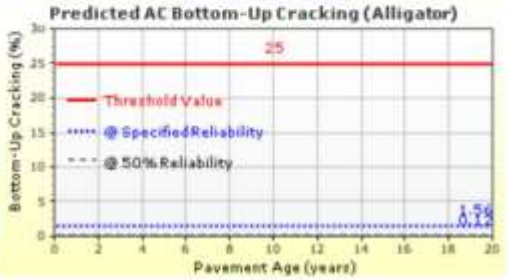

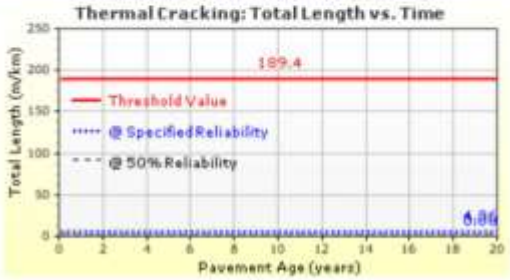

Traffic Inputs

Graphical Representation of Traffic Inputs

Initial two-way AADTT:	9,640	Percent of trucks in design direction (%):	50.0
Number of lanes in design direction:	3	Percent of trucks in design lane (%):	80.0
		Operational speed (kph)	100.0

Tabular Representation of Traffic Inputs

Volume Monthly Adjustment Factors

Level 3: Default MAF

Month	Vehicle Class									
	4	5	6	7	8	9	10	11	12	13
January	1.0	1.0	1.0	1.0	1.0	1.0	1.0	1.0	1.0	1.0
February	1.0	1.0	1.0	1.0	1.0	1.0	1.0	1.0	1.0	1.0
March	1.0	1.0	1.0	1.0	1.0	1.0	1.0	1.0	1.0	1.0
April	1.0	1.0	1.0	1.0	1.0	1.0	1.0	1.0	1.0	1.0
May	1.0	1.0	1.0	1.0	1.0	1.0	1.0	1.0	1.0	1.0
June	1.0	1.0	1.0	1.0	1.0	1.0	1.0	1.0	1.0	1.0
July	1.0	1.0	1.0	1.0	1.0	1.0	1.0	1.0	1.0	1.0
August	1.0	1.0	1.0	1.0	1.0	1.0	1.0	1.0	1.0	1.0
September	1.0	1.0	1.0	1.0	1.0	1.0	1.0	1.0	1.0	1.0
October	1.0	1.0	1.0	1.0	1.0	1.0	1.0	1.0	1.0	1.0
November	1.0	1.0	1.0	1.0	1.0	1.0	1.0	1.0	1.0	1.0
December	1.0	1.0	1.0	1.0	1.0	1.0	1.0	1.0	1.0	1.0

Distributions by Vehicle Class

Truck Distribution by Hour does not apply

Vehicle Class	AADTT Distribution (%) (Level 3)	Growth Factor	
		Rate (%)	Function
Class 4	3.3%	1%	Linear
Class 5	34%	1%	Linear
Class 6	11.7%	1%	Linear
Class 7	1.6%	1%	Linear
Class 8	9.9%	1%	Linear
Class 9	36.2%	1%	Linear
Class 10	1%	1%	Linear
Class 11	1.8%	1%	Linear
Class 12	0.2%	1%	Linear
Class 13	0.3%	1%	Linear

Axle Configuration

Traffic Wander	
Mean wheel location (mm)	460
Traffic wander standard deviation (mm)	254
Design lane width (m)	3.75

Axle Configuration	
Average axle width (m)	2.59
Dual tire spacing (mm)	305
Tire pressure (kPa)	827.4

Average Axle Spacing	
Tandem axle spacing (m)	1.45
Tridem axle spacing (m)	1.68
Quad axle spacing (m)	1.32

Wheelbase does not apply

Number of Axles per Truck

Vehicle Class	Single Axle	Tandem Axle	Tridem Axle	Quad Axle
Class 4	1.62	0.39	0	0
Class 5	2	0	0	0
Class 6	1.02	0.99	0	0
Class 7	1	0.26	0.83	0
Class 8	2.38	0.67	0	0
Class 9	1.13	1.93	0	0
Class 10	1.19	1.09	0.89	0
Class 11	4.29	0.26	0.06	0
Class 12	3.52	1.14	0.06	0
Class 13	2.15	2.13	0.35	0

AADTT (Average Annual Daily Truck Traffic) Growth

* Traffic cap is not enforced

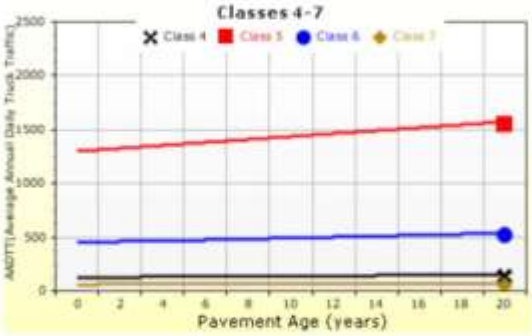

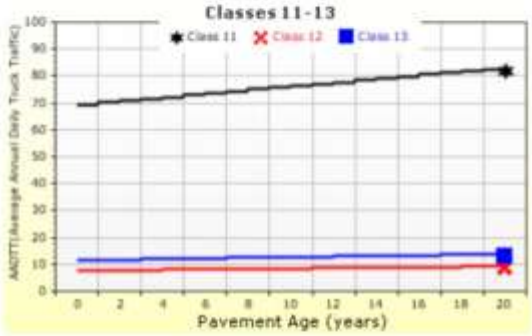

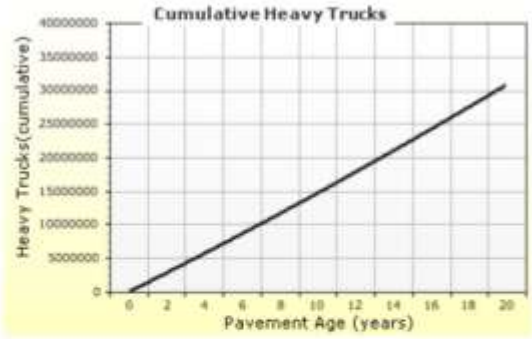

Climate Inputs

Climate Data Sources:

Climate Station Cities:	Location (lat lon elevation(m))
NIAGARA FALLS, NY	43.10700 -78.94500 178
BUFFALO, NY	42.94100 -78.73600 216
DUNKIRK, NY	42.49300 -79.27200 203

Annual Statistics:

Mean annual air temperature (°C)	9.73
Mean annual precipitation (mm)	902.46
Freezing index (°C - days)	358.44
Average annual number of freeze/thaw cycles	55.73

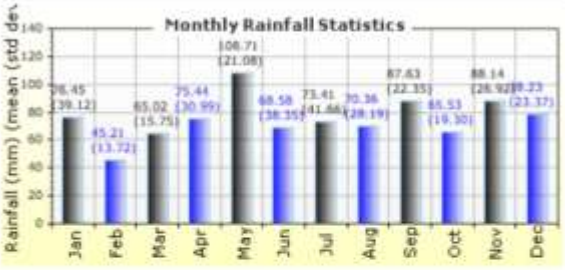

Water table depth (m)	10.00

Monthly Climate Summary:

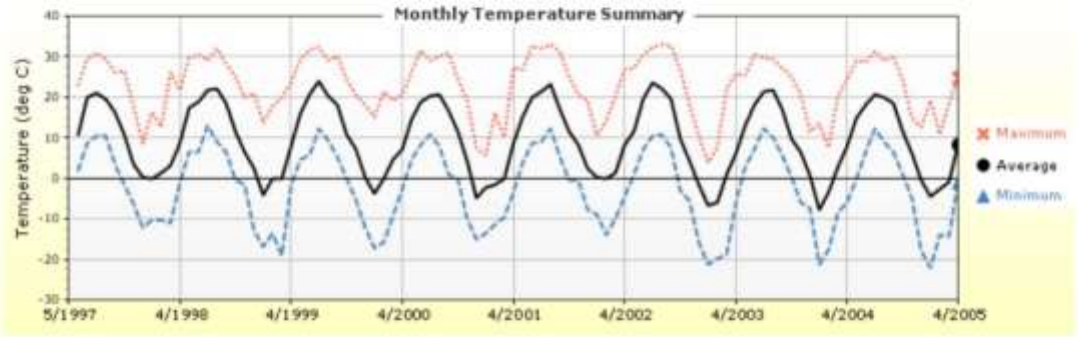

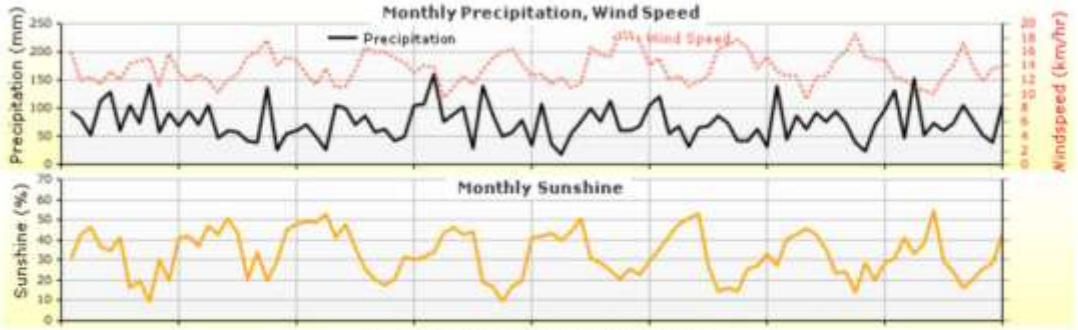

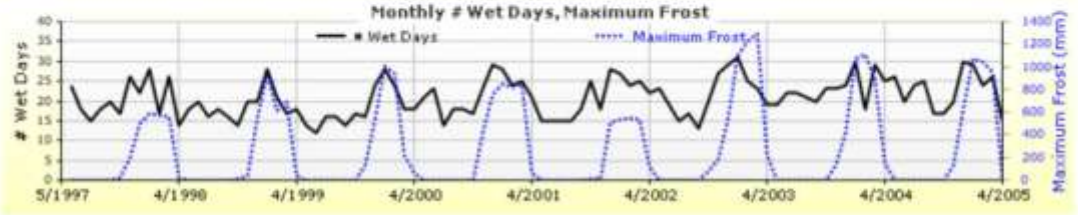

Hourly Air Temperature Distribution by Month:

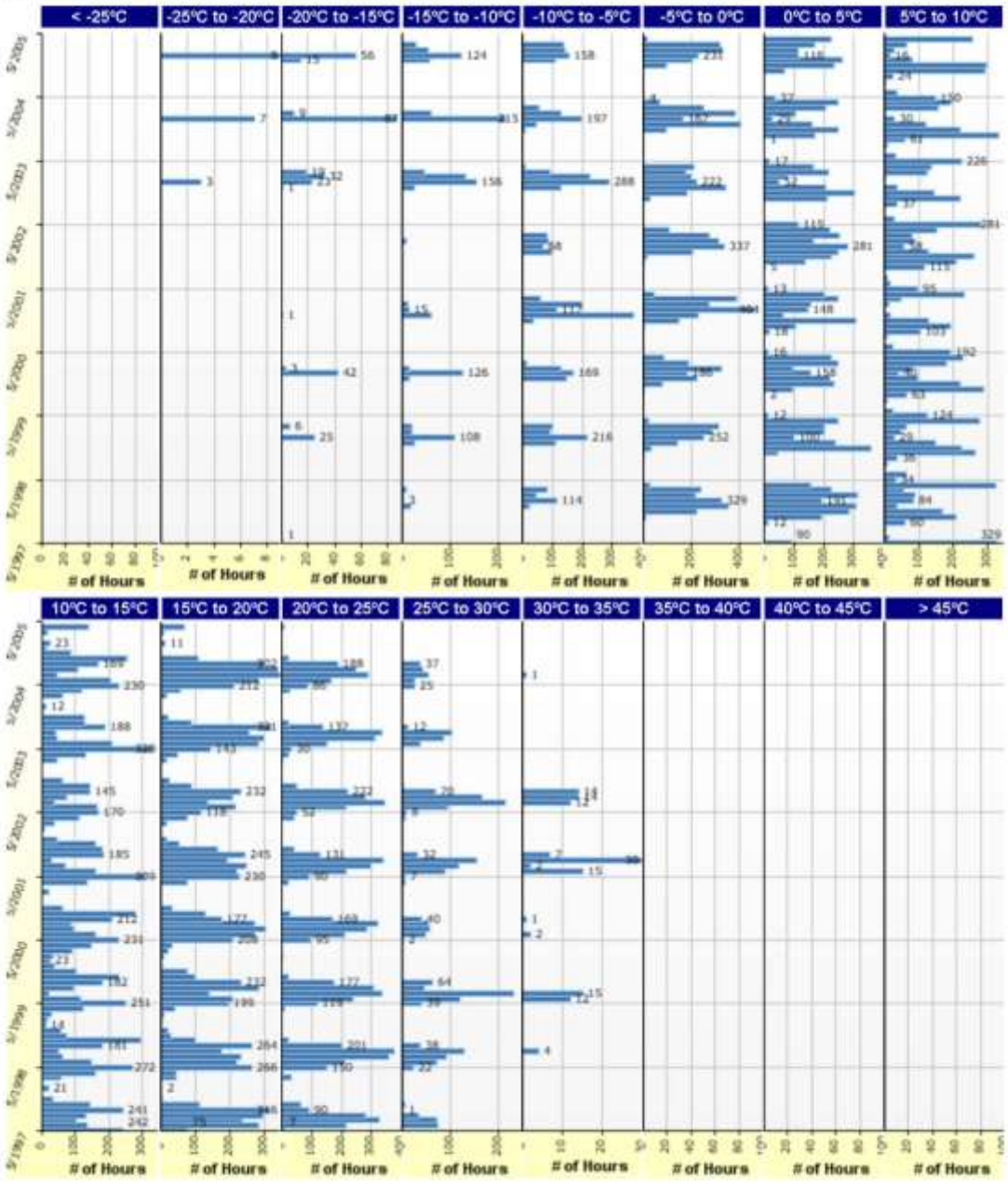

Design Properties

HMA Design Properties

Use Multilayer Rutting Model	False
Using G* based model (not nationally calibrated)	False
Is NCHRP 1-37A HMA Rutting Model Coefficients	True
Endurance Limit	-
Use Reflective Cracking	True

Structure - ICM Properties	
AC surface shortwave absorptivity	0.85

Layer Name	Layer Type	Interface Friction
Layer 1 Flexible : Default asphalt concrete	Flexible (1)	1.00
Layer 2 Flexible : Default asphalt concrete	Flexible (1)	1.00
Layer 3 Flexible : Default asphalt concrete	Flexible (1)	1.00
Layer 4 Non-stabilized Base : Permeable aggregate	Non-stabilized Base (4)	1.00
Layer 5 Non-stabilized Base : Crushed stone	Non-stabilized Base (4)	1.00
Layer 6 Subgrade : A-5	Subgrade (5)	-

Thermal Cracking (Input Level: 3)

Indirect tensile strength at -10 °C (MPa)	2.56

Thermal Contraction	
Is thermal contraction calculated?	True
Mix coefficient of thermal contraction (mm/mm/°C)	-
Aggregate coefficient of thermal contraction (mm/mm/°C)	9.0e-006
Voids in Mineral Aggregate (%)	15.9

	Creep Compliance (1/GPa)		
Loading time (sec)	-20 °C	-10 °C	0 °C
1	4.28e-002	5.53e-002	6.79e-002
2	4.61e-002	6.34e-002	8.47e-002
5	5.09e-002	7.60e-002	1.13e-001
10	5.48e-002	8.71e-002	1.42e-001
20	5.90e-002	9.99e-002	1.77e-001
50	6.50e-002	1.20e-001	2.37e-001
100	7.00e-002	1.37e-001	2.95e-001

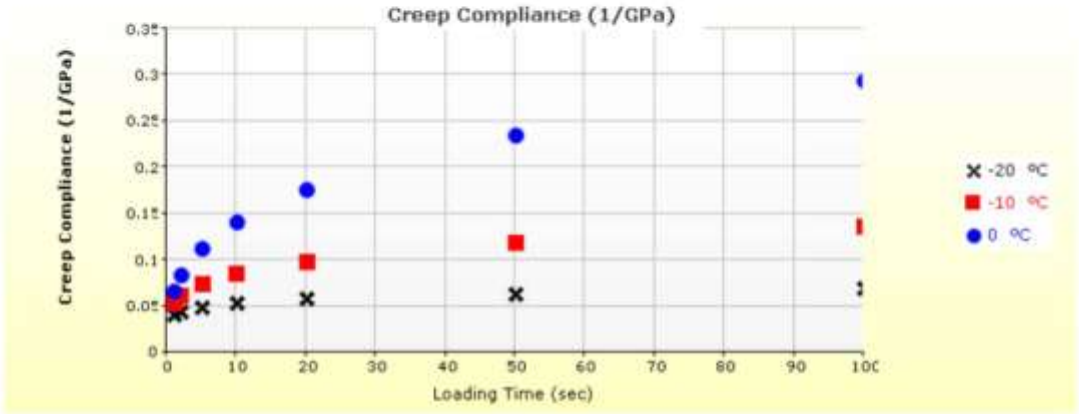

K1E_St49_St53

File Name: C:\Users\admin\Desktop\Amin's Final Dataset\AASHTOWARE RUNS\Round16\AC\Calibration\K1E_St49_St53.dgpx

HMA Layer 1: Layer 1 Flexible : Default asphalt concrete

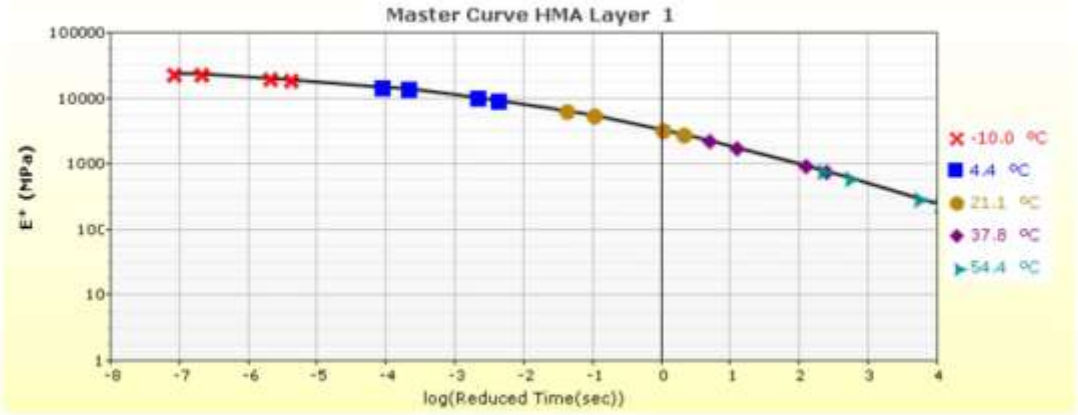

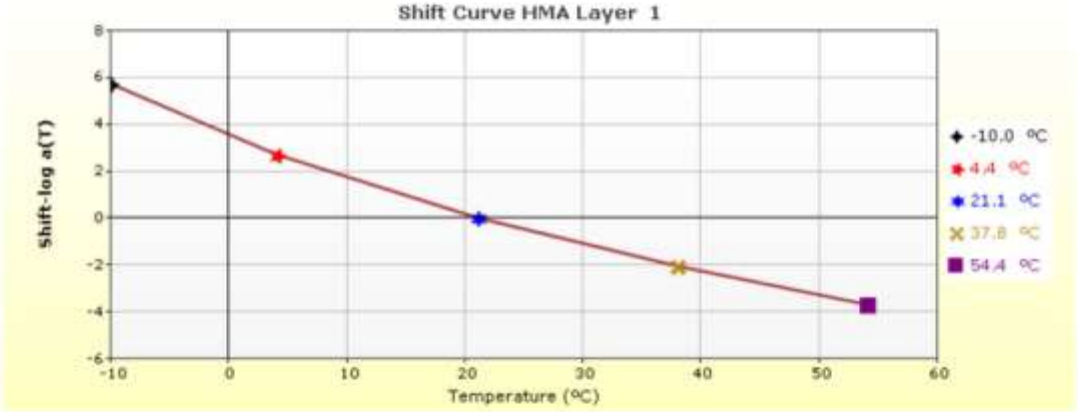

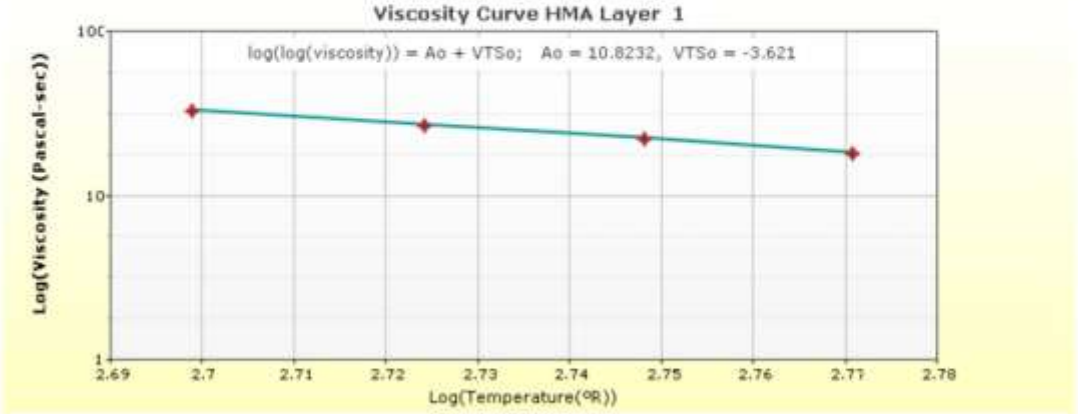

HMA Layer 2: Layer 2 Flexible : Default asphalt concrete

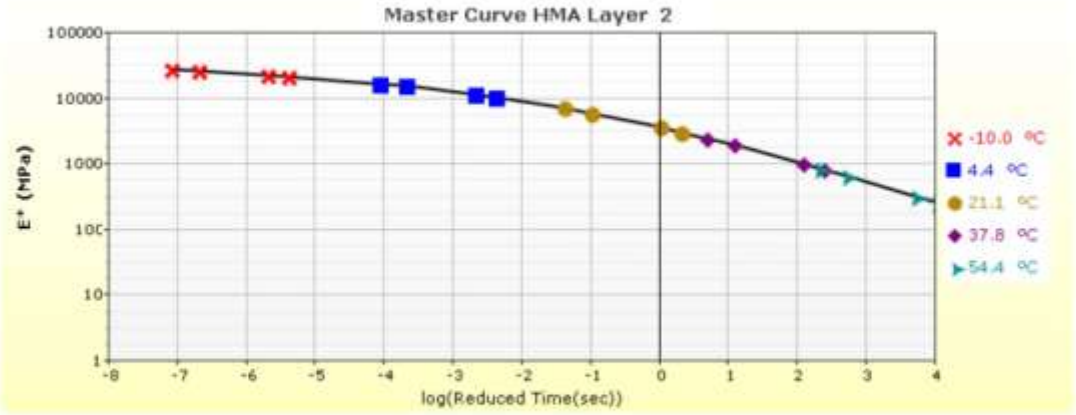

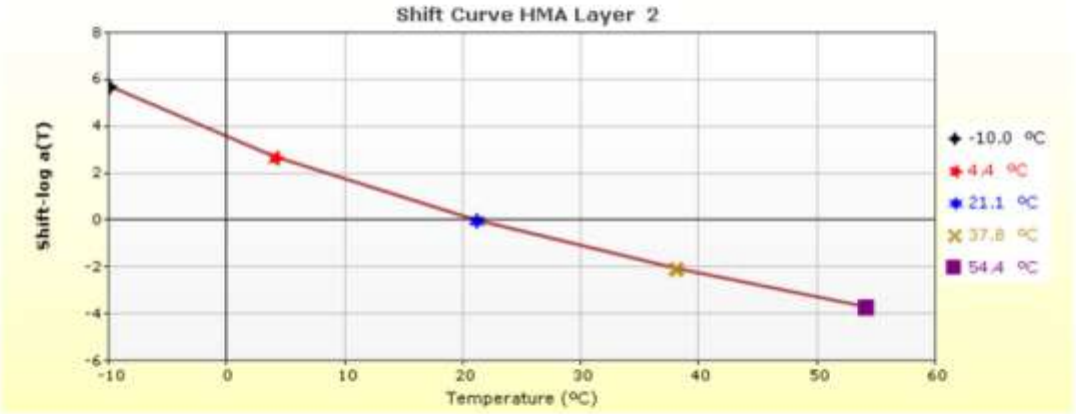

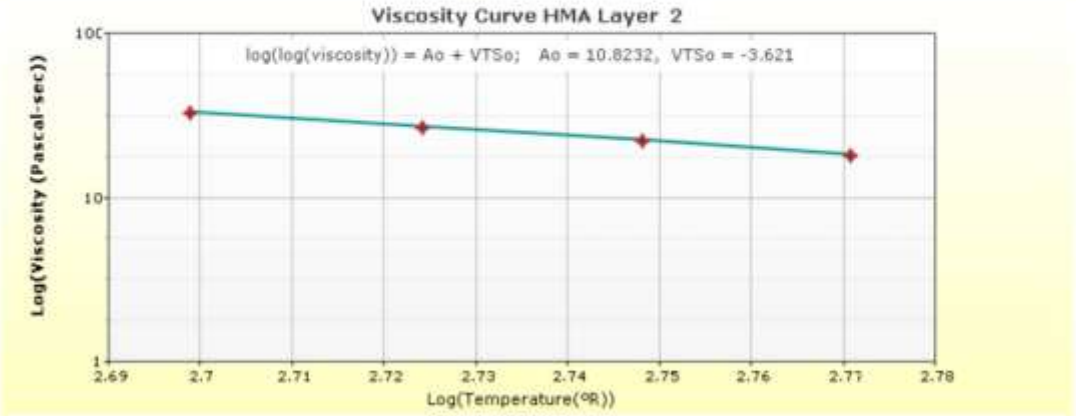

HMA Layer 3: Layer 3 Flexible : Default asphalt concrete

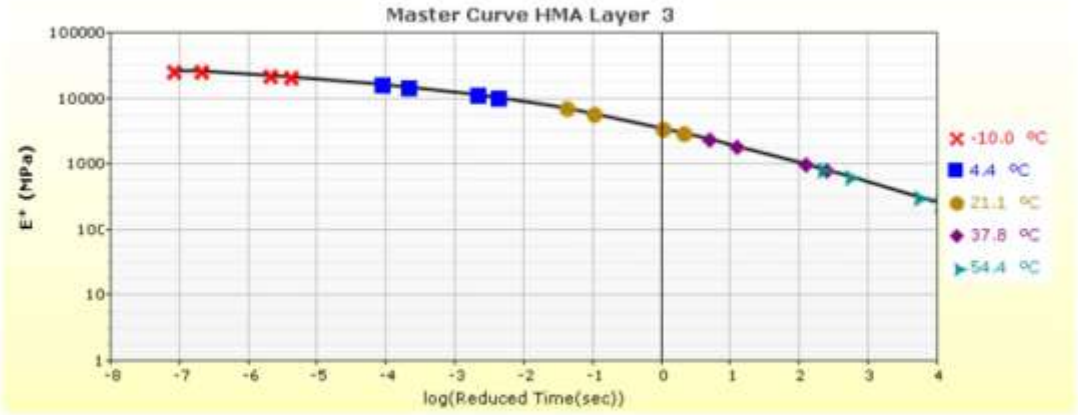

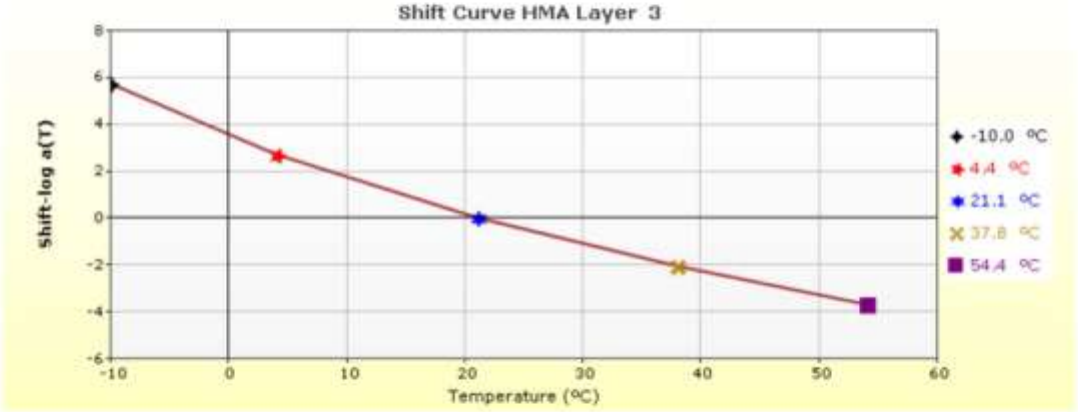

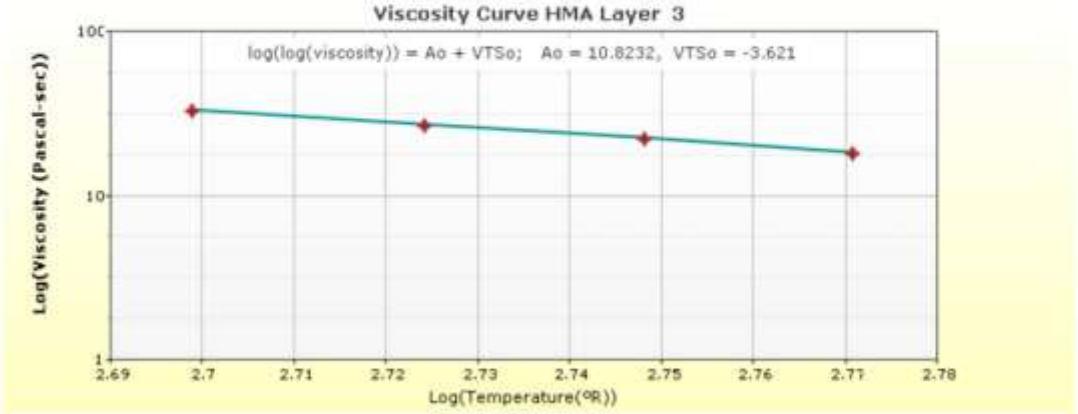

Analysis Output Charts

K1E_St49_St53

File Name: C:\Users\admin\Desktop\Amin's Final Dataset\AASHTOWARE RUNS\Round16\AC\Calibration\K1E_St49_St53.dgpx

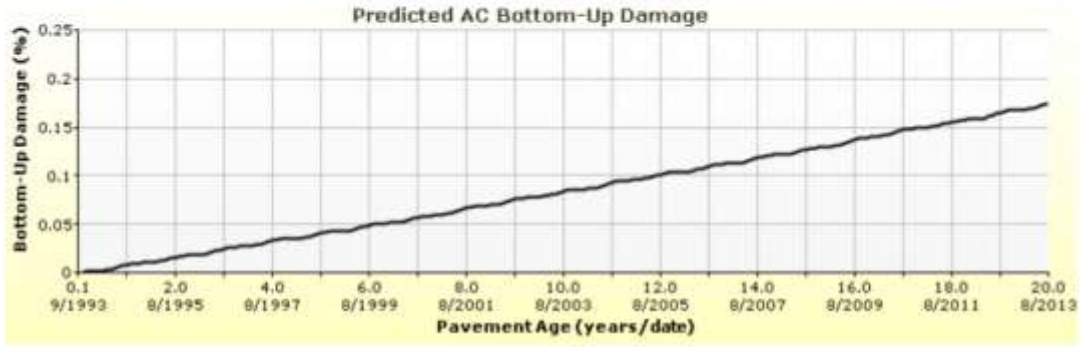

K1E_St49_St53

File Name: C:\Users\admin\Desktop\Amin's,Final Dataset\AASHTOWARE RUNS\Round16\AC\Calibration\K1E_St49_St53.dgpx

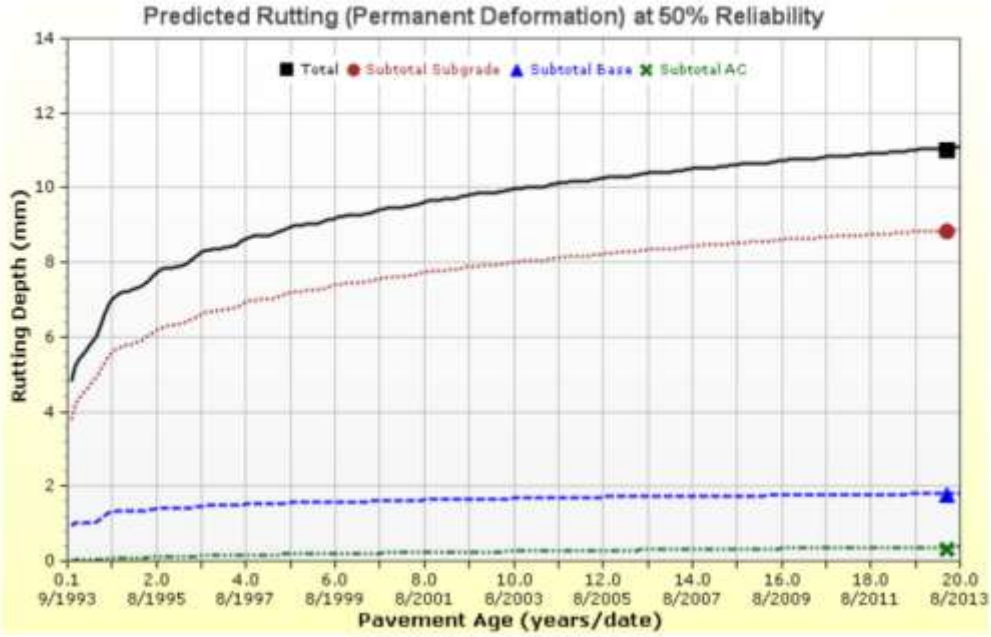

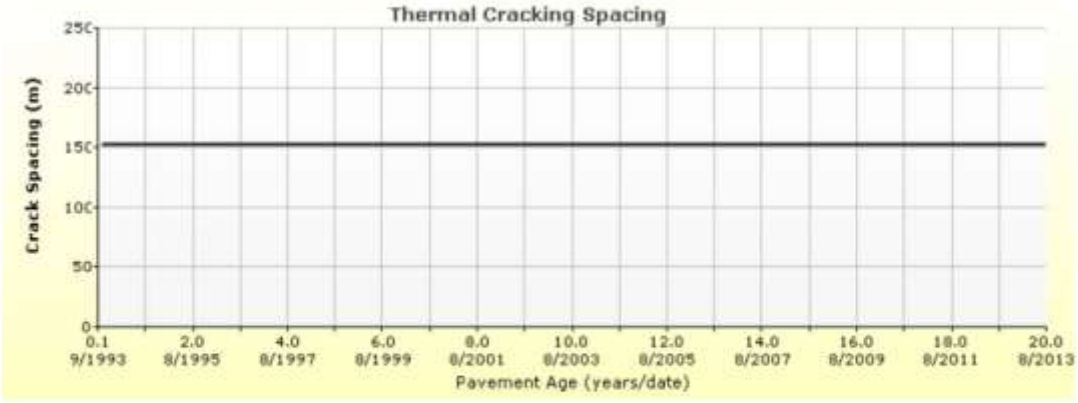
Thermal Cracking Spacing
Crack Spacing (m)
250
200
150
100
50
0
0.1
9/1993
2.0
8/1995
4.0
8/1997
6.0
8/1999
8.0
8/2001
10.0
8/2003
12.0
8/2005
14.0
8/2007
16.0
8/2009
18.0
8/2011
20.0
8/2013
Pavement Age (years/date)

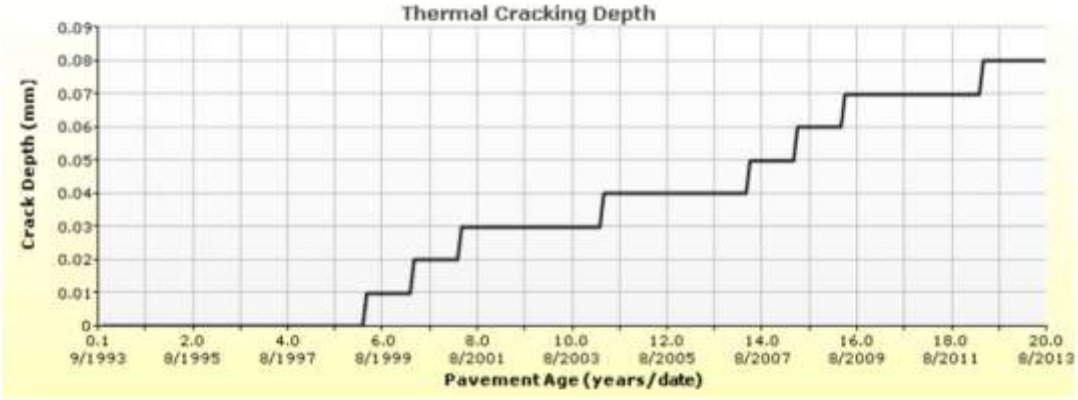
Thermal Cracking Depth
Crack Depth (mm)
0.09
0.08
0.07
0.06
0.05
0.04
0.03
0.02
0.01
0
0.1
9/1993
2.0
8/1995
4.0
8/1997
6.0
8/1999
8.0
8/2001
10.0
8/2003
12.0
8/2005
14.0
8/2007
16.0
8/2009
18.0
8/2011
20.0
8/2013
Pavement Age (years/date)

K1E_St49_St53

File Name: C:\Users\admin\Desktop\Amin's,Final Dataset\AASHTOWARE RUNS\Round16\AC\Calibration\K1E_St49_St53.dgpx

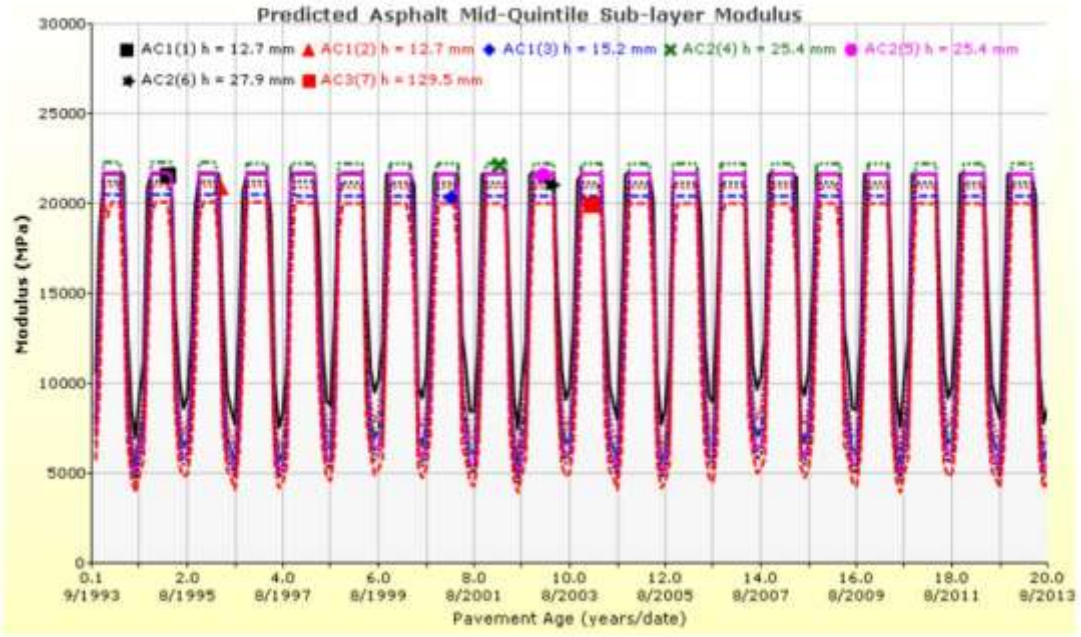

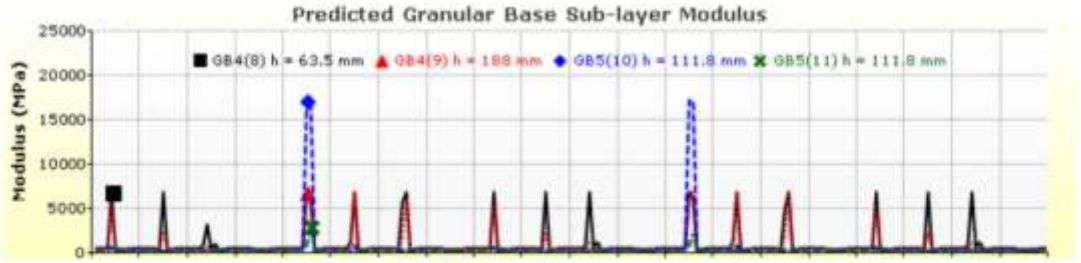

Layer Information

Layer 1 Flexible : Default asphalt concrete

Asphalt		
Thickness (mm)	40.0	
Unit weight (kgf/m^3)	2520.0	
Poisson's ratio	Is Calculated?	False
	Ratio	0.35
	Parameter A	-
	Parameter B	-

Asphalt Dynamic Modulus (Input Level: 3)

Gradation	Percent Passing
19 mm-inch sieve	100
9.5 mm sieve	82.5
4.75 mm sieve	52.5
0.075mm sieve	2.5

Asphalt Binder

Parameter	Value
Grade	Penetration Grade
Binder Type	Pen 85-100
A	10.8232
VTS	-3.621

General Info

Name	Value
Reference temperature (°C)	21.1
Effective binder content (%)	12.4
Air voids (%)	3.5
Thermal conductivity (watt/meter-kelvin)	1.16
Heat capacity (joule/kg-kelvin)	963

Identifiers

Field	Value
Display name/identifier	Default asphalt concrete
Description of object	
Author	
Date Created	16/09/2010 1:00:00 AM
Approver	
Date approved	16/09/2010 1:00:00 AM
State	
District	
County	
Highway	K1 - QEW
Direction of Travel	East
From station (km)	5.658
To station (km)	13.227
Province	
User defined field 2	
User defined field 3	
Revision Number	0

Layer 2 Flexible : Default asphalt concrete

Asphalt		
Thickness (mm)	80.0	
Unit weight (kgf/m^3)	2460.0	
Poisson's ratio	Is Calculated?	False
	Ratio	0.35
	Parameter A	-
	Parameter B	-

Asphalt Dynamic Modulus (Input Level: 3)

Gradation	Percent Passing
19 mm-inch sieve	97
9.5 mm sieve	63
4.75 mm sieve	43.5
0.075mm sieve	3

Asphalt Binder

Parameter	Value
Grade	Penetration Grade
Binder Type	Pen 85-100
A	10.8232
VTS	-3.621

General Info

Name	Value
Reference temperature (°C)	21.1
Effective binder content (%)	10.9
Air voids (%)	4
Thermal conductivity (watt/meter-kelvin)	1.16
Heat capacity (joule/kg-kelvin)	963

Identifiers

Field	Value
Display name/Identifier	Default asphalt concrete
Description of object	
Author	
Date Created	16/09/2010 1:00:00 AM
Approver	
Date approved	16/09/2010 1:00:00 AM
State	
District	
County	
Highway	
Direction of Travel	
From station (km)	
To station (km)	
Province	
User defined field 2	
User defined field 3	
Revision Number	0

Layer 3 Flexible : Default asphalt concrete

Asphalt		
Thickness (mm)	130.0	
Unit weight (kgf/m^3)	2460.0	
Poisson's ratio	Is Calculated?	False
	Ratio	0.35
	Parameter A	-
	Parameter B	-

Asphalt Dynamic Modulus (Input Level: 3)

Gradation	Percent Passing
19 mm-inch sieve	97
9.5 mm sieve	63
4.75 mm sieve	42.5
0.075mm sieve	3

Asphalt Binder

Parameter	Value
Grade	Penetration Grade
Binder Type	Pen 85-100
A	10.8232
VTS	-3.621

General Info

Name	Value
Reference temperature (°C)	21.1
Effective binder content (%)	10.9
Air voids (%)	4
Thermal conductivity (watt/meter-kelvin)	1.16
Heat capacity (joule/kg-kelvin)	963

Identifiers

Field	Value
Display name/identifier	Default asphalt concrete
Description of object	
Author	
Date Created	16/09/2010 1:00:00 AM
Approver	
Date approved	16/09/2010 1:00:00 AM
State	
District	
County	
Highway	
Direction of Travel	
From station (km)	
To station (km)	
Province	
User defined field 2	
User defined field 3	
Revision Number	0

Layer 4 Non-stabilized Base : Permeable aggregate

Unbound	
Layer thickness (mm)	250.0
Poisson's ratio	0.35
Coefficient of lateral earth pressure (k0)	0.5

Modulus (Input Level: 3)

Analysis Type:	Modify input values by temperature/moisture
Method:	Resilient Modulus (MPa)

Resilient Modulus (MPa)
400.0

Use Correction factor for NDT modulus?	-
NDT Correction Factor:	-

Identifiers

Field	Value
Display name/identifier	Permeable aggregate
Description of object	Default material
Author	AASHTO
Date Created	01/01/2011 12:00:00 AM
Approver	
Date approved	01/01/2011 12:00:00 AM
State	
District	
County	
Highway	
Direction of Travel	
From station (km)	
To station (km)	
Province	
User defined field 2	
User defined field 3	
Revision Number	0

Sieve

Liquid Limit	6.0
Plasticity Index	1.0
Is layer compacted?	False

	Is User Defined?	Value
Maximum dry unit weight (kgf/m^3)	False	2038.2
Saturated hydraulic conductivity (m/hr)	False	5.054e-02
Specific gravity of solids	False	2.7
Optimum gravimetric water content (%)	False	7.4

User-defined Soil Water Characteristic Curve (SWCC)	
Is User Defined?	False
af	7.2555
bf	1.3328
cf	0.8242
hr	117.4000

Sieve Size	% Passing
0.001mm	
0.002mm	
0.020mm	
0.075mm	8.7
0.150mm	
0.180mm	12.9
0.250mm	
0.300mm	
0.425mm	20.0
0.600mm	
0.850mm	
1.18mm	
2.0mm	33.8
2.36mm	
4.75mm	44.7
9.5mm	57.2
12.5mm	63.1
19.0mm	72.7
25.0mm	78.8
37.5mm	85.8
50.0mm	91.6
63.0mm	
75.0mm	
90.0mm	97.6

Layer 5 Non-stabilized Base : Crushed stone

Unbound	
Layer thickness (mm)	225.0
Poisson's ratio	0.35
Coefficient of lateral earth pressure (k0)	0.5

Modulus (Input Level: 3)

Analysis Type:	Modify input values by temperature/moisture
Method:	Resilient Modulus (MPa)

Resilient Modulus (MPa)
250.0

Use Correction factor for NDT modulus?	-
NDT Correction Factor:	-

Identifiers

Field	Value
Display name/identifier	Crushed stone
Description of object	Default material
Author	AASHTO
Date Created	01/01/2011 12:00:00 AM
Approver	
Date approved	01/01/2011 12:00:00 AM
State	
District	
County	
Highway	
Direction of Travel	
From station (km)	
To station (km)	
Province	
User defined field 2	
User defined field 3	
Revision Number	0

Sieve

Liquid Limit	6.0
Plasticity Index	0.0
Is layer compacted?	True

	Is User Defined?	Value
Maximum dry unit weight (kgf/m^3)	False	2048.3
Saturated hydraulic conductivity (m/hr)	False	2.376e-02
Specific gravity of solids	False	2.7
Optimum gravimetric water content (%)	False	5.7

User-defined Soil Water Characteristic Curve (SWCC)	
Is User Defined?	False
af	3.0201
bf	2.5984
cf	0.7539
hr	100.0000

Sieve Size	% Passing
0.001mm	
0.002mm	
0.020mm	
0.075mm	5.0
0.150mm	
0.180mm	
0.250mm	
0.300mm	13.5
0.425mm	
0.600mm	
0.850mm	
1.18mm	27.5
2.0mm	
2.36mm	
4.75mm	45.0
9.5mm	61.5
12.5mm	77.5
19.0mm	92.5
25.0mm	100.0
37.5mm	100.0
50.0mm	100.0
63.0mm	
75.0mm	
90.0mm	100.0

Layer 6 Subgrade : A-5

Unbound	
Layer thickness (mm)	Semi-infinite
Poisson's ratio	0.35
Coefficient of lateral earth pressure (k0)	0.5

Modulus (Input Level: 3)

Analysis Type:	Modify input values by temperature/moisture
Method:	Resilient Modulus (MPa)

Resilient Modulus (MPa)
34.5

Use Correction factor for NDT modulus?	-
NDT Correction Factor:	-

Identifiers

Field	Value
Display name/identifier	A-5
Description of object	Default material
Author	AASHTO
Date Created	01/01/2011 12:00:00 AM
Approver	
Date approved	01/01/2011 12:00:00 AM
State	
District	
County	
Highway	
Direction of Travel	
From station (km)	
To station (km)	
Province	
User defined field 2	
User defined field 3	
Revision Number	0

Sieve

Liquid Limit	42.0
Plasticity Index	15.0
Is layer compacted?	True

	Is User Defined?	Value
Maximum dry unit weight (kgf/m^3)	False	1706.7
Saturated hydraulic conductivity (m/hr)	False	2.849e-06
Specific gravity of solids	False	2.7
Optimum gravimetric water content (%)	False	18.2

User-defined Soil Water Characteristic Curve (SWCC)	
Is User Defined?	False
af	114.8407
bf	0.6389
cf	0.1739
hr	500.0000

Sieve Size	% Passing
0.001mm	
0.002mm	25.0
0.020mm	
0.075mm	82.0
0.150mm	
0.180mm	91.0
0.250mm	
0.300mm	
0.425mm	95.0
0.600mm	
0.850mm	
1.18mm	
2.0mm	98.0
2.36mm	
4.75mm	100.0
9.5mm	100.0
12.5mm	100.0
19.0mm	
25.0mm	
37.5mm	
50.0mm	
63.0mm	
75.0mm	
90.0mm	100.0

Calibration Coefficients

AC Fatigue	
$N_f = 0.00432 * C * \beta_{f1} k_1 \left(\frac{1}{\varepsilon_t}\right)^{k_2 \beta_{f2}} \left(\frac{1}{E}\right)^{k_3 \beta_{f3}}$ $C = 10^M$ $M = 4.84\left(\frac{V_b}{V_a + V_b} - 0.69\right)$	k1: 0.007566 k2: 3.9492 k3: 1.281 Bf1: 1 Bf2: 1 Bf3: 1

AC Rutting		
$\frac{\varepsilon_p}{\varepsilon_r} = k_z \beta_{r1} 10^{k_1 T^{k_2 \beta_{r2}} N^{k_3 \beta_{r3}}}$ $k_z = (C_1 + C_2 * depth) * 0.328196^{depth}$ $C_1 = -0.1039 * H_{ac}^2 + 2.4868 * H_{ac} - 17.342$ $C_2 = 0.0172 * H_{ac}^2 - 1.7331 * H_{ac} + 27.428$ *Where:* $H_{ac} = total\ AC\ thickness(in)$	$\varepsilon_p = plastic\ strain\left(^{in}/_{in}\right)$ $\varepsilon_r = resilient\ strain\left(^{in}/_{in}\right)$ $T = layer\ temperature(^{\circ}F)$ $N = number\ of\ load\ repetitions$	
AC Rutting Standard Deviation	0.24*Pow(RUT,0.8026)+0.001	
AC Layer	K1:-3.35412 K2:1.5606 K3:0.4791	Br1:0.7 Br2:0.6 Br3:1

Thermal Fracture	
$C_f = 400 * N\left(\frac{\log C / h_{ac}}{\sigma}\right)$ $\Delta C = (k * \beta t)^{n+1} * A * \Delta K^n$ $A = 10^{(4.389 - 2.52 * \log(E * \sigma_m * n))}$	C_f = observed amount of thermal cracking(ft/500ft) k = regression coefficient determined through field calibration $N(\ )$ = standard normal distribution evaluated at( ) σ = standard deviation of the log of the depth of cracks in the pavements C = crack depth(in) h_{ac} = thickness of asphalt layer(in) ΔC = Change in the crack depth due to a cooling cycle ΔK = Change in the stress intensity factor due to a cooling cycle A, n = Fracture parameters for the asphalt mixture E = mixture stiffness σ_m = Undamaged mixture tensile strength β_t = Calibration parameter
Level 1 K: 1.5	Level 1 Standard Deviation: 0.1468 * THERMAL + 65.027
Level 2 K: 0.5	Level 2 Standard Deviation: 0.2841 *THERMAL + 55.462
Level 3 K: 1.5	Level 3 Standard Deviation: 0.3972 * THERMAL + 20.422

CSM Fatigue			
$N_f = 10^{\left(\frac{k_1 \beta_{c1}\left(\frac{\sigma_s}{M_r}\right)}{k_2 \beta_{c2}}\right)}$	$N_f = number\ of\ repetitions\ to\ fatigue\ cracking$ $\sigma_s = Tensile\ stress(psi)$ $M_r = modulus\ of\ rupture(psi)$		
k1: 1	k2: 1	Bc1: 1	Bc2:1

Subgrade Rutting			
$\delta_a(N) = \beta_{s_1} k_1 \varepsilon_v h \left(\frac{\varepsilon_0}{\varepsilon_r}\right) \left\| e^{-\left(\frac{\rho}{N}\right)^{\beta}} \right\|$		δ_a = permanent deformation for the layer N = number of repetitions ε_v = average veritcal strain(in/in) $\varepsilon_0, \beta, \rho$ = material properties ε_r = resilient strain(in/in)	
Granular		**Fine**	
k1: 2.03	Bs1: 1	k1: 1.35	Bs1: 1
Standard Deviation (BASERUT) 0.1477*Pow(BASERUT,0.6711)+0.001		Standard Deviation (BASERUT) 0.1235*Pow(SUBRUT,0.5012)+0.001	

AC Cracking						
AC Top Down Cracking				**AC Bottom Up Cracking**		
$FC_{top} = \left(\frac{C_4}{1 + e^{(C_1 - C_2 \times log_{10}(Damage))}}\right) * 10.56$				$FC = \left(\frac{6000}{1 + e^{\left(C_1 + C_1' + C_2 + C_2' log_{10}(D*100)\right)}}\right) * \left(\frac{1}{60}\right)$ $C_2' = -2.40874 - 39.748 * (1 + h_{ac})^{-2.856}$ $C_1' = -2 * C_2'$		
c1: 7	c2: 3.5	c3: 0	c4: 1000	c1: 1	c2: 1	c3: 6000
AC Cracking Top Standard Deviation				**AC Cracking Bottom Standard Deviation**		
200 + 2300/(1+exp(1.072-2.1654*LOG10 (TOP+0.0001)))				1.13+13/(1+exp(7.57-15.5*LOG10 (BOTTOM+0.0001)))		

CSM Cracking				IRI Flexible Pavements			
$FC_{ctb} = C_1 + \frac{C_2}{1 + e^{C_3 - C_4 (Damage)}}$				C1 - Rutting C2 - Fatigue Crack		C3 - Transverse Crack C4 - Site Factors	
C1: 1	C2: 1	C3: 0	C4: 1000	C1: 40	C2: 0.3	C3: 0.008	C4: 0.011
CSM Standard Deviation							
CTB*1							

Root Mean Square Error for Iterations of AASHTOWare® local calibration for Low Traffic Volume Category

R	Low Traffic Volume Calibration								
	Rutting				IRI				
	Br_1	Br_2	Br_3	RMSE	C_1	C_2	C_3	C_4	RMSE
1	1	1	1	3.180	40	0.4	0.008	0.015	0.706
2	1	0.9	1	2.589	40	0.4	0.008	0.014	0.7097
3	1	0.8	1	2.361	40	0.4	0.008	0.013	0.7106
4	1	0.7	1	2.271	40	0.4	0.008	0.011	0.7146
5	1	0.6	1	2.232	40	0.4	0.008	0.009	1.2465
6	1	0.4	1	2.206	38	0.4	0.008	0.011	0.7156
7	1	0.6	0.8	2.207	36	0.4	0.008	0.011	0.7153
8	1	0.6	0.6	2.200	34	0.4	0.008	0.011	0.7208
9	1	0.6	1.2	2.346	35	0.4	0.008	0.011	0.7145
10	0.8	0.6	1	2.225	35	0.3	0.008	0.011	0.7205
11	1.2	0.6	1	2.239	42	0.4	0.008	0.011	0.7132
12	1.4	0.6	1	2.247	40	0.4	0.006	0.011	0.7167
13	1.38	0.6	1	2.246	40	0.4	0.01	0.011	0.7159
14	1.25	0.6	1	2.242	40	0.6	0.008	0.011	0.7156
15	1.2	0.6	0.8	2.209	42	0.4	0.008	0.015	0.7134
16	0.7	0.6	1	2.221	40	0.3	0.008	0.011	0.7174
17	0.6	0.6	1	2.218	40	0.8	0.008	0.011	0.7159
18	1.1	0.6	1	2.236	44	0.4	0.008	0.015	0.7102
19	0.65	0.6	1	2.220	48	0.4	0.008	0.015	0.7082
20	0.7	0.6	1.2	2.295	46	0.4	0.008	0.015	0.7067
21	0.7	0.6	0.8	2.2042	38	0.4	0.008	0.015	0.7165
22	0.7	0.6	0.9	2.2038	36	0.4	0.008	0.015	0.7189
23	0.7	0.6	0.98	2.218	38	0.8	0.008	0.015	0.7149

Root Mean Square Error for Iterations of AASHTOWare® local calibration for High Traffic Volume Category

R	High Traffic Volume Calibration								
	Rutting				IRI				
	Br_1	Br_2	Br_3	RMSE	C_1	C_2	C_3	C_4	RMSE
1	1	1	1	3.297	40	0.4	0.008	0.015	0.42235
2	1	0.9	1	2.193	40	0.4	0.008	0.014	0.39486
3	1	0.8	1	1.957	40	0.4	0.008	0.013	0.38240
4	1	0.7	1	1.862	40	0.4	0.008	0.011	0.37518
5	1	0.6	1	1.873	40	0.4	0.008	0.009	0.37196
6	1	0.4	1	1.895	38	0.4	0.008	0.011	0.37421
7	1	0.6	0.8	1.895	36	0.4	0.008	0.011	0.37258
8	1	0.6	0.6	1.903	34	0.4	0.008	0.011	0.37075
9	1	0.6	1.2	1.932	35	0.4	0.008	0.011	0.37825
10	0.8	0.6	1	1.878	35	0.3	0.008	0.011	0.37173
11	1.2	0.6	1	1.869	42	0.4	0.008	0.011	0.37523
12	1.4	0.6	1	1.866	40	0.4	0.006	0.011	0.37379
13	1.38	0.6	1	1.866	40	0.4	0.01	0.011	0.37334
14	1.25	0.6	1	1.868	40	0.6	0.008	0.011	0.37344
15	1.2	0.6	0.8	1.894	42	0.4	0.008	0.015	0.38161
16	0.7	0.6	1	1.880	40	0.3	0.008	0.011	0.37347
17	0.6	0.6	1	1.883	40	0.8	0.008	0.011	0.37268
18	1.1	0.6	1	1.871	44	0.4	0.008	0.015	0.38662
19	0.65	0.6	1	1.882	48	0.4	0.008	0.015	0.39228
20	0.7	0.6	1.2	1.879	46	0.4	0.008	0.015	0.39635
21	0.7	0.6	0.8	1.920	38	0.4	0.008	0.015	0.37586
22	0.7	0.6	0.9	1.903	36	0.4	0.008	0.015	0.37406
23	0.7	0.6	0.98	1.883	38	0.8	0.008	0.015	0.37752

Root Mean Square Error for Iterations of AASHTOWare® local calibration for Overall Network Category

R	Overall Network Calibration								
	Rutting				IRI				
	Br_1	Br_2	Br_3	RMSE	C_1	C_2	C_3	C_4	RMSE
1	1	1	1	3.255	40	0.4	0.008	0.015	0.5776
2	1	0.9	1	2.368	40	0.4	0.008	0.014	0.56362
3	1	0.8	1	2.137	40	0.4	0.008	0.013	0.55946
4	1	0.7	1	2.046	40	0.4	0.008	0.011	0.55196
5	1	0.6	1	2.0355	40	0.4	0.008	0.009	0.8767
6	1	0.4	1	2.0364	38	0.4	0.008	0.011	0.5593
7	1	0.6	0.8	2.03662	36	0.4	0.008	0.011	0.5589
8	1	0.6	0.6	2.0381	34	0.4	0.008	0.011	0.56134
9	1	0.6	1.2	2.16456	35	0.4	0.008	0.011	0.56065
10	0.8	0.6	1	2.03503	35	0.3	0.008	0.011	0.5614
11	1.2	0.6	1	2.03642	42	0.4	0.008	0.011	0.55813
12	1.4	0.6	1	2.03734	40	0.4	0.006	0.011	0.559661
13	1.38	0.6	1	2.03804	40	0.4	0.01	0.011	0.558998
14	1.25	0.6	1	2.03702	40	0.6	0.008	0.011	0.55895
15	1.2	0.6	0.8	2.03665	42	0.4	0.008	0.015	0.560467
16	0.7	0.6	1	2.03482	40	0.3	0.008	0.011	0.55982
17	0.6	0.6	1	2.03494	40	0.8	0.008	0.011	0.558646
18	1.1	0.6	1	2.03582	44	0.4	0.008	0.015	0.560229
19	0.65	0.6	1	2.03489	48	0.4	0.008	0.015	0.561484
20	0.7	0.6	1.2	2.06696	46	0.4	0.008	0.015	0.562147
21	0.7	0.6	0.8	2.04882	38	0.4	0.008	0.015	0.560284
22	0.7	0.6	0.9	2.03681	36	0.4	0.008	0.015	0.561085
23	0.7	0.6	0.98	2.03507	38	0.8	0.008	0.015	0.559909

Appendix C

Statistical Analysis

In this Appendix summary of t-Test: Paired Two Sample for Means for each category is presented here.

Low Traffic Volume Calibration

Rutting- Default Values

	Observed	*Predicted*
Mean	4.063848039	6.026622549
Variance	4.392522189	8.157423704
Observations	204	204
Pearson Correlation	0.522896111	
Hypothesized Mean Difference	0	
Df	203	
t Stat	-11.17800529	
P(T<=t) two-tail	6.46378E-23	
t Critical two-tail	1.971718802	

Rutting- Calibration Coefficients

	Observed	*Predicted*
Mean	4.042230392	3.838803922
Variance	4.472816306	5.004277764
Observations	204	204
Pearson Correlation	0.491770715	
Hypothesized Mean Difference	0	
Df	203	
t Stat	1.32289299	
P(T<=t) two-tail	0.187359216	
t Critical two-tail	1.971718802	

Rutting- Validation

	Observed	*Predicted*
Mean	4.56609375	4.50521875
Variance	4.165778604	4.247577789
Observations	32	32
Pearson Correlation	0.810570283	
Hypothesized Mean Difference	0	

Df	31
t Stat	0.27274786
P(T<=t) two-tail	0.786855739
t Critical two-tail	2.039513438

IRI- Default Values

	Observed	*Predicted*
Mean	1.433254848	1.40700831
Variance	0.280707363	0.023073247
Observations	361	361
Pearson Correlation	-0.104436972	
Hypothesized Mean Difference	0	
Df	360	
t Stat	0.880745182	
P(T<=t) two-tail	0.379043356	
t Critical two-tail	1.966575389	

IRI- Calibration Coefficients

	Observed	*Predicted*
Mean	1.414210526	1.407091413
Variance	0.266374306	0.022420128
Observations	361	361
Pearson Correlation	-0.018160195	
Hypothesized Mean Difference	0	
Df	360	
t Stat	0.250486788	
P(T<=t) two-tail	0.802353813	
t Critical two-tail	1.966575389	

IRI- Validation

	Observed	*Predicted*
Mean	1.498482143	1.396785714
Variance	0.246349018	0.01660039
Observations	56	56
Pearson Correlation	0.045711565	
Hypothesized Mean Difference	0	
Df	55	
t Critical one-tail	1.673033966	
P(T<=t) two-tail	0.13910582	
t Critical two-tail	2.004044769	

High Traffic Volume Calibration

Rutting- Default Values

	Observed	*Predicted*
Mean	4.422827988	6.487247813
Variance	4.600931599	10.09199878
Observations	343	343
Pearson Correlation	0.591759131	
Hypothesized Mean Difference	0	
Df	342	
t Stat	-14.85064125	
P(T<=t) two-tail	7.55149E-39	
t Critical two-tail	1.966924576	

Rutting- Calibration Coefficients

	Observed	*Predicted*
Mean	4.391093	4.211746356
Variance	4.69928	4.00698919
Observations	343	343
Pearson Correlation	0.627374	
Hypothesized Mean Difference	0	
Df	342	
t Stat	1.839221	
P(T<=t) two-tail	0.066749	
t Critical two-tail	1.966925	

Rutting- Validation

	Observed	*Predicted*
Mean	5.3029375	4.9250875
Variance	8.400439047	7.297982942
Observations	80	80
Pearson Correlation	0.42995179	
Hypothesized Mean Difference	0	
Df	79	
t Stat	1.128695082	
P(T<=t) two-tail	0.262442407	
t Critical two-tail	1.990450177	

IRI- Default Values

	Observed	*Predicted*
Mean	1.273610478	1.419453303
Variance	0.131270211	0.024630751
Observations	439	439
Pearson Correlation	-0.013745273	
Hypothesized Mean Difference	0	
Df	438	
t Stat	-7.700634496	
P(T<=t) two-tail	9.1025E-14	
t Critical two-tail	1.965394793	

IRI Calibration Coefficients

	Observed	*Predicted*
Mean	1.273610478	1.276537585
Variance	0.131270211	0.010528624
Observations	439	439
Pearson Correlation	0.054318642	
Hypothesized Mean Difference	0	
Df	438	
t Stat	-0.165237714	
P(T<=t) two-tail	0.868833117	
t Critical two-tail	1.965394793	

IRI Validation

	Observed	*Predicted*
Mean	1.233010753	1.283763441
Variance	0.054579967	0.010595465
Observations	93	93
Pearson Correlation	-0.037336651	
Hypothesized Mean Difference	0	
Df	92	
t Stat	-1.891283322	
P(T<=t) two-tail	0.061732774	
t Critical two-tail	1.986086272	

Overall Network Calibration

Rutting - Default Values

	Observed	*Predicted*
Mean	4.299516129	6.326775891
Variance	4.620503039	9.393341069
Observations	589	589
Pearson Correlation	0.570168283	
Hypothesized Mean Difference	0	
Df	588	
t Stat	-19.29600238	
P(T<=t) two-tail	1.21957E-64	
t Critical two-tail	1.964006547	

Rutting – Calibration Coefficients

	Observed	*Predicted*
Mean	4.299516129	4.269001698
Variance	4.620503039	4.203265682
Observations	589	589
Pearson Correlation	0.530660421	
Hypothesized Mean Difference	0	
Df	588	
t Stat	0.36367866	
P(T<=t) two-tail	0.716228701	
t Critical two-tail	1.964006547	

Rutting – Validation

	Observed	*Predicted*
Mean	5.009344262	4.861475
Variance	6.969514029	7.166685
Observations	122	122
Pearson Correlation	0.416813205	
Hypothesized Mean Difference	0	
Df	121	
t Stat	0.568815402	
P(T<=t) two-tail	0.570535691	
t Critical two-tail	1.979763738	

IRI- Default Values

	Observed	*Predicted*
Mean	1.37729425	1.415975197
Variance	0.260622806	0.024243263
Observations	887	887
Pearson Correlation	-0.05260612	
Hypothesized Mean Difference	0	
Df	886	
t Stat	-2.127430163	
P(T<=t) two-tail	0.033659973	
t Critical two-tail	1.962645047	

IRI Calibration Coefficients

	Observed	*Predicted*
Mean	1.380264938	1.336629087
Variance	0.265756956	0.004843199
Observations	887	887
Pearson Correlation	-0.058444529	
Hypothesized Mean Difference	0	
df	886	
t Stat	1.767810231	
P(T<=t) two-tail	0.057036749	
t Critical two-tail	1.962645047	

IRI Validation

	Observed	*Predicted*
Mean	1.278764368	1.342413793
Variance	0.153026355	0.011435758
Observations	174	174
Pearson Correlation	-0.142935411	
Hypothesized Mean Difference	0	
df	173	
t Stat	-1.998914193	
P(T<=t) two-tail	0.047183429	
t Critical two-tail	1.973771297	